Presence and Stability of SARS-Cov-2 on Indoor Surfaces and Masks

Jin Pan

Dissertation submitted to the faculty of the Virginia Polytechnic Institute and State University in partial fulfillment of the requirements for the degree of

Doctor of Philosophy

In

Civil Engineering

Linsey C. Marr, Committee Chair

Nisha K. Duggal

David G. Schmale

Peter J. Vikesland

May 2nd, 2022

Blacksburg, VA

Keywords: SARS-CoV-2, mask, airborne transmission, fomite transmission

Presence and Stability of SARS-Cov-2 on Indoor Surfaces and Masks

Jin Pan

Abstract

The emergence of coronavirus disease 2019 (COVID-19) has resulted in more than 300 million cases and 5 million deaths worldwide and innumerable economic losses. COVID-19 is acknowledged to transmit via air, but whether it is capable of transmitting via contaminated surfaces, also known as fomites, remains controversial. The overarching goal of this study was to investigate the presence and stability of SARS-CoV-2, the virus that causes COVID-19, on indoor surfaces and masks, and to provide insight into the possibility of fomite transmission. Since most transmission occurs indoors where humans spent 90% of their time, we first focused on quantifying the contamination level of SARS-CoV-2, including both viral RNA and viable virus, on commonly touched surfaces and in the heating, ventilation, and air cleaning (HVAC) systems in two university dormitories. Although we found up to 10^4 gene copies per ~10×10 cm^2 on surfaces, we did not detect any viable virus, suggesting that the possibility of transmission via indoor surfaces is low. As universal masking has been recommended as an effective practice to prevent transmission of SARS-CoV-2, we shifted our focus to masks, both their effectiveness at filtering the virus from the air and their potential to serve as fomites. We evaluated the effectiveness of 11 face coverings for material filtration efficiency, inward protection efficiency on a manikin, and outward protection efficiency on a manikin. Masks made of filter materials, such as vacuum cleaner bag and HVAC filters, achieved a high material filtration efficiency whereas common textiles like cotton and acrylic usually showed the worst performance. The material filtration efficiency was generally positively correlated with either inward or outward protection effectiveness, but stiffer materials were an exception to this relationship as they did not fit as closely to the manikin's face and thus leaked substantially. Subsequently, we analyzed the survival of aerosolized SARS-CoV-2 in saliva on masks. Results suggested that the virus lost infectivity within one hour on an N95 respirator,

surgical mask, polyester mask, and two types of cotton masks but not on a nylon/spandex mask. This study also highlighted the importance of applying virus in aerosols of realistic sizes when analyzing the stability of SARS-CoV-2 on surfaces.

Presence and Stability of SARS-Cov-2 on Indoor Surfaces and Masks

Jin Pan

General audiences abstract

The emergence of coronavirus disease 2019 (COVID-19) has resulted in more than 300 million cases and 5 million deaths worldwide and innumerable economic losses. Researchers are debating if COVID-19 can transmit via surfaces contaminated with SARS-CoV-2, the virus that causes the disease. The goal of this study was to investigate whether SARS-CoV-2 is present and remains viable on indoor surfaces and masks, and to provide insight into the possibility of transmission via contaminated surfaces. Since most transmission occurs indoors where humans spent 90% of their time, we first focused on quantifying number of SARS-CoV-2 on commonly touched surfaces and in the heating, ventilation, and air cleaning (HVAC) systems in two university dormitories. Although we found a high concentration of SARS-CoV-2 genes on surfaces, we did not detect any viable virus, suggesting that the possibility of transmission via indoor surfaces is low. As universal masking has been recommended as an effective practice to prevent transmission of SARS-CoV-2, we shifted our focus to masks. We evaluated the effectiveness of 11 face coverings regarding their ability to trap viruses, protect wearers from inhaling viruses, and prevent infected individuals from expelling viruses into the surrounding air. Masks made of filter materials, such as a vacuum cleaner bag and HVAC filter, trapped the most viruses whereas common textiles like cotton and acrylic usually performed worst. It is also crucial that masks fit closely to the wearer's face to achieve better protection. Subsequently, we analyzed the ability of SARS-CoV-2 in aerosols, microscopic particles such as those exhaled by an infected person, to survive on different types of masks. Results suggested that the virus died within one hour on a majority of the masks. This study also highlighted the importance of applying aerosols of realistic sizes instead of large droplets when analyzing the survival of SARS-CoV-2 on surfaces.

Acknowledgements

I have received much support, both personally and professionally, from many people to help me continue my career in academia. I cannot express enough my gratitude to my advisor and life mentor, Dr. Linsey Marr, for she has been constantly providing me insightful guidance and supporting me in pursuing my academic goals. She is always inspiring, encouraging, and patient, which is extremely valuable to me especially during the pandemic, when everything was out of order. She is a great role model not only for me but for all women in STEM.

I would also like to thank my committee members, Dr. Nisha Duggal, Dr. David Schmale, and Dr. Peter Vikesland. Their time, efforts, support, and care have been indispensable to my research and completion of the degree. I am so grateful to Dr. Nisha Duggal, for she has taught me all the essential techniques to deal with SARS-CoV-2, allowed me to use her lab and equipment, and offered me great inputs on my experiments, without all of which I could not have conducted and completed my favorite study. I am also very thankful to Dr. David Schmale, for I learnt all the basics and received the first trainings regarding biological experiments in his lab, which has been a good start and will be continuously useful in my future research. My gratitude also goes to Dr. Amy Pruden for granting me access to her lab and supplies, where I completed many qPCR experiments, and Dr. Gabriel Issacman-Vanwertz and Dr. Shane Ross for their perceptive comments on my research.

Research can be much more painful and tougher if without the support of the EWR program. I must express my thanks to Dr. AJ Prussin, who has been very approachable and willing to share his expertise whenever I need help, and Dr. Weinan Leng, who has offered much assistance to me during my time in Kelly Hall. I also benefited from the discussion with AIR^2 group and CEEair group, where I received numerous insights on my research and presentation skills. I must also highlight the help from Duggal lab, particularly from Mr. Seth Hawks, who has been a great teacher for all the virus-related experiments and a patient friend for many questions and requests I had. I am also grateful for the support from Schmale lab, including Ms. Regina Hanlon, who contributed

a lot to my study and the transition of my research direction, and Ms. Hope Gruszewski, and Ms. Niki McMaster, who have been constantly helpful and kind to me. I would like to specifically thank IGEP BIOTRANS program, Pratt Fellowship, and Sussman Fellowship for providing me valuable funding and resources.

My friends are always reliable and willing to listen to me, without whom I cannot progress far. I will never forget all those philosophical discussions with James Hurley and how wise, knowledgeable, and good-hearted he is. I am also thankful to Jiaqi Sun, who has been supporting me from my undergraduate to the end of my Ph.D. with her liveliness and energy, and Wenchuo Yao, who offered mental support and provided much happiness and company to me. I am fortunate to have Charbel Harb as both a collaborator and a friend, and I enjoyed every moment I spent with Wei, Meng, Chenyang, Xinyue, Huan, Chunyi, Kaisen, Minzhe, Qishen, and Ran, when I experienced much joy and relax.

Last but not least, I would like to thank my beloved parents. You give me endless support, allowing to pursue my goals in academia, comforting and encouraging me whenever I was doubtful about myself, and respecting my life choices. I can never reward you enough, and I hope that you can be proud of me in the past, present, and future.

Table of contents

Lists of figures

Lists of tables

1. Introduction

1.1. Overview

Since the emergence of coronavirus disease 2019 (COVID-19) in Wuhan, China, it has spread to over 200 countries and territories,[1,2] resulting in more than 300 million cases and 5 million deaths worldwide, as of January 2022.[2] In the United States, the total numbers of cases and deaths reached 66 million and 850,000, respectively.[3] COVID-19 is caused by severe acute respiratory syndrome coronavirus-2 (SARS-CoV-2).[4] It primarily attacks the respiratory system of humans, and it can also affect the cardiovascular, neurological, reproductive, gastrointestinal, and urinary systems.[5-10]

The high infection rate of COVID-19 is in part due to the high transmissibility of SARS-CoV-2. It is likely that transmission of SARS-CoV-2 occurs mainly via the airborne route (i.e., inhalation of virus-laden aerosols).[11-15] Droplet transmission (i.e. transmission via large droplets that are sprayed onto the mucus membranes) is important only when individuals are very close (usually < 0.2 m).[13] Some evidence suggests that fomite transmission (i.e., transmission via contaminated surfaces) also occurs, at least among hamsters.[16] Several studies have demonstrated that SARS-CoV-2 in droplets can survive on a variety of surfaces for hours to days under laboratory-controlled conditions, indicating that transmission via surfaces is possible.[17-22] Furthermore, a spate of research has recovered SARS-CoV-2 RNA from surfaces in both healthcare and non-healthcare settings where infected individuals have lingered or resided.[23-27] Despite the prolonged survival of SARS-CoV-2 on multiple types of surfaces and the discovery of its RNA in the environment, debates continue with regards to the likelihood and importance of fomite transmission in real-life conditions.[28-30]

Given that airborne transmission of SARS-CoV-2 is widely recognized as the primary route, multiple measures can be implemented to minimize the risk of transmission in the indoor environment, where most transmission occurs.[31,32] These measures include ventilation, high-efficiency filtration, and universal masking.[15,33,34] All of these approaches aim to reduce the

concentration of virus in indoor air, with masking acting as source control. Masking also reduces the wearer's exposure to virus in the air. Even though systematic reviews have investigated the efficacy of masks regarding protection against other airborne viruses,[35,36] we knew little about the effectiveness of cloth masks against SARS-CoV-2 aerosols at the time we began the study. Moreover, masks contaminated with virus-laden aerosols might serve as fomites, should someone touch the virus and transfer it to their mucus membranes.[37,38] Investigating the role of masks at the interface of airborne and fomite transmission of SARS-CoV-2 is essential to develop guidance for controlling the COVID-19 pandemic.

1.2. Transmission of SARS-CoV-2 and controversy

There are three commonly recognized transmission routes of SARS-CoV-2: airborne (i.e., aerosol), droplet, and fomite. Both aerosols and droplets are generated from respiratory activities, including breathing, talking, singing, coughing, and sneezing.[39-41] While it is likely that airborne transmission is dominant, the exact breakdown of transmission among the different routes is not known.

1.2.1. Airborne and droplet transmission

Before the COVID-19 pandemic, airborne transmission was traditionally defined as involving aerosols or "droplet nuclei" (evaporated droplets) with a diameter smaller than 5 μm. In contrast, droplet transmission was defined as transmission via droplets larger than 5 μm. However, this conventional cut-off size of 5 μm to distinguish aerosols and droplets lacks solid evidence; instead, aerosol scientists have updated the size threshold to 100 μm based on differences in aerodynamic behavior.[13,42-45] This threshold is the upper size limit of a particle that can be inhaled, and a particle of this size will fall to the ground in 5 s from the height of 1.5 m.[13] The updated size distinction is used as the foundation for the following discussion.

Whether airborne or droplet transmission was dominant remained controversial since the beginning of the COVID-19 pandemic. At the early stage of the pandemic, both the World Health Organization (WHO) and the Centers for Disease Control and Prevention (CDC) emphasized

droplet transmission rather than airborne transmission.[44] As more research on airborne transmission emerged, new discoveries seemed to reverse the original opinion. Scientists have recovered both viable SARS-CoV-2 and SARS-CoV2- RNA from aerosols ranging from 0.25 to >4 μm in real-life settings,[46-50] and SARS-CoV-2 aerosols can maintain infectivity for up to 3 hours in laboratory-controlled environments.[22,51,52] Animal studies have demonstrated that airborne transmission of SARS-CoV-2 may occur among hamsters[11,16,53] and ferrets.[12,54,55] The superspreading event occurring at a choir practice in Skagit, Washington further suggested that long-range airborne transmission was possible.[56] The accumulation of this evidence shifted the emphasis of studies on SARS-CoV-2 transmission study from droplets to aerosols.

1.2.2. Fomite transmission

Fomite transmission raised much concern at the beginning of the pandemic, but ample evidence has suggested that airborne transmission is likely to be more important. However, the possibility of fomite transmission cannot be completely ruled out. Numerous studies have recovered SARS-CoV-2 RNA on various indoor surfaces in both healthcare and non-healthcare settings.[20,23-27,46,57-60] SARS-CoV-2 in droplets can survive on surfaces for several days in studies involving droplets with an initial volume ranging from 5 μL to 50 μL.[17-22] Moreover, fomite transmission has been shown to occur among hamsters, yet it resulted in milder symptoms and lower viral load in the respiratory system than airborne transmission.[16] These results indicate that fomite transmission may contribute to the overall transmission of SARS-CoV-2, though its relative importance and relationship with airborne transmission in humans is still unclear. Of note, the majority of the studies regarding fomite sampling in real-life situations focused on healthcare settings. Most transmission takes place in the community, rather than in hospitals and other healthcare facilities, so the results of such studies may not be broadly representative.[31,32] At the time we conducted our experiment, there had been few large-scale, quantitative, and comprehensive studies to investigate the risk of fomite transmission in a non-healthcare setting. In addition, the interaction of fomites with aerosols and droplets in indoor environments through

deposition and resuspension requires further research.

1.3. Prevention of transmission using masks

Universal masking has proven to be an effective and practical way to mitigate airborne transmission of SARS-CoV-2,[61-63] with mask performance depending mainly on materials and fit. The former defines the filtration efficiency of the mask, which represents its ability to filter virus-laden aerosols and droplets. The latter determines the degree of air leakage, which compromises the overall performance, via gaps between the mask and the face. As the pandemic surged in the U.S. and worldwide, there was a lack of respirators (e.g., N95) that are known to provide highly efficient filtration against aerosols and a tight fit to ensure no leakage. Amid this shortage, some public agencies suggested that people wear cloth masks. Although ample studies have examined the filtration efficiency and breathability of a variety of cloth materials,[64-69] at the time of this study, people knew little about the effectiveness of these cloth masks with regard to both inward protection for reducing the wearer's exposure and outward protection for source control. Even if commercial cloth masks and medical masks in developed countries were replenished, homemade cloth masks still accounted for a good portion of masks being used in the developing world due to limited resources.[70,71] Therefore, it is essential to conduct a comprehensive evaluation of homemade cloth masks regarding both inward and outward protection.

Due to their function of collecting inhaled and exhaled aerosols and droplets, masks can be a potential reservoir of viruses. Researchers have successfully recovered SARS-CoV-2 RNA from masks worn by infected individuals.[37,38] SARS-CoV-2 in droplets can survive on surgical masks for 4-7 days at ~22°C and 45-65% RH,[17,72,73] and on an N95 for 2 days at 25°C and 70% RH[74] and for up to 21 days at 20°C and 35-40% RH.[21] The virus can remain infectious on cotton from 4 hours to 5.57 days, depending on the temperature and RH.[21,72,73,75] SARS-CoV-2 in droplets seemed to persist on polyester for only a short duration: 2.5 hours on a t-shirt made of 85% polyester and 15% elastane,[73] and 4 hours on 65% polyester and 35% cotton,[19] both at 22°C and 40-50% RH. Though these studies shed light on the possibility of masks serving as fomites, only

limited types of materials were examined, and unrealistically large droplets (> 5 μL) were used in these studies, whereas typical aerosols are smaller than 100 μm with a volume of $<5\times10^{-4}$ μL. It is crucial to examine aerosols of realistic size on a wide range of materials when exploring the survival of viruses on masks.

1.4. Objectives

After reviewing the current knowledge of SARS-CoV-2 transmission and mitigation using masks, we identified gaps and defined the overarching goals of this study, which were to elucidate the potential for fomite transmission in a real-life setting, evaluate the efficacy of homemade cloth masks, and investigate masks for their potential to act as fomites, at the interface of airborne and fomite transmission. Specific objectives are to:

1) quantify SARS-CoV-2 RNA concentration and evaluate virus viability in surface swab samples and on HVAC filters collected from university dormitory rooms housing students who tested positive for COVID-19.

2) evaluate the efficiency of cloth masks compared to a surgical mask and a face shield at blocking aerosols and droplets over a wide range of sizes.

3) evaluate the persistence of aerosolized SARS-CoV-2 on different types of masks.

1.5. References

1. Zhang J, Litvinova M, Wang W, et al. Evolving epidemiology and transmission dynamics of coronavirus disease 2019 outside Hubei province, China: a descriptive and modelling study. *The Lancet Infectious Diseases.* 2020;20(7):793-802.
2. World Health Organization. https://covid19.who.int/table. Accessed 1/19, 2022.
3. Centers for Disease Control and Prevention. https://covid.cdc.gov/covid-data-tracker/#cases_totalcases. Accessed 1/19, 2022.
4. Ksiazek TG, Erdman D, Goldsmith CS, et al. A Novel Coronavirus Associated with Severe Acute Respiratory Syndrome. *New England Journal of Medicine.* 2003;348(20):1953-1966.
5. Chen N, Zhou M, Dong X, et al. Epidemiological and clinical characteristics of 99 cases of 2019 novel coronavirus pneumonia in Wuhan, China: a descriptive study. *The Lancet.* 2020;395(10223):507-513.
6. Huang C, Wang Y, Li X, et al. Clinical features of patients infected with 2019 novel coronavirus in Wuhan, China. *The Lancet.* 2020;395(10223):497-506.
7. Wang D, Hu B, Hu C, et al. Clinical Characteristics of 138 Hospitalized Patients With 2019 Novel Coronavirus–Infected Pneumonia in Wuhan, China. *JAMA.* 2020;323(11):1061-1069.
8. Yang X, Yu Y, Xu J, et al. Clinical course and outcomes of critically ill patients with SARS-CoV-2 pneumonia in Wuhan, China: a single-centered, retrospective, observational study. *Lancet Respir Med.* 2020;8(5):475-481.
9. Song E, Zhang C, Israelow B, et al. Neuroinvasion of SARS-CoV-2 in human and mouse brainNeuroinvasion of SARS-CoV-2 in humans and mice. *Journal of Experimental Medicine.* 2021;218(3):e20202135.
10. Xiao F, Tang M, Zheng X, Liu Y, Li X, Shan H. Evidence for Gastrointestinal Infection of SARS-CoV-2. *Gastroenterology.* 2020;158(6):1831-1833.e1833.
11. Hawks Seth A, Prussin Aaron J, Kuchinsky Sarah C, et al. Infectious SARS-CoV-2 Is Emitted in Aerosol Particles. *mBio.* 2021;12(5):e02527-02521.
12. Kutter JS, de Meulder D, Bestebroer TM, et al. SARS-CoV and SARS-CoV-2 are transmitted through the air between ferrets over more than one meter distance. *Nature Communications.* 2021;12(1):1653.
13. Wang Chia C, Prather Kimberly A, Sznitman J, et al. Airborne transmission of respiratory viruses. *Science.* 2021;373(6558):eabd9149.
14. Sills J, Prather Kimberly A, Marr Linsey C, et al. Airborne transmission of SARS-CoV-2. *Science.* 2020;370(6514):303-304.
15. Allen JG, Marr LC. Recognizing and controlling airborne transmission of SARS-CoV-2 in indoor environments. *Indoor Air.* 2020;30(4):557-558.
16. Port JR, Yinda CK, Owusu IO, et al. SARS-CoV-2 disease severity and transmission efficiency is increased for airborne compared to fomite exposure in Syrian hamsters. *Nature Communications.* 2021;12(1):4985.

17. Chin AWH, Chu JTS, Perera MRA, et al. Stability of SARS-CoV-2 in different environmental conditions. *The Lancet Microbe.* 2020;1(1):e10.
18. Hirose R, Ikegaya H, Naito Y, et al. Survival of Severe Acute Respiratory Syndrome Coronavirus 2 (SARS-CoV-2) and Influenza Virus on Human Skin: Importance of Hand Hygiene in Coronavirus Disease 2019 (COVID-19). *Clin Infect Dis.* 2021;73(11):e4329-e4335.
19. Harbourt DE, Haddow AD, Piper AE, et al. Modeling the stability of severe acute respiratory syndrome coronavirus 2 (SARS-CoV-2) on skin, currency, and clothing. *PLOS Neglected Tropical Diseases.* 2020;14(11):e0008831.
20. Kampf G, Todt D, Pfaender S, Steinmann E. Persistence of coronaviruses on inanimate surfaces and their inactivation with biocidal agents. *Journal of Hospital Infection.* 2020;104(3):246-251.
21. Kasloff SB, Leung A, Strong JE, Funk D, Cutts T. Stability of SARS-CoV-2 on critical personal protective equipment. *Scientific Reports.* 2021;11(1):984.
22. van Doremalen N, Bushmaker T, Morris DH, et al. Aerosol and Surface Stability of SARS-CoV-2 as Compared with SARS-CoV-1. *New England Journal of Medicine.* 2020;382(16):1564-1567.
23. Bedrosian N, Mitchell E, Rohm E, et al. A Systematic Review of Surface Contamination, Stability, and Disinfection Data on SARS-CoV-2 (Through July 10, 2020). *Environmental Science & Technology.* 2021;55(7):4162-4173.
24. Ben-Shmuel A, Brosh-Nissimov T, Glinert I, et al. Detection and infectivity potential of severe acute respiratory syndrome coronavirus 2 (SARS-CoV-2) environmental contamination in isolation units and quarantine facilities. *Clinical Microbiology and Infection.* 2020;26(12):1658-1662.
25. Chia PY, Coleman KK, Tan YK, et al. Detection of air and surface contamination by SARS-CoV-2 in hospital rooms of infected patients. *Nature Communications.* 2020;11(1):2800.
26. Colaneri M, Seminari E, Novati S, et al. Severe acute respiratory syndrome coronavirus 2 RNA contamination of inanimate surfaces and virus viability in a health care emergency unit. *Clin Microbiol Infect.* 2020;26(8):1094.e1091-1094.e1095.
27. Döhla M, Wilbring G, Schulte B, et al. SARS-CoV-2 in environmental samples of quarantined households. *medRxiv.* 2020:2020.2005.2028.20114041.
28. Rocha ALS, Pinheiro JR, Nakamura TC, et al. Fomites and the environment did not have an important role in COVID-19 transmission in a Brazilian mid-sized city. *Scientific Reports.* 2021;11(1):15960.
29. Mondelli MU, Colaneri M, Seminari EM, Baldanti F, Bruno R. Low risk of SARS-CoV-2 transmission by fomites in real-life conditions. *The Lancet Infectious Diseases.* 2021;21(5):e112.
30. Goldman E. Exaggerated risk of transmission of COVID-19 by fomites. *The Lancet Infectious Diseases.* 2020;20(8):892-893.

31. Qian H, Miao T, Liu L, Zheng X, Luo D, Li Y. Indoor transmission of SARS-CoV-2. *Indoor Air.* 2021;31(3):639-645.
32. Madewell ZJ, Yang Y, Longini IM, Jr., Halloran ME, Dean NE. Household Transmission of SARS-CoV-2: A Systematic Review and Meta-analysis. *JAMA Network Open.* 2020;3(12):e2031756-e2031756.
33. Prather KA, Wang CC, Schooley RT. Reducing transmission of SARS-CoV-2. *Science.* 2020;368(6498):1422.
34. Morawska L, Tang JW, Bahnfleth W, et al. How can airborne transmission of COVID-19 indoors be minimised? *Environment International.* 2020;142:105832.
35. Jefferson T, Foxlee R, Del Mar C, et al. Physical interventions to interrupt or reduce the spread of respiratory viruses: systematic review. *BMJ.* 2008;336(7635):77-80.
36. Xiao J, Shiu EYC, Gao H, et al. Nonpharmaceutical Measures for Pandemic Influenza in Nonhealthcare Settings-Personal Protective and Environmental Measures. *Emerging infectious diseases.* 2020;26(5):967-975.
37. Ruiz-Bastián M, Rodríguez-Tejedor M, Rivera-Núñez MA, Group SA-C-W. Detection of SARS-CoV-2 genomic RNA on surgical masks worn by patients: Proof of concept. *Enferm Infecc Microbiol Clin (Engl Ed).* 2021;39(10):528-530.
38. Dargahi A, Jeddi F, Ghobadi H, et al. Evaluation of masks' internal and external surfaces used by health care workers and patients in coronavirus-2 (SARS-CoV-2) wards. *Environmental Research.* 2021;196:110948.
39. Johnson GR, Morawska L, Ristovski ZD, et al. Modality of human expired aerosol size distributions. *Journal of Aerosol Science.* 2011;42(12):839-851.
40. Duguid JP. The size and the duration of air-carriage of respiratory droplets and droplet-nuclei. *Epidemiology and Infection.* 1946;44(6):471-479.
41. Morawska L, Johnson GR, Ristovski ZD, et al. Size distribution and sites of origin of droplets expelled from the human respiratory tract during expiratory activities. *Journal of Aerosol Science.* 2009;40(3):256-269.
42. Prather KA, Marr LC, Schooley RT, McDiarmid MA, Wilson ME, Milton DK. Airborne transmission of SARS-CoV-2. *Science.* 2020;370(6514):303.
43. Wells WF. ON AIR-BORNE INFECTION*: STUDY II. DROPLETS AND DROPLET NUCLEI. *American Journal of Epidemiology.* 1934;20(3):611-618.
44. Samet JM, Burke TA, Lakdawala SS, et al. SARS-CoV-2 indoor air transmission is a threat that can be addressed with science. *Proceedings of the National Academy of Sciences.* 2021;118(45):e2116155118.
45. Samet JM, Prather K, Benjamin G, et al. Airborne Transmission of Severe Acute Respiratory Syndrome Coronavirus 2 (SARS-CoV-2): What We Know. *Clinical Infectious Diseases.* 2021;73(10):1924-1926.
46. Santarpia JL, Rivera DN, Herrera VL, et al. Aerosol and surface contamination of SARS-CoV-2 observed in quarantine and isolation care. *Scientific Reports.* 2020;10(1):12732.

47. Lednicky JA, Lauzardo M, Fan ZH, et al. Viable SARS-CoV-2 in the air of a hospital room with COVID-19 patients. *International Journal of Infectious Diseases.* 2020;100:476-482.
48. Liu Y, Ning Z, Chen Y, et al. Aerodynamic analysis of SARS-CoV-2 in two Wuhan hospitals. *Nature.* 2020;582(7813):557-560.
49. Lednicky JA, Lauzardo M, Alam MM, et al. Isolation of SARS-CoV-2 from the air in a car driven by a COVID patient with mild illness. *International Journal of Infectious Diseases.* 2021;108:212-216.
50. Hu J, Lei C, Chen Z, et al. Distribution of airborne SARS-CoV-2 and possible aerosol transmission in Wuhan hospitals, China. *National Science Review.* 2020;7(12):1865-1867.
51. Schuit M, Ratnesar-Shumate S, Yolitz J, et al. Airborne SARS-CoV-2 Is Rapidly Inactivated by Simulated Sunlight. *The Journal of Infectious Diseases.* 2020;222(4):564-571.
52. Smither SJ, Eastaugh LS, Findlay JS, Lever MS. Experimental aerosol survival of SARS-CoV-2 in artificial saliva and tissue culture media at medium and high humidity. *Emerging Microbes & Infections.* 2020;9(1):1415-1417.
53. Sia SF, Yan L-M, Chin AWH, et al. Pathogenesis and transmission of SARS-CoV-2 in golden hamsters. *Nature.* 2020;583(7818):834-838.
54. Kim Y-I, Kim S-G, Kim S-M, et al. Infection and Rapid Transmission of SARS-CoV-2 in Ferrets. *Cell Host & Microbe.* 2020;27(5):704-709.e702.
55. Richard M, Kok A, de Meulder D, et al. SARS-CoV-2 is transmitted via contact and via the air between ferrets. *Nature Communications.* 2020;11(1):3496.
56. Miller SL, Nazaroff WW, Jimenez JL, et al. Transmission of SARS-CoV-2 by inhalation of respiratory aerosol in the Skagit Valley Chorale superspreading event. *Indoor Air.* 2021;31(2):314-323.
57. Guo Z-D, Wang Z-Y, Zhang S-F, et al. Aerosol and Surface Distribution of Severe Acute Respiratory Syndrome Coronavirus 2 in Hospital Wards, Wuhan, China, 2020. *Emerging infectious diseases.* 2020;26(7):1583-1591.
58. Jiang F-C, Jiang X-L, Wang Z-G, et al. Detection of Severe Acute Respiratory Syndrome Coronavirus 2 RNA on Surfaces in Quarantine Rooms. *Emerging infectious diseases.* 2020;26(9):2162-2164.
59. Ong SWX, Tan YK, Chia PY, et al. Air, Surface Environmental, and Personal Protective Equipment Contamination by Severe Acute Respiratory Syndrome Coronavirus 2 (SARS-CoV-2) From a Symptomatic Patient. *JAMA.* 2020;323(16):1610-1612.
60. Wang J, Feng H, Zhang S, et al. SARS-CoV-2 RNA detection of hospital isolation wards hygiene monitoring during the Coronavirus Disease 2019 outbreak in a Chinese hospital. *Int J Infect Dis.* 2020;94:103-106.
61. Chu DK, Akl EA, Duda S, et al. Physical distancing, face masks, and eye protection to prevent person-to-person transmission of SARS-CoV-2 and COVID-19: a systematic review and meta-analysis. *The Lancet.* 2020;395(10242):1973-1987.

62. Howard J, Huang A, Li Z, et al. An evidence review of face masks against COVID-19. *Proceedings of the National Academy of Sciences.* 2021;118(4):e2014564118.
63. Lyu W, Wehby GL. Community Use Of Face Masks And COVID-19: Evidence From A Natural Experiment Of State Mandates In The US. *Health Affairs.* 2020;39(8):1419-1425.
64. Drewnick F, Pikmann J, Fachinger F, Moormann L, Sprang F, Borrmann S. Aerosol filtration efficiency of household materials for homemade face masks: Influence of material properties, particle size, particle electrical charge, face velocity, and leaks. *Aerosol Science and Technology.* 2021;55(1):63-79.
65. Konda A, Prakash A, Moss GA, Schmoldt M, Grant GD, Guha S. Response to Letters to the Editor on Aerosol Filtration Efficiency of Common Fabrics Used in Respiratory Cloth Masks: Revised and Expanded Results. *ACS Nano.* 2020;14(9):10764-10770.
66. Konda A, Prakash A, Moss GA, Schmoldt M, Grant GD, Guha S. Aerosol Filtration Efficiency of Common Fabrics Used in Respiratory Cloth Masks. *ACS Nano.* 2020;14(5):6339-6347.
67. Leung NHL, Chu DKW, Shiu EYC, et al. Respiratory virus shedding in exhaled breath and efficacy of face masks. *Nature Medicine.* 2020;26(5):676-680.
68. Lindsley WG, Blachere FM, Law BF, Beezhold DH, Noti JD. Efficacy of face masks, neck gaiters and face shields for reducing the expulsion of simulated cough-generated aerosols. *Aerosol Science and Technology.* 2020:1-9.
69. Zangmeister CD, Radney JG, Vicenzi EP, Weaver JL. Filtration Efficiencies of Nanoscale Aerosol by Cloth Mask Materials Used to Slow the Spread of SARS-CoV-2. *ACS Nano.* 2020;14(7):9188-9200.
70. Morais FG, Sakano VK, Lima LNd, et al. Filtration efficiency of a large set of COVID-19 face masks commonly used in Brazil. *Aerosol Science and Technology.* 2021;55(9):1028-1041.
71. Benson NU, Fred-Ahmadu OH, Bassey DE, Atayero AA. COVID-19 pandemic and emerging plastic-based personal protective equipment waste pollution and management in Africa. *Journal of Environmental Chemical Engineering.* 2021;9(3):105222.
72. Liu Y, Li T, Deng Y, et al. Stability of SARS-CoV-2 on environmental surfaces and in human excreta. *Journal of Hospital Infection.* 2021;107:105-107.
73. Paton S, Spencer A, Garratt I, et al. Persistence of Severe Acute Respiratory Syndrome Coronavirus 2 (SARS-CoV-2) Virus and Viral RNA in Relation to Surface Type and Contamination Concentration. *Applied and Environmental Microbiology.* 2021;87(14):e00526-00521.
74. Kwon T, Gaudreault NN, Richt JA. Environmental Stability of SARS-CoV-2 on Different Types of Surfaces under Indoor and Seasonal Climate Conditions. *Pathogens.* 2021;10(2).
75. Riddell S, Goldie S, Hill A, Eagles D, Drew TW. The effect of temperature on persistence of SARS-CoV-2 on common surfaces. *Virology Journal.* 2020;17(1):145.

2. SARS-CoV-2 on surfaces and HVAC filters in dormitory rooms

Jin Pan[a], Seth A. Hawks[b], Aaron J. Prussin II[a], Nisha K. Duggal[b], Linsey C. Marr[a*]

[a] Civil and Environmental Engineering, Virginia Tech, Blacksburg, VA 24061, USA

[b] Department of Biomedical Sciences and Pathobiology, Virginia-Maryland College of Veterinary Medicine, Blacksburg, VA 24061, USA

[*] Corresponding author: lmarr@vt.edu (L. Marr).

Reprinted with permission from Pan, J., Hawks, S. A., Prussin, A. J., Duggal, N. K., & Marr, L. C. (2021). SARS-CoV-2 on Surfaces and HVAC Filters in Dormitory Rooms. *Environmental Science & Technology Letters.*

2.1. Abstract

While there have been many studies of SARS-CoV-2 contamination in hospital patients' rooms, less is known about the virus' presence in non-healthcare environments, which is where most transmission takes place. We investigated virus contamination in university dormitories housing students who were in quarantine or isolation. We collected surface swab samples and heating, ventilation, and air conditioning (HVAC) filters from 24 rooms that had been occupied by students who tested positive for COVID-19, and we measured viral RNA by quantitative reverse transcription polymerase chain reaction (RT-qPCR). We detected viral RNA on or in 15/21 (71.4%) HVAC filters, 71/125 (56.8%) surface samples, and 4/6 (66.7%) bathroom exhaust grilles in the two dormitories combined. Viral RNA was present in all five surface sample types, including sink handles, sink countertops, floors near the sink, door handles, and thermostat panels. Viral RNA levels on surfaces varied widely, from 10 to $>10^4$ gene copies per swabbed area of ~10×10 cm^2. Additionally, we tested the infectivity of samples with a Ct value lower than 33, and none of them were positive. This information will be valuable for assessing the risk of airborne and fomite transmission of COVID-19.

2.2. Introduction

The majority of studies on surface contamination with SARS-CoV-2 have taken place in healthcare settings, where viral RNA has been found on many types of surfaces, including beds, electronics, utensils, and floors.[1,2] Less is known about environmental contamination in other types of settings. The majority of those infected with COVID-19 do not visit a hospital, and we can assume that most transmission occurs in non-healthcare settings. Thus, further investigation of environmental contamination with SARS-CoV-2 in non-healthcare settings is warranted to support risk assessments of transmission.

There is limited quantitative information about SARS-CoV-2 in non-healthcare settings. Many such studies are relatively small, focusing on 1-4 rooms or households, or lack assessment of virus viability.[3-12] Among these studies, the positive rate of surface samples ranged from 0 to ~50%, and these results were mostly qualitative or semi-quantitative with only positivity or Ct values reported, except in one residential study, in which concentrations up to 10^4 SARS-CoV-2 N2 gene copies/cm^2 were found on the floor,[7] and one community study, in which concentrations up to 10^2 gene copies/cm^2 were found on a door handle.[12] Three of the studies attempted to culture virus from the samples; no cytopathic effects by SARS-CoV-2 were observed, indicating that the virus was not culturable and its viability was below the detection limit of the assay.[3,9,10] Studies that include both quantification and viability analyses are needed to provide a more comprehensive understanding of SARS-CoV-2 contamination and the potential for transmission in the built environment.

Data on the presence of SARS-CoV-2 in heating, ventilation, and air conditioning (HVAC) systems in non-healthcare settings are also limited. Studies have recovered SARS-CoV-2 RNA from air ducts, ventilation grates, and HVAC filters in healthcare settings, showing that the virus had been present in the air.[13-17] In one study in a home, Maestre et al. reported 10^4 to 10^5 SARS-CoV-2 N2 gene copies/g of dust gathered from HVAC filters.[7] For comparison, other respiratory viruses have been found on HVAC filters: respiratory syncytial virus (RSV) and seasonal coronaviruses in a daycare center[18] and influenza A virus, influenza B virus, and parainfluenza

virus in two public buildings.[19]

Improved characterization of environmental contamination with SARS-CoV-2 is needed in the types of settings where transmission is common, such as residences. The objective of this study was to quantify SARS-CoV-2 RNA concentration and evaluate virus viability in surface swab samples and on HVAC filters collected from university dormitory rooms housing students who tested positive for COVID-19. Results will contribute to an improved understanding of the potential for the airborne and fomite transmission in non-healthcare settings.

2.3. Materials and methods

2.3.1. Quarantine and isolation dormitories

The university allocated two dormitories for housing of students in quarantine or isolation in single-occupancy rooms. The quarantine dormitory housed students who had been exposed and were waiting for their test results, while the isolation dormitory housed students who had already tested positive. In the quarantine dormitory, we only sampled rooms that had been occupied by students who tested positive. We assumed that those in quarantine were at an earlier stage of infection compared to those in isolation, but we were not able to obtain details about their symptoms. We obtained anonymous move-in and move-out dates of the students who had occupied the rooms. Further details about quarantine and isolation procedures can be found in the Supporting Information (SI).

Each room in the quarantine dormitory had a private sink, but students had to use a shared bathroom on the hall for the shower and toilet. All quarantine rooms had a window HVAC unit with a MERV-8 filter. Each room in the isolation dormitory had a full bathroom. These rooms were connected to a central HVAC system and had an air supply vent and an air return vent with a MERV-8 filter. After a student vacated a room, personnel sprayed surfaces in the room with a disinfectant and replaced the HVAC filter before a new student moved in.

2.3.2. Sample collection

We sampled 10 quarantine rooms and 14 isolation rooms that were occupied by 28 students. One of the quarantine rooms was occupied by three different students at different times, and

another quarantine room was occupied by two different students. One of the isolation rooms was occupied by two different students. We collected most samples within 24 hours after the student had moved out, with a maximum gap of 4 days between move-out and sample collection in two cases, and before the room was disinfected.

In the quarantine rooms, we swabbed four high-touch surfaces: the inside door handle, the floor near the sink (sink floor), the right sink handle, and the thermostat panel (Figure S1). In the isolation rooms, we swabbed the same sites as in the quarantine dormitories, along with the sink countertop. Quarantine rooms had hard vinyl flooring near the sink, whereas isolation rooms had carpeted floor near the sink, so we added the sink countertop as a hard-surface sampling site. Additionally, we swabbed the air exhaust grilles in the public bathrooms in the quarantine dormitory. To collect samples, we swabbed a ~10×10 cm^2 area with a sterile, flocked nylon swab and immediately placed the swab in a vial containing 1 mL of universal viral transport medium (BD Diagnostics, Sparks, MD) according to the manufacturer's instructions. For the door and sink handles, we swabbed the entire surface, whose area may have been somewhat less than or greater than 100 cm^2. The swabs were stored at -80 °C before processing. We also collected HVAC filters from each room, if available, cut them into ~3×8 cm^2 pieces, and stored them at -80 °C.

2.3.3. RNA extraction, RT-qPCR, and plaque assays

We vortexed the swabs in their medium for 15 s and removed 200 µL for RNA extraction. We eluted each HVAC filter piece in a conical tube with 20 mL BA-1 buffer[20] by shaking at 250 rpm for 15 min. We then centrifuged the eluates at 4300 × g for 2 min and used 200 µL of supernatant for RNA extraction. To extract RNA, we used the Qiagen QIAamp Viral RNA Mini kit (Qiagen, Hilden, Germany) according to the manufacturer's protocol. The elution volume was 60 µL. We quantified RNA by RT-qPCR using the 2019-nCoV RUO primer/probe kit (10006713, IDT, Coralville, IA) targeting the N1 gene and the BioRad iTaq Universal Probes One-Step kit (BioRad, Hercules, CA).[21] We used synthetic SARS-CoV-2 RNA (NR-52358, BEI Resources, Manassas, VA) as standards.[22] Each plate contained duplicates of standard points, samples, and no-template controls. The limit of detection (LOD) occurred at 40 cycles, which equated to 0.2 gc/reaction, or

9.4 gc per swab and 114 gc per 3×8 cm^2 filter piece. We also extracted RNA from blank swabs in triplicate; they were negative. The RNA quantity was indicated by the Ct value, which is the number of cycles required for the signal to pass the threshold above the background level. The higher the Ct value, the lower the amount of RNA. We calculated the number of RNA copies using standard curves developed with serial dilutions of a known amount of RNA. Details of the reaction matrix and RT-qPCR program and a discussion of the LOD can be found in the SI.

We further used original Vero cells and Vero cells expressing TMPRSS2 receptor for plaque assay to detect any viable virus from those samples with a Ct<33.[23] We added 200 μL of the sample to each well with fully confluent Vero cells on a 6-well plate. We incubated the plates at 37 °C for 1 h, and then overlaid 2 mL agarose medium comprising 0.8% agarose and Ye-Lah medium[24] to each well, followed by incubation for 1 day at 37 °C. Then, we added the second 2 mL agarose overlay with additional 3% neutral red. A day later, we counted the plaques. As a positive control, we inoculated the Vero cells with a SARS-CoV-2 stock, with six 10-fold dilutions. The lowest dilution was negative and served as the negative control.[25]

2.3.4. Statistics

We conducted the Wilcoxon ranked sum test to examine whether there were significant differences between samples from the quarantine dormitory and the isolation dormitory, and Tukey's test to compare multiple surface swab samples from the same dormitory.

2.4. Results and discussion

2.4.1. Detection of SARS-CoV-2 RNA on high-touch surfaces

We detected viral RNA on or in 15/21 (71.4%) HVAC filters, 71/125 (56.8%) surface samples, and 4/6 (66.7%) bathroom exhaust grilles in the two dormitories combined (Figure 2-1, Figure 2-2, Table S1). In the quarantine rooms, viral RNA was present in all five surface sample types; all sink floor samples were positive (13/13, 100%), followed by the thermostat panel (7/13, 53.8%) and the sink handle (6/13, 46.2%) (Figure 2-1a, c). The door handle showed the lowest positivity (4/13, 30.8%). The finding of such a high positive rate for samples collected from the floor is consistent

with a previous study, in which researchers found that floor dust can serve as a matrix for preserving SARS-CoV-2 RNA for up to 4 weeks.[26] However, the positive rate of other surface sampling sites was much higher than has been reported in previous large studies: <4% in a study involving 21 households[10] and <13% in a study involving 39 quarantine hotel rooms.[11] The thermostat panel exhibited a high positive rate, which indicated that either the individuals manipulated the control panel quite frequently, or perhaps this spot was neglected during disinfection of the room. In contrast to the quarantine rooms, the highest positive rate occurred on the door handles in the isolation dormitory (10/15, 66.7%), followed by the sink handle (9/15, 60.0%), the thermostat panel (9/15, 60.0%), the sink floor (9/15, 60.0%), and the sink countertop (5/13, 38.5%) (Figure 2-1b, d).

Viral RNA levels on these surfaces varied widely, from $10^{0.8}$ to $10^{4.5}$ genome copies per swabbed area (Figure 2-1a-b). For each type of sampling site, there was at least one sample with greater than 10^4 gene copies, much higher than the amount found on similar surfaces in a household.[7] This might be explained by the infected individual being confined to the smaller area of a dormitory room compared to that of an apartment unit or house. The concentrations per swabbed area in the dormitory were comparable to those detected in intensive care units (ICU).[13,27] Across different types of sampling sites, we found the SARS-CoV-2 RNA concentration on sink floors was significantly higher than that of the other sites in the quarantine dormitory (Tukey's test, $p<0.05$). In the isolation dormitory, we observed no significant differences among all surface sampling sites (Figure 2-2b). In these rooms, the floor near the sink was carpeted, and the recovery efficiency on this material was probably lower than on all the other solid surface types sampled.[28]

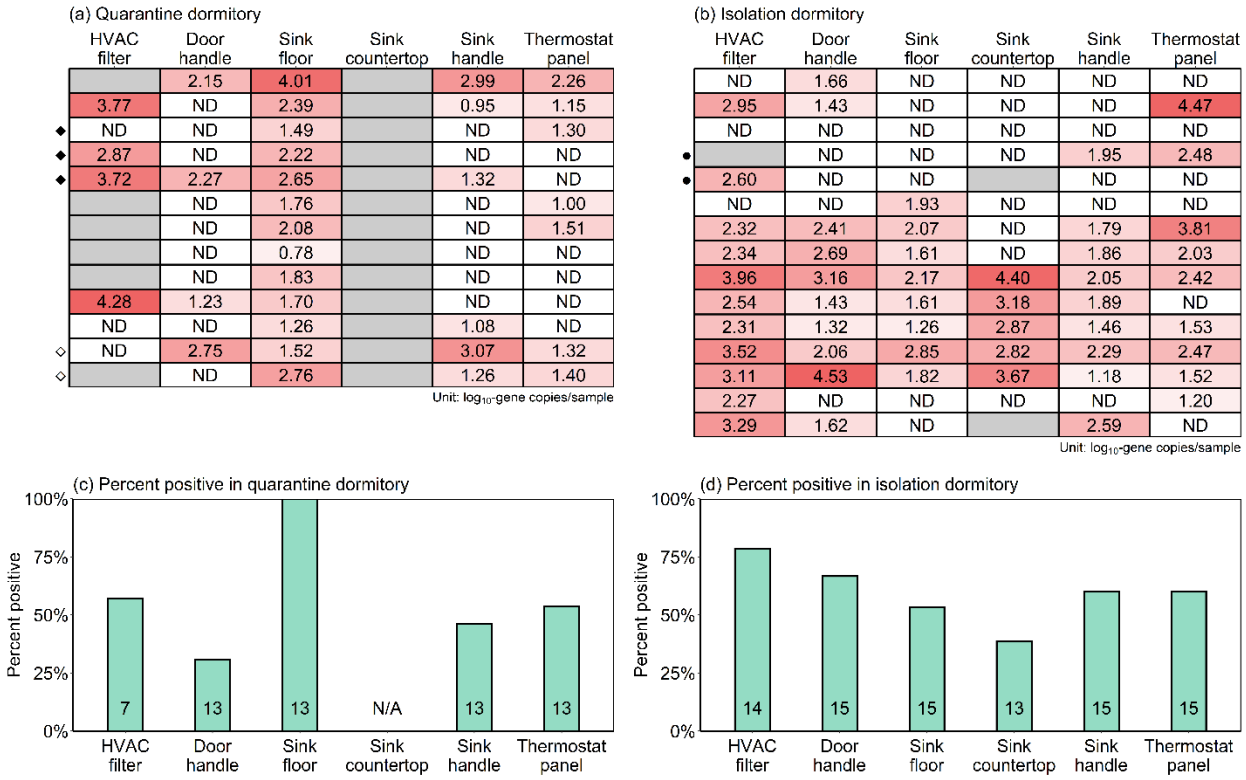

Figure 2-1. $\log_{10}$ SARS-CoV-2 RNA gene copies per swab or 3×8 cm^2 HVAC filter piece in the (a) quarantine dormitory and (b) isolation dormitory. Each row represents one room. Rows with shared symbols indicate that these rooms were the same room sampled at different points in time following occupancy by different individuals. Red shading indicates $\log_{10}$-gene copies per sample; white with "ND" means "not detected"; gray means "not collected" for the sink countertop or "not available" for the HVAC filters. Percentage of positive samples for each type of sampling site in the (c) quarantine dormitory and (d) isolation dormitory. The numbers at the bottom of each column indicate the number of samples.

The average duration of occupancy of the sampled rooms was 5 days (±3.6 days) in the quarantine dormitory and 9 days (±2.8 days) in the isolation dormitory. We might expect to find more virus in rooms that were occupied longer, but there were no significant correlations (Student's t-test, $p>0.05$) between duration and virus concentration in the quarantine dormitory (Figure S2). However, in the isolation dormitory, the viral RNA loadings on sink handle, sink countertop, and HVAC filters were negatively correlated with the occupancy duration (Student's t-test, $p<0.05$) (Figure S2). We speculated that the recovering students in the isolation rooms tended to shed less over time,[29] and the viral RNA shed at the earlier period of occupancy slightly degraded,[30] especially given that there were three individuals who spent 14 days in the isolation dormitory.

However, as the students in the quarantine rooms were most likely to be in the early or middle course of the infection, they would have shed higher amounts of virus even toward the end of their stay.

2.4.2. Detection of SARS-CoV-2 RNA from HVAC filters and exhaust grilles

We detected SARS-CoV-2 RNA on 4/7 (57.1%) HVAC filters in quarantine rooms and 11/14 (78.6%) HVAC filters in isolation rooms. Additionally, we observed high SARS-CoV-2 RNA concentrations (up to 10^4 gene copies per 3×8 cm^2 filter piece) on the HVAC filters (Figure 2-1, Figure 2-2. (a) Comparisons between quarantine and isolation dormitories by sampling site. (b) Comparisons among sampling sites in the same dormitory; HVAC filters were excluded from the comparison because they were eluted and quantified differently from surface samples. The letters below each site indicate similarities and differences between sites. Those with the same letter are not significantly different from each other, and those with different letters are significantly different from each other. Dashed lines represent the LOD.).

The presence of viral RNA on the HVAC filters indicated that virus was present in the air. Previous studies have found SARS-CoV-2 RNA on filters in the central HVAC system, distant from patients in a hospital.[14] Because the filter is not 100% efficient, some viral particles can penetrate the filter, enter the supply air ducts, and be recirculated.[14,16] There is also the possibility of re-entrainment of particles that had deposited on the filters, especially if there is a sudden change in air velocity in the system.[31] These results highlight the importance of additional research examining the role of HVAC systems in virus transmission.

We attempted to estimate the viral RNA concentration in the air from the filter results. The air flow rate through the filters was approximately 8495 L min^{-1} (300 ft^3 min^{-1}) in the quarantine rooms and 10,194 L min^{-1} (360 ft^3 min^{-1}) in the isolation rooms. If we assume that the HVAC systems were running half the time and that the filters were 50% efficient at capturing viral particles,[32] then the concentration of virus in the air ranged from 0.3 to 115 gene copies/m^3 of air in the quarantine rooms and from 0.2 to 24 gene copies/m^3 of air in the isolation rooms, with an average of 31 and 3 gene copies/m^3 of air, respectively. These estimates are within the range of concentrations of 0 to 10^3 RNA copies/m^3 of air reported in healthcare settings.[17,33,34] A study in a residential building

reported a much higher concentration of 5.69×10^4 gene copies/m^3 of air.[9] We expect these values to vary widely with the virus shedding rate of the occupant and the ventilation rate of the room. Of note, our estimates are very rough because the flow rate of the HVAC system in both dormitories was adjustable by the occupant, and the actual running times are not known.

SARS-CoV-2 RNA was also detected on public bathroom exhaust grilles in the quarantine dormitory, with a positivity of 4/6 (66.7%) and concentration up to $10^{2.7}$ gene copies per swabbed area (Table S1). These exhaust vents were likely contaminated by deposition of virus exhaled by bathroom users or other residents on the hallway. As the exhaust vent was located right above the toilets, fecal aerosols containing SARS-CoV-2 generated during flushing might have deposited on the grilles as well.[35]

2.4.3. Infectivity test

We attempted to culture those samples with a Ct value lower than 33, and none of them contained culturable virus. For reference, we have successfully cultured SARS-CoV-2 in respiratory aerosol particles freshly emitted by hamsters.[25] Thus far, most studies that attempted to detect viable viruses from environmental surfaces have not detected them, including samples from both healthcare and non-healthcare settings.[3,9,10,36-42] Santarpia et al. observed some evidence of replication of competent virus in a sample collected on the windowsill.[17] Our results indicate that SARS-CoV-2 decays within the amount of time between the student vacating the room and sampling in this study (ranging from 6 hours to 4 days). These results also suggest low possibility of fomite transmission even if high levels of SARS-CoV-2 RNA are present.

2.4.4. Comparisons of shedding to environment between early and middle-to-late infection stage

The quarantine dormitory likely housed students who were at an earlier stage of infection, whereas the isolation dormitory housed the students who were at a later stage. Since patients shed more virus earlier in the course of infection, especially for cases not requiring hospitalization,[34,43] we hypothesized that environmental contamination with virus would be higher in quarantine rooms than isolation rooms. However, we found no significant differences (Wilcoxon ranked sum test,

p>0.05) in viral RNA concentrations between quarantine and isolation rooms except on the floor (Wilcoxon ranked sum test, p<0.05) (Figure 2-2a), and the contrast is likely due to different flooring types: vinyl vs. carpet. We also found no significant differences (Wilcoxon ranked sum test, p>0.05) in the rate of positive samples between the two dormitories (Figure S3). However, this comparison is limited because we were not able to compare shedding from the same individual at different stages of infection. In addition, there were uncertainties regarding the timing of exposure and onset of symptoms for these students. Further study is required to elucidate the relationship between the course of disease and environmental contamination.

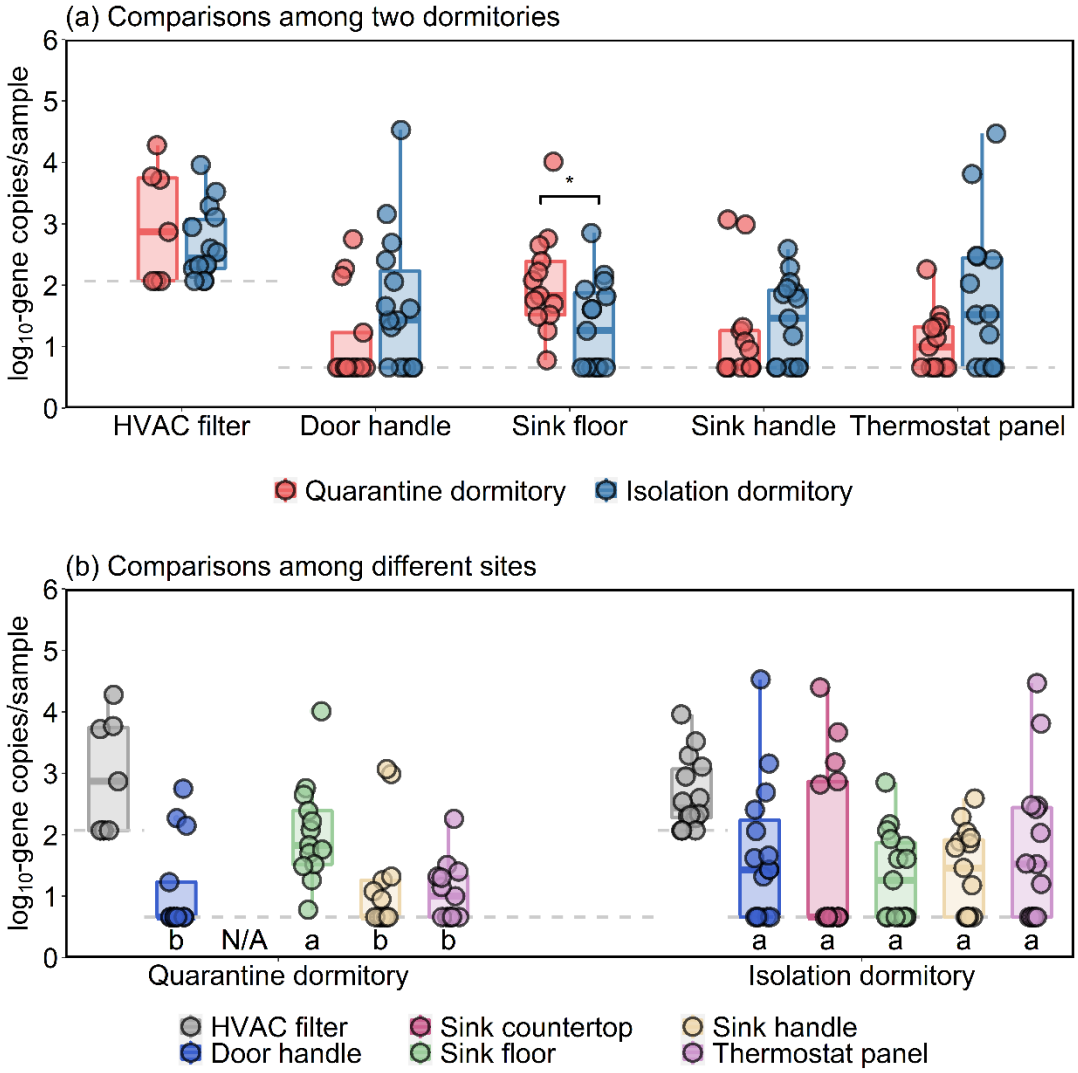

Figure 2-2. (a) Comparisons between quarantine and isolation dormitories by sampling site. (b) Comparisons among

sampling sites in the same dormitory; HVAC filters were excluded from the comparison because they were eluted and quantified differently from surface samples. The letters below each site indicate similarities and differences between sites. Those with the same letter are not significantly different from each other, and those with different letters are significantly different from each other. Dashed lines represent the LOD.

Acknowledgements

Virginia Tech's Center for Emerging, Zoonotic, and Arthropod-borne Pathogens, Fralin Life Sciences Institute, and Institute for Critical Technology and Applied Science provided support for this work. The authors thank Dr. Peter Vikesland and Dr. David Schmale at Virginia Tech for helpful discussions. The authors also thank Todd Pignataro and Kenneth Belcher for coordinating sampling in the dormitories.

Supporting information

MATERIALS AND METHODS

Quarantine and isolation procedures

Quarantined students received a COVID-19 test on day 8 after moving in, or sooner if they developed symptoms. The test results came back two days later, and only students who tested positive with no or mild symptoms transferred from the quarantine dorm to the isolation dorm. Then, the vacant rooms were sprayed with a disinfectant containing sodium dichloro-s-triazinetrione, and the HVAC filters were replaced. Quarantined students usually stayed in their rooms, but isolated students had leisure hours from 2:00 pm to 5:00 pm when they could leave the building and spend time in a fenced area outdoors.

Sampling sites

We sampled 5-6 sites per room, as shown in Figure S1.

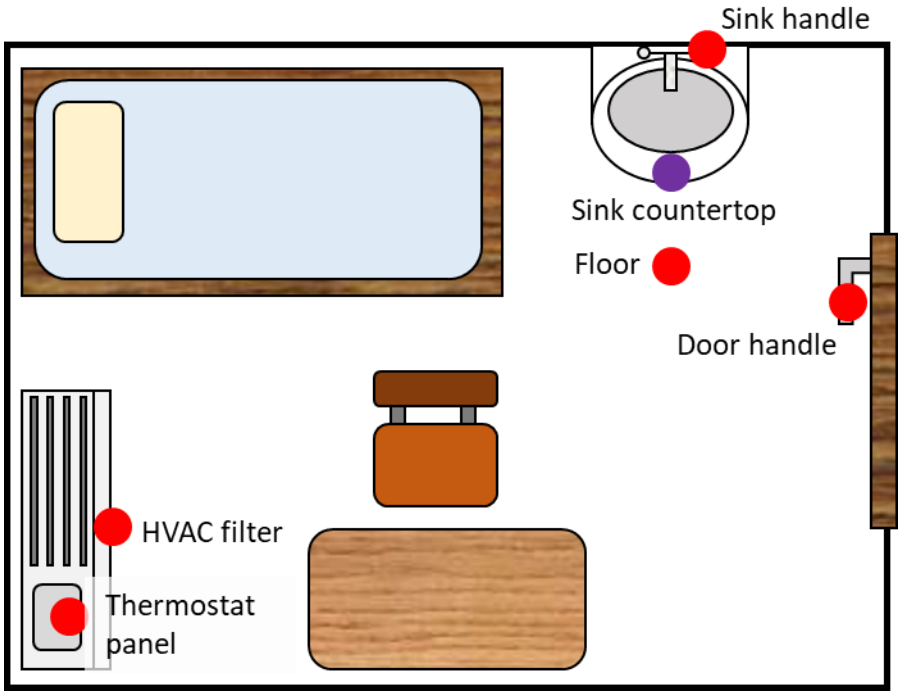

Figure S1. Schematic of sampling sites, highlighted by red dots. Of note, sink countertops were only sampled in the isolation dormitory rooms.

Recovery efficiency

While the efficiency of recovering SARS-CoV-2 from environmental surfaces remains an important factor to assess the data quality, this issue has been addressed in previous literature only sparsely for SARS-CoV-2 surveillance in the environment. This limitation is in part due to the difficulty of obtaining the same surface materials for laboratory-controlled experiments, as in our case, and in part due to safety concerns of conducting these experiments in the real environment. Garnett et al. have compared seven different swabs and reported a recovery efficiency of 22-68% when swabbing a sterile tray coated with 500 μL SARS-CoV-2 at concentrations of 5.5×10^{-4} to 5.5×10^{5} PFU/mL.[44] Another study spiked bovine respiratory syncytial virus (BRSV), a surrogate for SARS-CoV-2, into filter dust and floor dust and onto swabs, and found recovery efficiencies of 6%, 8%, and 25%, respectively.[7] As a reference, the recovery efficiency of BRSV from wastewater was 7.6%.[45] These data did not address the question of recovery efficiency from environmental surfaces, but they provide insight into underestimation of environmental contamination by SARS-CoV-2 due to losses during sample collection and processing. Interpretation of these results in the context of transmission should also consider the transfer efficiency from surfaces to human skin.

RT-qPCR methods

Each well (i.e. each RT-qPCR reaction) consisted of 5 μL RNA sample, 3.25 μL molecular grade water, 10 μL Master Mix and 0.25 μL reverse transcriptase (both from BioRad iTaq Universal Probes One-Step kit), and 1.5 μL 2019-nCoV RUO primer/probe. The RT-qPCR program consisted of initial conditions of 30 min at 55 °C and 15 min at 95 °C then 39 cycles of 95 °C for 15 s and 60 °C for 1 min. The lowest amplified point occurred at around 40 cycles consistently across all the plates, and the duplicates of the no-template control were always negative. Therefore, we averaged all standard curves and chose the average Ct value that represented the lowest amplified point as the LOD, which equaled 0.2 gc/reaction, or 9.4 gc per swab and 114 gc per 3×8 cm^2 filter piece. We ran 11 plates for a total of 152 samples.

RESULTS AND DISCUSSION

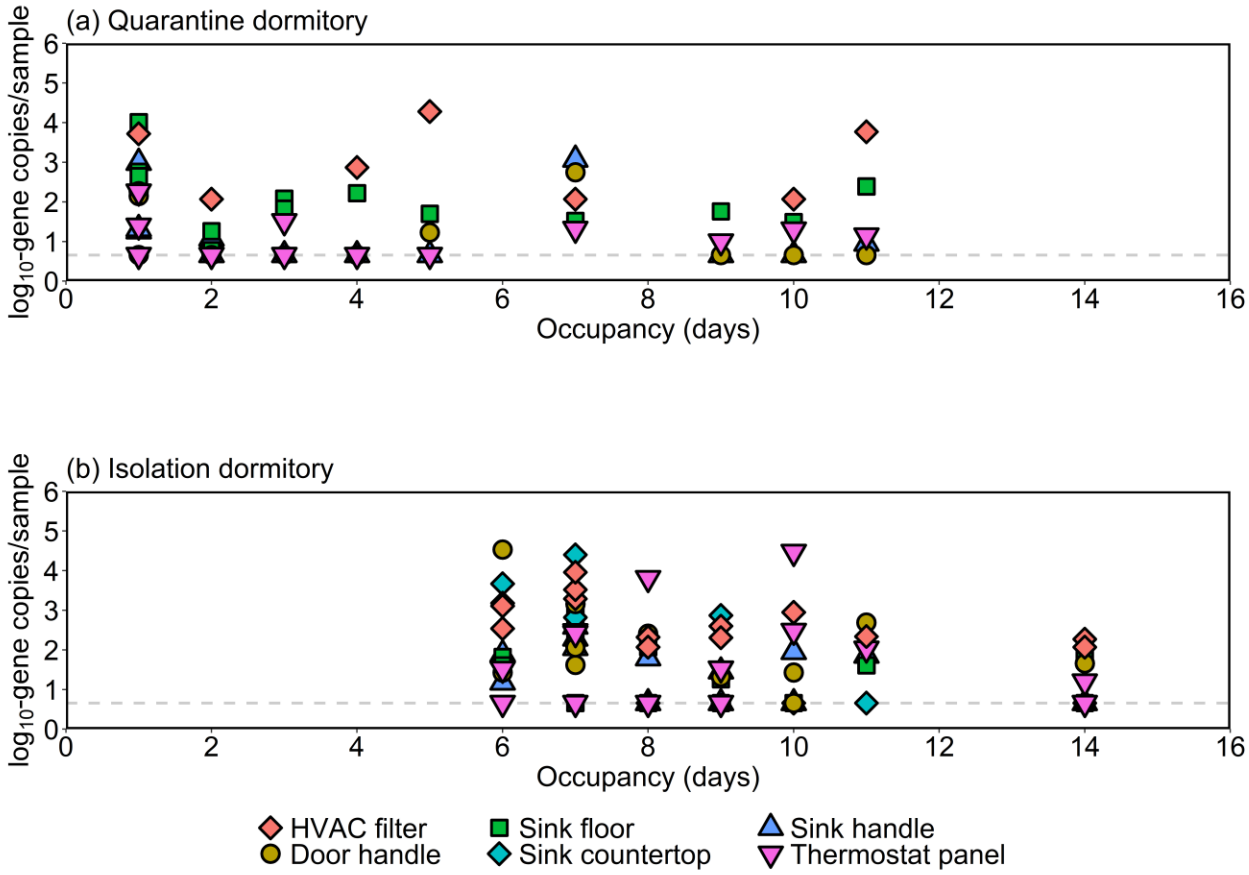

Figure S2. Gene copies per sample versus duration of occupancy in the (a) quarantine and (b) isolation dormitories.

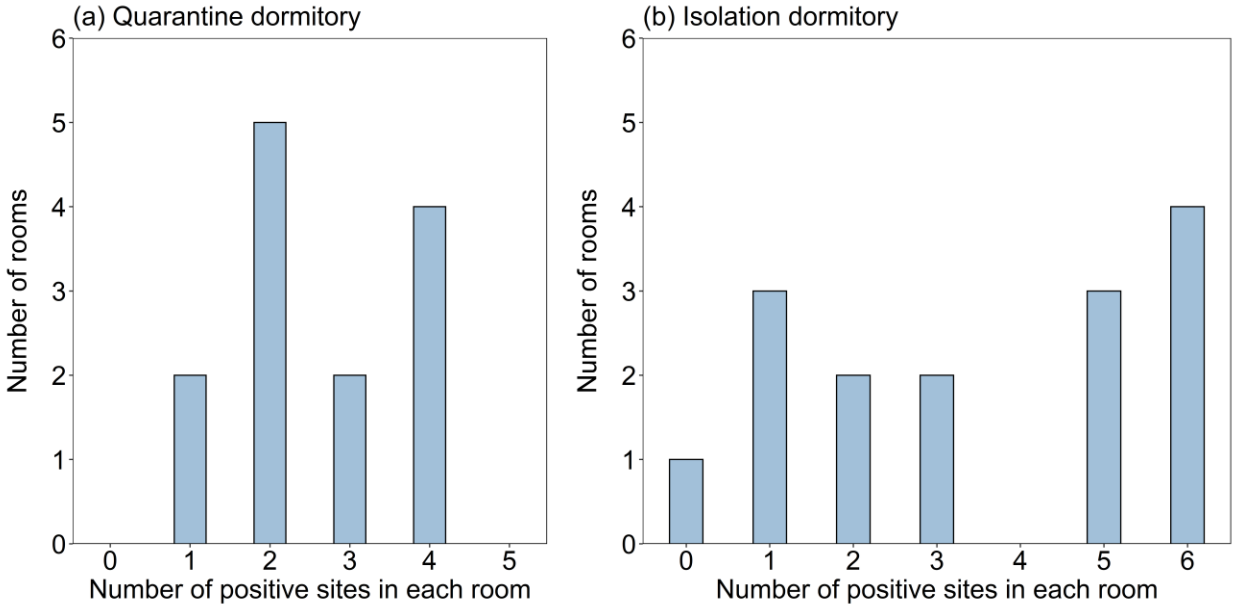

Figure S3. The frequencies of the number of positive sites in the (a) quarantine and (b) isolation dormitories. The number of sampling sites in each room varied from 4 to 5 in the quarantine dormitory and 5 to 6 in the isolation dormitory. We compared these two distributions after converting the number to the rate of positive sites to account for the differences in sample size.

Table S1. SARS-CoV-2 RNA concentration on the exhaust grilles collected from four public bathrooms in the quarantine dormitory.

Bathroom #	Date	Log_{10}-gene copies/sample
Bathroom 1	2/24/2021	2.7
	3/5/2021	2.6
Bathroom 2	2/24/2021	Not detected
	3/5/2021	1.9
Bathroom 3	3/3/2021	2.6
Bathroom 4	3/3/2021	Not detected

References

1. Onakpoya IJ, Heneghan CJ, Spencer EA, et al. SARS-CoV-2 and the role of fomite transmission: a systematic review. *F1000Res.* 2021;10:233-233.
2. Bedrosian N, Mitchell E, Rohm E, et al. A Systematic Review of Surface Contamination, Stability, and Disinfection Data on SARS-CoV-2 (Through July 10, 2020). *Environmental Science & Technology.* 2021;55(7):4162-4173.
3. Ben-Shmuel A, Brosh-Nissimov T, Glinert I, et al. Detection and infectivity potential of severe acute respiratory syndrome coronavirus 2 (SARS-CoV-2) environmental contamination in isolation units and quarantine facilities. *Clinical Microbiology and Infection.* 2020;26(12):1658-1662.
4. Hu X, Xing Y, Ni W, et al. Environmental contamination by SARS-CoV-2 of an imported case during incubation period. *Science of The Total Environment.* 2020;742:140620.
5. Jiang F-C, Jiang X-L, Wang Z-G, et al. Detection of Severe Acute Respiratory Syndrome Coronavirus 2 RNA on Surfaces in Quarantine Rooms. *Emerging infectious diseases.* 2020;26(9):2162-2164.
6. Lee S-E, Lee D-Y, Lee W-G, et al. Detection of Novel Coronavirus on the Surface of Environmental Materials Contaminated by COVID-19 Patients in the Republic of Korea. *Osong Public Health Res Perspect.* 2020;11(3):128-132.
7. Maestre JP, Jarma D, Yu J-RF, Siegel JA, Horner SD, Kinney KA. Distribution of SARS-CoV-2 RNA signal in a home with COVID-19 positive occupants. *Science of The Total Environment.* 2021;778:146201.
8. Wong JC, Hapuarachchi HC, Arivalan S, et al. Environmental Contamination of SARS-CoV-2 in a Non-Healthcare Setting. *International Journal of Environmental Research and Public Health.* 2021;18(1).
9. Nannu Shankar S, Witanachchi CT, Morea AF, et al. SARS-CoV-2 in residential rooms of two self-isolating persons with COVID-19. *Journal of Aerosol Science.* 2022;159:105870.
10. Döhla M, Wilbring G, Schulte B, et al. SARS-CoV-2 in environmental samples of quarantined households. *medRxiv.* 2020:2020.2005.2028.20114041.
11. Liu J, Liu J, He Z, et al. Duration of SARS-CoV-2 positive in quarantine room environments: A perspective analysis. *International Journal of Infectious Diseases.* 2021;105:68-74.
12. Harvey AP, Fuhrmeister ER, Cantrell ME, et al. Longitudinal Monitoring of SARS-CoV-2 RNA on High-Touch Surfaces in a Community Setting. *Environmental Science & Technology Letters.* 2021;8(2):168-175.
13. Guo Z-D, Wang Z-Y, Zhang S-F, et al. Aerosol and Surface Distribution of Severe Acute Respiratory Syndrome Coronavirus 2 in Hospital Wards, Wuhan, China, 2020. *Emerging infectious diseases.* 2020;26(7):1583-1591.
14. Horve PF, Dietz LG, Fretz M, et al. Identification of SARS-CoV-2 RNA in healthcare heating, ventilation, and air conditioning units. *Indoor Air.* 2021;n/a(n/a).
15. Mouchtouri VA, Koureas M, Kyritsi M, et al. Environmental contamination of SARS-CoV-

2 on surfaces, air-conditioner and ventilation systems. *International Journal of Hygiene and Environmental Health.* 2020;230:113599.
16. Nissen K, Krambrich J, Akaberi D, et al. Long-distance airborne dispersal of SARS-CoV-2 in COVID-19 wards. *Scientific Reports.* 2020;10(1):19589.
17. Santarpia JL, Rivera DN, Herrera VL, et al. Aerosol and surface contamination of SARS-CoV-2 observed in quarantine and isolation care. *Scientific Reports.* 2020;10(1):12732.
18. Prussin AJ, II, Vikram A, Bibby KJ, Marr LC. Seasonal Dynamics of the Airborne Bacterial Community and Selected Viruses in a Children's Daycare Center. *PLOS ONE.* 2016;11(3):e0151004.
19. Goyal SM, Anantharaman S, Ramakrishnan MA, et al. Detection of viruses in used ventilation filters from two large public buildings. *American Journal of Infection Control.* 2011;39(7):e30-e38.
20. Bunning ML, Bowen RA, Cropp CB, et al. Experimental infection of horses with West Nile virus. *Emerging infectious diseases.* 2002;8(4):380-386.
21. Lu X, Wang L, Sakthivel SK, et al. US CDC real-time reverse transcription PCR panel for detection of severe acute respiratory syndrome coronavirus 2. *Emerging infectious diseases.* 2020;26(8):1654.
22. Huang Z, Tian D, Liu Y, et al. Ultra-sensitive and high-throughput CRISPR-p owered COVID-19 diagnosis. *Biosensors and Bioelectronics.* 2020;164:112316.
23. La Scola B, Le Bideau M, Andreani J, et al. Viral RNA load as determined by cell culture as a management tool for discharge of SARS-CoV-2 patients from infectious disease wards. *Eur J Clin Microbiol Infect Dis.* 2020;39(6):1059-1061.
24. Poole-Smith BK, Hemme RR, Delorey M, et al. Comparison of Vector Competence of Aedes mediovittatus and Aedes aegypti for Dengue Virus: Implications for Dengue Control in the Caribbean. *PLOS Neglected Tropical Diseases.* 2015;9(2):e0003462.
25. Hawks Seth A, Prussin Aaron J, Kuchinsky Sarah C, et al. Infectious SARS-CoV-2 Is Emitted in Aerosol Particles. *mBio.*12(5):e02527-02521.
26. Renninger N, Nastasi N, Bope A, et al. Indoor Dust as a Matrix for Surveillance of COVID-19. *mSystems.*6(2):e01350-01320.
27. Hu J, Lei C, Chen Z, et al. Distribution of airborne SARS-CoV-2 and possible aerosol transmission in Wuhan hospitals, China. *National Science Review.* 2020;7(12):1865-1867.
28. Yeargin T, Fraser A, Huang G, Jiang X. Recovery and Disinfection of Two Human Norovirus Surrogates, Feline Calicivirus and Murine Norovirus, from Hard Nonporous and Soft Porous Surfaces. *Journal of Food Protection.* 2015;78(10):1842-1850.
29. Sun J, Tang X, Bai R, et al. The kinetics of viral load and antibodies to SARS-CoV-2. *Clinical Microbiology and Infection.* 2020;26(12):1690.e1691-1690.e1694.
30. Paton S, Spencer A, Garratt I, et al. Persistence of Severe Acute Respiratory Syndrome Coronavirus 2 (SARS-CoV-2) Virus and Viral RNA in Relation to Surface Type and Contamination Concentration. *Applied and Environmental Microbiology.*87(14):e00526-00521.
31. Jankowska E, Reponen T, Willeke K, Grinshpun SA, Choi K-J. Collection of fungal spores

on air filters and spore reentrainment from filters into air. *Journal of Aerosol Science.* 2000;31(8):969-978.
32. Azimi P, Zhao D, Stephens B. Estimates of HVAC filtration efficiency for fine and ultrafine particles of outdoor origin. *Atmospheric Environment.* 2014;98:337-346.
33. Chia PY, Coleman KK, Tan YK, et al. Detection of air and surface contamination by SARS-CoV-2 in hospital rooms of infected patients. *Nature Communications.* 2020;11(1):2800.
34. Liu Y, Yan L-M, Wan L, et al. Viral dynamics in mild and severe cases of COVID-19. *The Lancet Infectious Diseases.* 2020;20(6):656-657.
35. Dancer SJ, Li Y, Hart A, Tang JW, Jones DL. What is the risk of acquiring SARS-CoV-2 from the use of public toilets? *Science of The Total Environment.* 2021;792:148341.
36. Yamagishi T, Ohnishi M, Matsunaga N, et al. Environmental Sampling for Severe Acute Respiratory Syndrome Coronavirus 2 During a COVID-19 Outbreak on the Diamond Princess Cruise Ship. *J Infect Dis.* 2020;222(7):1098-1102.
37. Wang J, Feng H, Zhang S, et al. SARS-CoV-2 RNA detection of hospital isolation wards hygiene monitoring during the Coronavirus Disease 2019 outbreak in a Chinese hospital. *Int J Infect Dis.* 2020;94:103-106.
38. Zhou J, Otter JA, Price JR, et al. Investigating SARS-CoV-2 surface and air contamination in an acute healthcare setting during the peak of the COVID-19 pandemic in London. *Clinical Infectious Diseases.* 2020.
39. Ong SWX, Tan YK, Chia PY, et al. Air, Surface Environmental, and Personal Protective Equipment Contamination by Severe Acute Respiratory Syndrome Coronavirus 2 (SARS-CoV-2) From a Symptomatic Patient. *JAMA.* 2020;323(16):1610-1612.
40. Moore G, Rickard H, Stevenson D, et al. Detection of SARS-CoV-2 within the healthcare environment: a multi-centre study conducted during the first wave of the COVID-19 outbreak in England. *Journal of Hospital Infection.* 2021;108:189-196.
41. Colaneri M, Seminari E, Novati S, et al. Severe acute respiratory syndrome coronavirus 2 RNA contamination of inanimate surfaces and virus viability in a health care emergency unit. *Clin Microbiol Infect.* 2020;26(8):1094.e1091-1094.e1095.
42. Kampf G, Pfaender S, Goldman E, Steinmann E. SARS-CoV-2 Detection Rates from Surface Samples Do Not Implicate Public Surfaces as Relevant Sources for Transmission. *Hygiene.* 2021;1(1).
43. Zou L, Ruan F, Huang M, et al. SARS-CoV-2 Viral Load in Upper Respiratory Specimens of Infected Patients. *New England Journal of Medicine.* 2020;382(12):1177-1179.
44. Garnett L, Bello A, Tran KN, et al. Comparison analysis of different swabs and transport mediums suitable for SARS-CoV-2 testing following shortages. *Journal of Virological Methods.* 2020;285:113947.
45. Gonzalez R, Curtis K, Bivins A, et al. COVID-19 surveillance in Southeastern Virginia using wastewater-based epidemiology. *Water Research.* 2020;186:116296.

3. Inward and outward effectiveness of cloth masks, a surgical mask, and a face shield

Jin Pan, Charbel Harb, Weinan Leng, Linsey C. Marr*

Civil and Environmental Engineering, Virginia Tech, Blacksburg, VA 24061

*Corresponding author: lmarr@vt.edu

Keywords: masks, aerosol, transmission, COVID-19, SARS-CoV-2, face coverings

Reprinted with permission from Pan, J., Harb, C., Leng, W., & Marr, L. C. (2021). Inward and outward effectiveness of cloth masks, a surgical mask, and a face shield. *Aerosol Science and Technology*, 55(6), 718-733.

3.1. Abstract

We evaluated the effectiveness of 11 face coverings for material filtration efficiency, inward protection efficiency on a manikin, and outward protection efficiency on a manikin. At the most penetrating particle size, the vacuum bag, microfiber cloth, and single-layer surgical-type mask had material filtration efficiencies >50%, while the other materials had much lower filtration efficiencies. However, these efficiencies increased rapidly with particle size, and many materials had efficiencies >50% at 2 μm and >75% at 5 μm. The vacuum bag performed best, with efficiencies of 54-96% for all three metrics, depending on particle size. The thin acrylic and face shield performed worst. Inward protection efficiency and outward protection efficiency, defined for close-range, face-to-face interactions, were similar for many masks; the two efficiencies diverged for stiffer materials and those worn more loosely (e.g., bandana) or more tightly (e.g., wrapped around the head) compared to an earloop mask. Discrepancies between material filtration efficiency and inward/outward protection efficiency indicated that the fit of the mask was important. We calculated that the particle size most likely to deposit in the respiratory tract when wearing a mask is ~2 μm. Based on these findings, we recommend a three-layer mask consisting of outer layers of a flexible, tightly woven fabric and an inner layer consisting of a material designed to filter out particles. This combination should produce an overall efficiency of >70% at the most penetrating particle size and >90% for particles 1 μm and larger if the mask fits well.

3.2. Introduction

Amid mounting evidence that COVID-19 is transmitted via inhalation of virus-laden aerosols, [1-5] universal masking has emerged as one of a suite of intervention strategies for reducing community transmission of the disease.[6] There is a correlation between widespread mask wearing,[7] or at least interest in masks,[8] and lower incidence of COVID-19 by country and between mask mandates and county-level COVID-19 growth rates in the US,[9] but a causal relationship has not been confirmed.

Due to a shortage of medical masks and respirators, some public health agencies have recommended the use of cloth face coverings. While there have been numerous studies on the ability of surgical masks and N95 respirators to filter out particles, less is known about the ability of cloth masks to provide both inward protection for reducing the wearer's exposure and outward protection for source control. In response to the pandemic, there has been a spate of studies on the filtration efficiency of different materials, but how this translates to both inward and outward protection over a wide range of particle sizes is not well known.

Reviews on the use of masks in both healthcare and non-healthcare settings to reduce transmission of other respiratory diseases mostly show a protective effect. A systematic review and meta-analysis of interventions against respiratory viruses found that wearing simple masks was highly effective at reducing transmission of severe acute respiratory syndrome (SARS) in five case control studies.[10] In contrast, a review of 10 randomized controlled trials of mask wearing in non-healthcare settings concluded that there was not a substantial effect on influenza transmission in terms of risk ratio, although most of the studies were underpowered and compliance was not perfect.[11] A systematic review of interventions against SARS-CoV-2 and the coronaviruses that cause SARS and Middle East respiratory syndrome found that the use of face masks could result in a large reduction in the risk of infection.[12]

Laboratory studies have demonstrated the ability of surgical masks to provide both inward and outward protection against viruses. Testing of eight different surgical masks on a manikin with influenza virus in droplets/aerosols of size 1–200 μm found that the amount of virus detected

behind the mask was reduced by an average of 83%, with a range of 9% to 98%.[13] The ability of a mask to block influenza virus was correlated with its ability to block droplets/aerosols containing only phosphate buffered saline (PBS) and bovine serum albumin (BSA). Surgical masks used for source control on influenza patients during breathing and coughing reduced the amount of virus released into the air in coarse (> 5 μm) and fine (≤ 5 μm) aerosols by 96% and 64%, respectively.[14] In a follow-up study, surgical masks blocked the release of seasonal coronaviruses in coarse and fine aerosols to undetectable levels, while they blocked influenza virus in most but not all patients.[15]

There have been some studies of cloth masks, which have been found to be less protective than surgical masks in most, but not all, cases. A variety of cloth materials mounted in a filter holder removed 49% to 86% of aerosolized bacteriophage MS2, compared to 89% removal by a surgical mask.[13] According to fit tests on 21 adults in the same study, homemade, 100% cotton masks provided median inward filtration efficiencies of 50%, compared to 80% for surgical masks. Homemade masks made from tea cloths and worn by volunteers had a median inward filtration efficiency of 60%, compared to 76% for a surgical mask.[16]

Several recent studies have evaluated the filtration efficiency of different materials and the ability of different types of face coverings to block cough-generated particles. The filtration efficiencies of 44 materials and medical masks, challenged with sodium chloride (NaCl) particles of diameter 0.03–0.25 μm, ranged from <10% for polyurethane foam to nearly 100% for a vacuum cleaner bag.[17] Other studies involving NaCl test particles have also found a wide range of material filtration efficiencies for common fabrics, including cotton, polyester, nylon, and silk; many materials had low filtration efficiencies for submicron particles.[18-21] Pieces of a bandana, veil, shawl, handkerchief, and cotton t-shirt mounted in a filter holder and challenged with volcanic ash particles were found to have filtration efficiencies of 18% to 43% in terms of mass concentration.[22] A study involving particles generated by coughing human subjects reported an outward protection efficiency of 77% at a distance of 0.3 m from the source for a cloth mask, but only 4% for a face shield.[23] Similarly, a study of outward protection efficiency using simulated coughs found that a

three-ply cotton mask, single-layer polyester neck gaiter, double-layer polyester neck gaiter, and face shield blocked 51%, 47%, 60%, and 2% of particles, respectively.[24]

N95 respirators and cloth masks serve different purposes, so the testing procedure for N95s is not necessarily well-suited for cloth masks. An N95 must be able to protect an individual worker in high-risk situations. A critical component of its efficacy is the fit test to ensure that the respirator seals completely to the face with no leaks. On the other hand, the overall goal of wearing cloth masks during the COVID-19 pandemic is to reduce community transmission. Cloth masks provide some degree of both source control and exposure reduction. While an N95 must block at least 95% of NaCl particles of the most penetrating size, 0.3 μm, cloth masks can be effective if they remove at least some particles, particularly those of the size that is most relevant for transmission. Although we do not yet know which size particles are most important, we can make some inferences from existing studies. SARS-CoV-2 and other viruses are carried by particles ranging in size from <1 μm to >5 μm.[12,25-27] A SARS-CoV-2 virion is 0.1 μm in diameter, but it is carried in respiratory droplets that also contain salts, proteins, and other components of respiratory fluid. Even if all the water evaporates, the mass of the non-volatile components is expected to be orders of magnitude larger than that of any viruses that might be present,[28] so the size of a particle carrying an intact virus must be quite a bit larger than 0.1 μm. The smaller mode of respiratory particles produced during breathing and speaking is centered around 1 μm, and there are relatively few particles smaller than 0.5 μm.[29] Influenza transmission between ferrets has been shown to be mediated by particles larger than 1.5 μm.[30] Thus, it seems prudent to evaluate mask performance over a range of particle sizes, particularly those larger than 0.3 μm.

Given the advice of public health agencies for the general public to wear face coverings and the paucity of knowledge about their effectiveness, the objective of this study is to evaluate the efficiency of cloth masks compared to a surgical mask and a face shield at blocking particles over a wide range of sizes. We first measure the filtration efficiency of materials under ideal conditions and then investigate both inward and outward protection efficiency of the materials when worn as masks on a manikin. We expect that efficiency on a manikin will be lower than in a filter holder

due to leakage around the mask and that outward efficiency will be higher than inward efficiency due to differences in velocity of the particles as they approach the material. The results of this study will contribute to understanding how universal masking might reduce transmission of COVID-19 and other respiratory diseases.

3.3. Methods

3.3.1. Masks

We tested nine materials that were fashioned into masks, one surgical mask, and one face shield, shown in Figure 3-1. To make the masks, we cut materials into 15.5 cm × 10 cm rectangles and securely taped them to a frame tailored from a procedure mask, except for two designs that followed instructions from the US Centers for Disease Control and Prevention (CDC). These included a sewn mask made of two layers of a 200-thread count cotton pillowcase and a non-sewn mask cut from a cotton t-shirt.[31] The instructions for the non-sewn mask used in this study have been supplanted with an updated design involving a large square of fabric and rubber bands. For masks with earloops, we secured the loops around the manikin's ears using pins to hold them in place. We did not tape the face coverings to the manikin's face. The surgical-type mask, technically a procedure mask, had a single layer and was advertised to meet ASTM level 1 specifications, which require ≥95% filtration efficiency of particles larger than 1 μm. We characterized the texture and structure of the masks using a scanning electron microscope (FEI Quanta 600 FEG). Because it is not possible to generate or characterize particles spanning a wide range of sizes with a single experimental setup, we designed several different protocols for testing masks, optimizing among different types of equipment and detection limits, as described below.

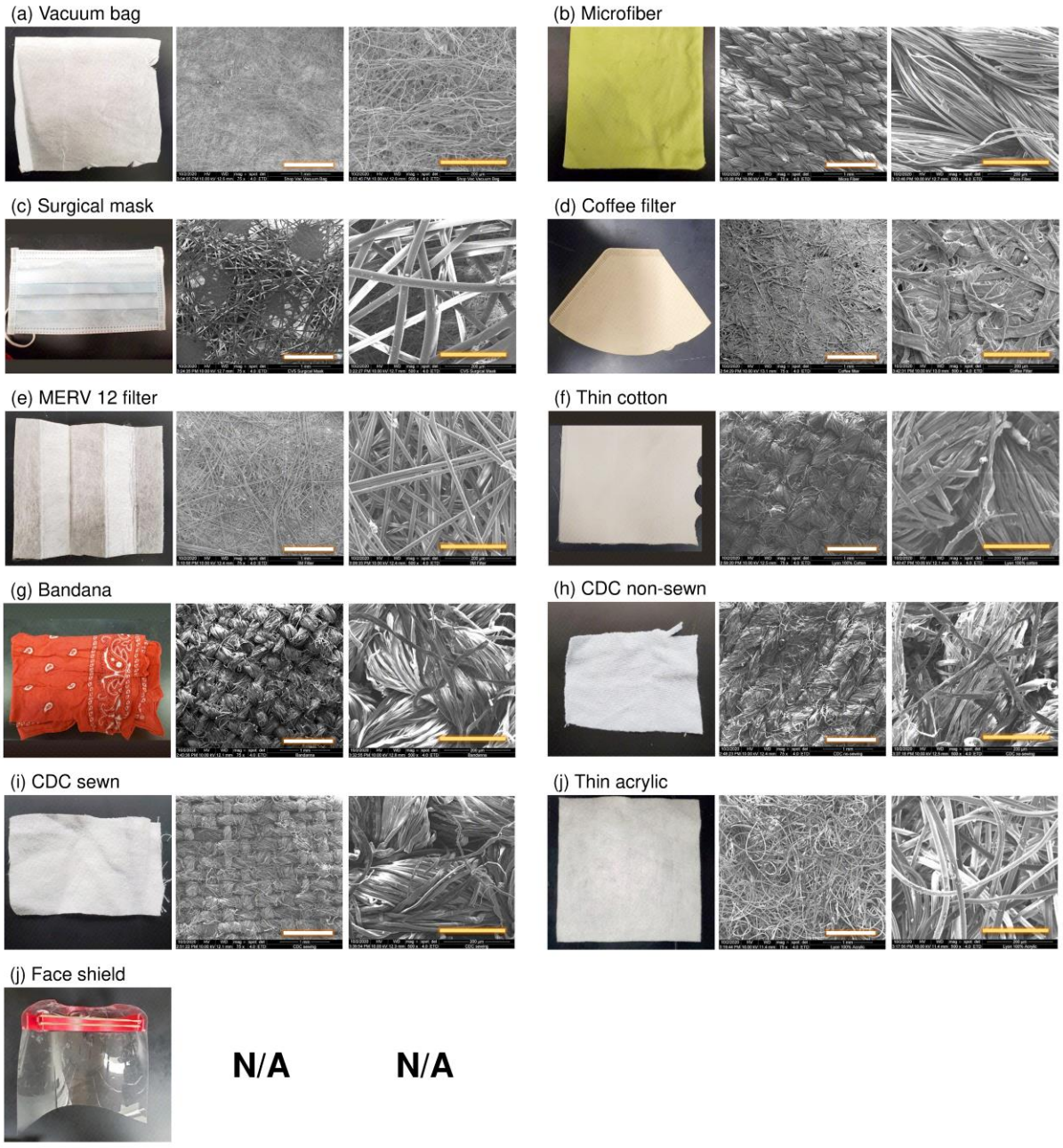

Figure 3-1. Ten mask materials and a face shield. All materials have a single layer except the thin cotton, which has two layers. SEM images are shown at two scales: the white scale bar represents 1 mm and the yellow one represents 200 μm. There are no SEM images for the face shield, which was made of a plastic sheet.

3.3.2. Material filtration efficiency

Evaluation of the materials for filtration efficiency followed a protocol based on National Institute of Occupational Safety and Health (NIOSH) testing procedures. Using a Collison 3-jet

nebulizer (BGI MRE-3, BGI Inc., MA, USA), we generated challenge particles of size 0.04 to 1 μm from a 2% NaCl solution. The particles filled a 280 L polyethylene chamber (Sigma AtmosBag, Sigma–Aldrich, ON, Canada), in which we placed a small fan to promote mixing. The temperature and humidity inside the chamber were 22 °C and 25-35% RH, respectively. We measured particle concentrations and size distributions over the range from 0.04 to 1 μm using a scanning mobility particle sizer (SMPS 3936, TSI Inc., MN, USA), with the particle density set to 2.165 g/cm^3 (NaCl) to convert from mobility diameter to aerodynamic diameter.

We cut out circular pieces of each material to mount in a 25 mm stainless steel filter holder (Advantec, Cole Parmer, IL, USA) that was connected to a vacuum line whose flow rate was maintained at 2.7 L/min by a mass flow controller (32907-53, Cole Parmer, IL, USA). The SMPS sampled from this line at a rate of 0.3 L/min, producing a total flow rate of 3.0 L/min and a corresponding face velocity of 10 cm/s through the material. Clean make-up air flow to the chamber was provided through a high-efficiency particulate air filter capsule (12144, Pall Corporation, MA, USA). We checked the material filtration efficiency of an N95 respirator and the microfiber cloth with and without a Kr-85 radioactive neutralizer (3012, TSI Inc., MN, USA) or soft x-ray neutralizer (XRC-05, HCT CO., Ltd, Republic of Korea) after the nebulizer, and did not find significant differences (Figures S1-S3), so we did not employ a neutralizer in subsequent tests. To calculate the size-resolved filtration efficiency, we compared measurements with the material in the filter holder to those made with an empty filter holder, as shown in equation (3-1), where FE is the material filtration efficiency; D_P is the particle diameter; C_{blank} is the concentration of challenge particles measured downstream of the empty filter holder, and $C_{material}$ is the concentration of particles downstream of the material:

$$FE(D_P) = \left(1 - \frac{C_{material}(D_P)}{C_{blank}(D_P)}\right) \times 100\% \quad (3\text{-}1)$$

For C_{blank}, we used the average of measurements conducted immediately before and after testing each material; these measurements differed by less than 10%. We conducted these experiments in triplicate using three different pieces cut from each material.

In addition to challenging the masks with submicron particles generated by the Collison

nebulizer, we also tested larger particles ranging in size from 2 to 5 μm. We generated these from a 2% NaCl solution using a flow focusing monodisperse aerosol generator (FMAG, TSI Inc., MN, USA). We measured the particles using an aerodynamic particle sizer spectrometer (APS 3321, TSI Inc., MN, USA), which covers the size range from 0.5 to 20 μm. Because the APS samples at a flow rate of 1.0 L/min, we adjusted the vacuum line to 2.0 L/min to produce a total flow rate of 3.0 L/min, the same as used for testing smaller particles. Clean make-up air was also applied as described above. We calculated the filtration efficiency according to equation (1) in triplicate. We also measured the pressure drop of each material in the filter holder using a differential pressure gauge (Minihelic II 2-5005, Dwyer Instruments, IN, USA).

3.3.3. Inward and outward protection efficiency at close distance

We evaluated both inward protection efficiency (*IPE*) for the ability to reduce the wearer's exposure and outward protection efficiency (*OPE*) for source control using two manikins mounted on opposite sides of a 57-L acrylic chamber (51 cm × 34 cm × 33 cm), mimicking the situation of close talking with a mouth-to-mouth distance of 33 cm (Figure 3-2a, b). Due to constraints of the experimental setup, the *IPE* and *OPE* should be interpreted to apply in the face-to-face direction at 33 cm distance. The *IPE* combines the effects of filtration and reduction in exposure to a respiratory plume directed at the wearer, and the *OPE* combines the effects of filtration and reduction in exposure resulting from the diversion of flow by the face covering. Thus, the *IPE* and *OPE* are indicators of protection afforded to the wearer and source control, respectively, but are not necessarily generalizable to all conditions.

The "exhaling" manikin was connected to a medical nebulizer (AIRIAL) filled with 2% NaCl solution, that produced a flow rate of 5.3 L/min through 0.79 cm i.d. tubing. The "inhaling" manikin was connected to both the APS and a vacuum line, with flow rates of 1 L/min and 14 L/min, respectively, resulting in a total flow rate of 15 L/min through 1 cm i.d. tubing. The air velocity at both manikin's mouths was 3.2–3.4 m/s, similar to that of breathing and talking.[32,33] Make-up air entered the chamber around the top perimeter, to minimize disruption to air flow that might be introduced by a port. At a flow rate of 5 L/min, the average downward velocity would be

0.05 cm/s, so downward motion of the aerosols is expected to be negligible during their brief transit time between the manikins. The make-up air had a background particle concentration of at most 0.5% (around 50 #/cm^3 for particles detectable by the APS) of that generated in the chamber by the nebulizer. We also estimated the impact of losses due to particle settling. If the exhaling manikin was maskless, then the aerosol flow travelled in a jet directly toward the inhaling manikin. We calculated that it would take less than 1 s for particles along the centerline to travel between the two manikins, while it would take 60 seconds for 5-μm particles to settle from this height to the bottom of the chamber. If the exhaling manikin was masked, then the travel time would be longer for particles that escaped sideways from the mask and were then pulled toward the inhaling manikin, but we still expect settling losses to be minor in this system. The relatively small size of the chamber introduced physical constraints to the aerosol flow but was required for concentrations to be maintained above the limit of detection, particularly for the larger particles. To minimize losses of particles, we used conductive tubing in lengths as short as possible.

To evaluate inward protection efficiency, we attached face coverings to the inhaling manikin (Figure 3-2a, Figure S4) and tested two scenarios. In scenario 1, we ran the medical nebulizer for 3 s through the exhaling manikin, generating particles of size 0.5–2 μm. Using a three-way valve, we set up the APS to sample either through the inhaling manikin's mouth or through tubing whose inlet was placed outside the face covering, near the manikin's mouth. The flow rate through the inhaling manikin remained constant at 15 L/min. We then waited 30 s for particle concentrations to decay below the upper limit of detection of the APS, switched the valve to sample from outside the mask, and measured the size distribution in the chamber for 5 s, denoted C_{c1}. We then switched the valve so that the APS sampled through the inhaling manikin's mouth and measured particles that penetrated the mask, denoted C_m. We discarded the measurements for 1 s after each switch to allow for flushing of the tubing, to avoid interference among C_{c1}, C_{c2}, and C_m. To account for the continually decaying particle concentration in the chamber, we then switched back to measuring particles in the chamber again, denoted as C_{c2}. The difference between C_{c1} and C_{c2} was less than 10% in all cases. Therefore, we used the average of C_{c1} and C_{c2} to represent C_c at the time when

we measured C_m. We calculated the inward protection efficiency based on equation (3-1). The temperature and humidity inside the chamber were 22 °C and 50–70% RH, respectively. In a separate experiment, we demonstrated that the three-way valve and the location of sampling inlets did not bias the calculation. There was no difference in the concentration and size distribution of particles whether the APS sampled directly from the chamber or through the inhaling manikin without the mask. Measurements in scenario 2 followed a similar protocol as in scenario 1 except that the medical nebulizer ran for 30 s instead of 3 s to generate larger particles, up to 5 μm, thanks to coagulation.

$$IPE(D_P) = \left(1 - \frac{C_m(D_P)}{\frac{C_{c1}(D_P) + C_{c2}(D_P)}{2}}\right) \times 100\% \tag{3-2}$$

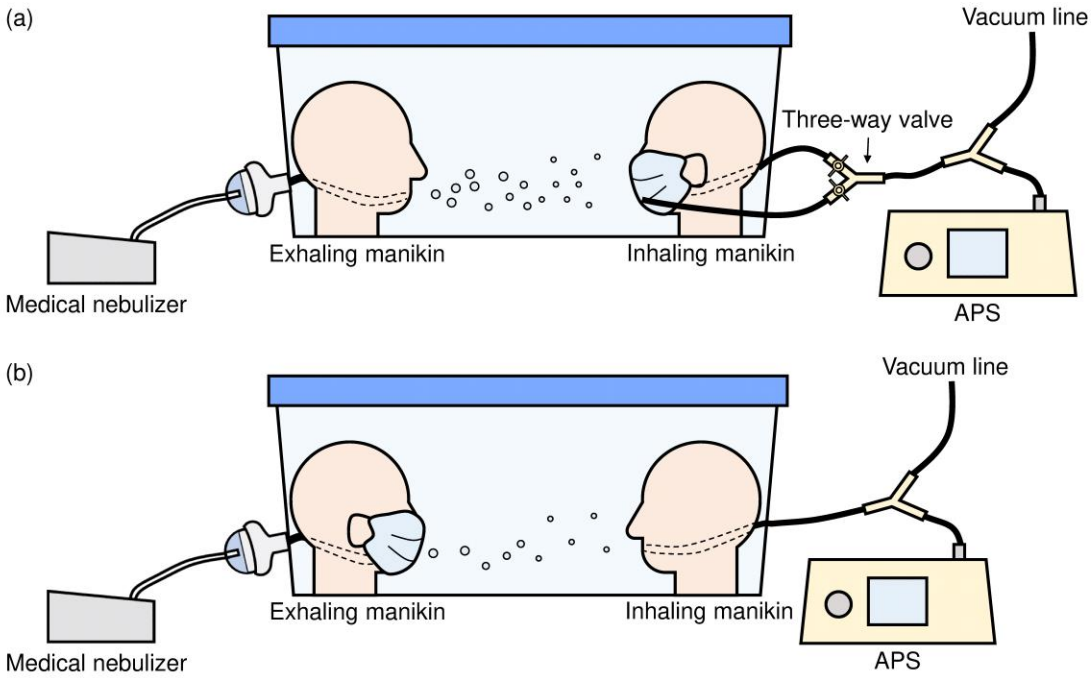

Figure 3-2. Schematic of experimental setup for determining (a) inward protection efficiency and (b) outward protection efficiency.

To evaluate outward protection efficiency, we removed the three-way valve and connected the APS and vacuum line directly to the inhaling manikin (Figure 3-2b). In each test, we ran the

medical nebulizer for 30 s and then allowed particle concentrations to decay, as in scenario 2 of the inward protection protocol, and we measured the chamber concentration (C_{c1}) using the APS at 1-s resolution. After introducing the HEPA-filtered air to flush particles from the chamber, we then put the mask or face shield on the exhaling manikin and ran the medical nebulizer for 30 s again to measure the concentration (C_m). Then we flushed the chamber again, ran the nebulizer to measure the chamber concentration C_{c2}, and calculated the average C_c as described in scenario 1. We calculated the outward protection efficiency according to equation (3-1) as well. We conducted all measurements in triplicate and applied a Student's t-test to compare the differences between two data points.

$$OPE(D_P) = \left(1 - \frac{C_m(D_P)}{\frac{C_{c1}(D_P) + C_{c2}(D_P)}{2}}\right) \times 100\% \quad (3\text{-}3)$$

3.3.4. Droplet deposition analysis

We evaluated the ability of the face coverings to block droplets larger than 20 μm, which can be generated by talking, coughing, and sneezing and which exceed the upper limit of the APS, using a modified droplet deposition analysis (DDA).[29,33] The setup was similar to that of the outward protection protocol but with an air brush (MP290001AV, Campbell Hausfeld, OH, USA) in place of the medical nebulizer to generate larger droplets.[34] We connected the air brush to HEPA-filtered air and a gas regulator set at 165.5 kPa, resulting in a total flow rate of 10 L/min, the same as the flow rate of the medical nebulizer. We filled the air brush with 2% NaCl solution and red food dye at a ratio of 4:1. We taped five glass slides (75 mm × 25 mm) to the face of the inhaling manikin. We pre-cleaned each slide using 70% isopropyl alcohol wipes.

First, we sprayed the air brush for 3 s without the face covering on the exhaling manikin. We then removed the glass slides from the inhaling manikin and inspected them under an optical microscope at 10× magnification (EVOS FL Auto, Life Technologies, CA, USA). We put the face covering on the exhaling manikin and repeated the same steps. To identify droplets on the slides, we processed the images using ImageJ and then manually counted the stains and measured their

size with a limit of detection of 12.3 μm/pixel. Because the droplets spread upon impaction with the slides, we corrected their size assuming a spread factor of 1.5, the ratio of the size of the stain to the original diameter of the droplet.[29] We conducted all measurements in triplicate.

3.4. Results

3.4.1. Size of challenge particles

We used four different types of aerosol generators to cover a broad size range and to accommodate different setups. The Collison nebulizer and FMAG, used to determine material filtration efficiency, generated particles ranging in size from 0.04 to 1 μm and from 2 to 5 μm, respectively (Figure 3-3a, b). The Collison nebulizer produced particles with a geometric mean diameter (GMD) of 0.12 μm and geometric standard deviation (GSD) of 1.4, and the FMAG a GMD of 4 μm and GSD of 1.21. The figure also shows the size distribution measured downstream of a MERV 12 filter to illustrate the data used to calculate filtration and protection efficiencies. The medical nebulizer produced particles ranging in size from 0.5 to 5 μm; the GMD was below the detection limit of the APS (Figure 3-3c). As the medical nebulizer covered a relatively large size range, we chose to use it to evaluate the inward and outward protection efficiencies Figure 3-3c). The air brush generated large particles ranging in size from 20 μm to greater than 135 μm (Figure 3-3d).

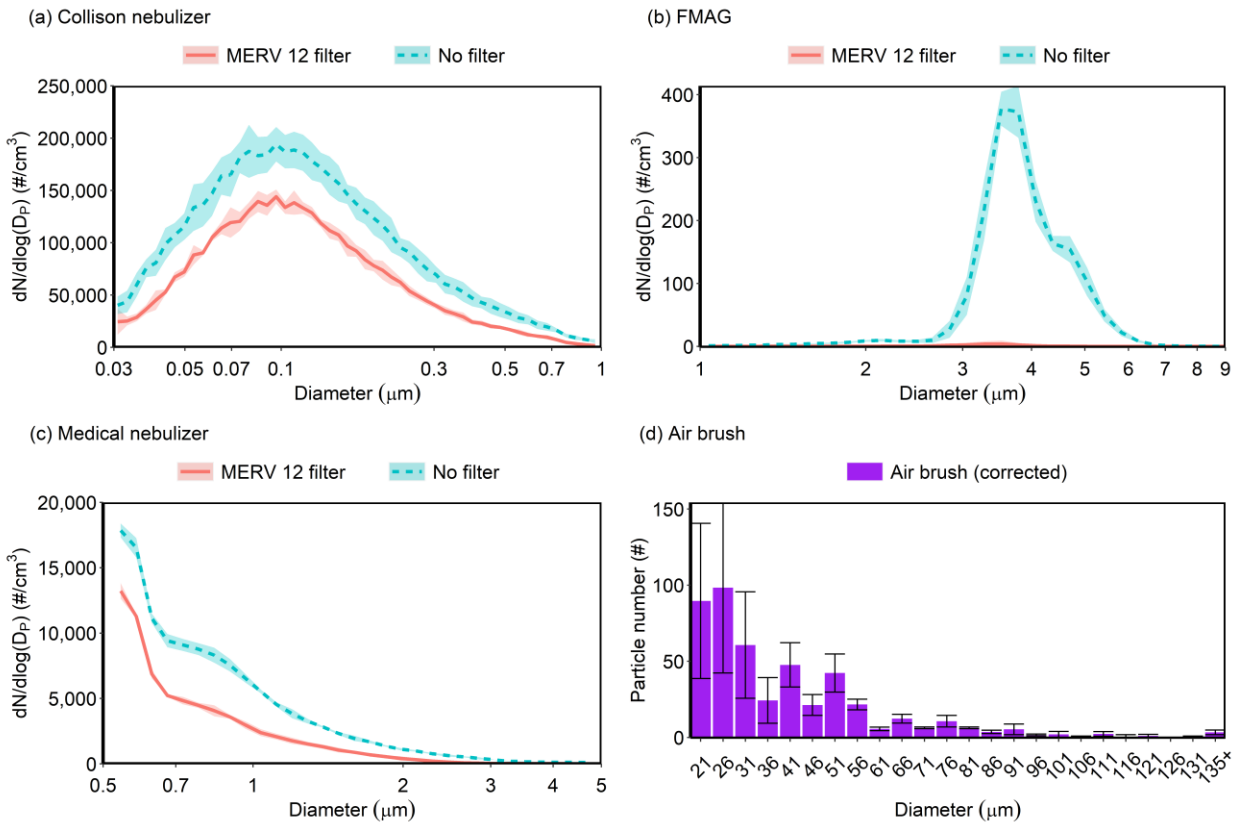

Figure 3-3. Concentration and size distribution of particles as a function of aerodynamic diameter generated by (a) Collison nebulizer, (b) FMAG, (c) medical nebulizer, without a filter (blue dashed line) or downstream of a MERV 12 filter (red solid line), and (d) air brush. In panel (d), the diameter was corrected from the measured size of the droplet stains on the slide by a factor of 1.5. Shading and error bars represent the standard deviations of triplicates.

3.4.2. Material filtration efficiency

We tested the material filtration efficiency of nine common homemade mask materials and one surgical mask. We did not test the face shield because it does not allow air flow through it. Figure 3-4 shows results obtained using the Collison nebulizer and SMPS over the size range 0.04 to 1 μm. The efficiency curves exhibit the expected U shape with a minimum in most cases in the range 0.1–0.3 μm, where no collection mechanism is especially efficient.[35]

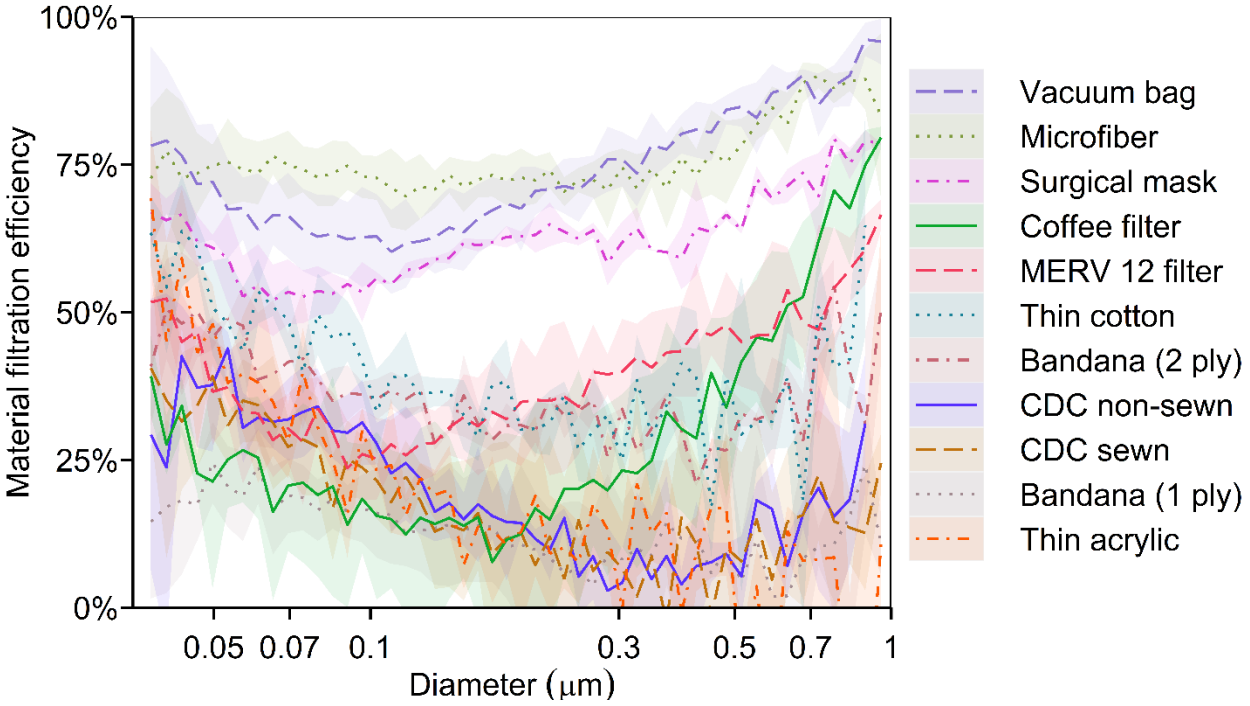

Figure 3-4. Material filtration efficiency of 10 mask materials as a function of aerodynamic diameter. The bandana appears twice because it was tested in both 1-ply and 2-ply configurations. Shading represents the standard deviations of triplicates.

The vacuum bag and microfiber performed best, with a minimum efficiency of 60%. Other studies have also reported that vacuum bags have high filtration efficiencies,[17,20] whereas the performance of microfiber varies depending on the manufacturer and fabric structure.[17,19] Following the top two, the surgical mask was ~50–75% efficient over this size range, falling with the range reported for surgical masks in previous studies.[13,19,20,36] The minimum efficiency of the coffee filter was only 10% for particles at 0.17 μm, lower than the reported value of 34.4% in another study (at a face velocity of 6.3 cm/s),[20] but its efficiency rapidly increased with particle size to 75% for particles at 1 μm. The MERV 12 filter reached its lowest efficiency of 25% at 0.1 μm and had an efficiency > 50% at the extremes shown in Figure 3-4. Common fabrics, including the thin cotton and bandana (2 ply), had low efficiencies, mostly between 30% and 50%. The fabrics fashioned into the CDC non-sewn and CDC sewn masks, bandana (1 ply), and thin acrylic had even lower efficiencies of 5–40% for submicron particles.

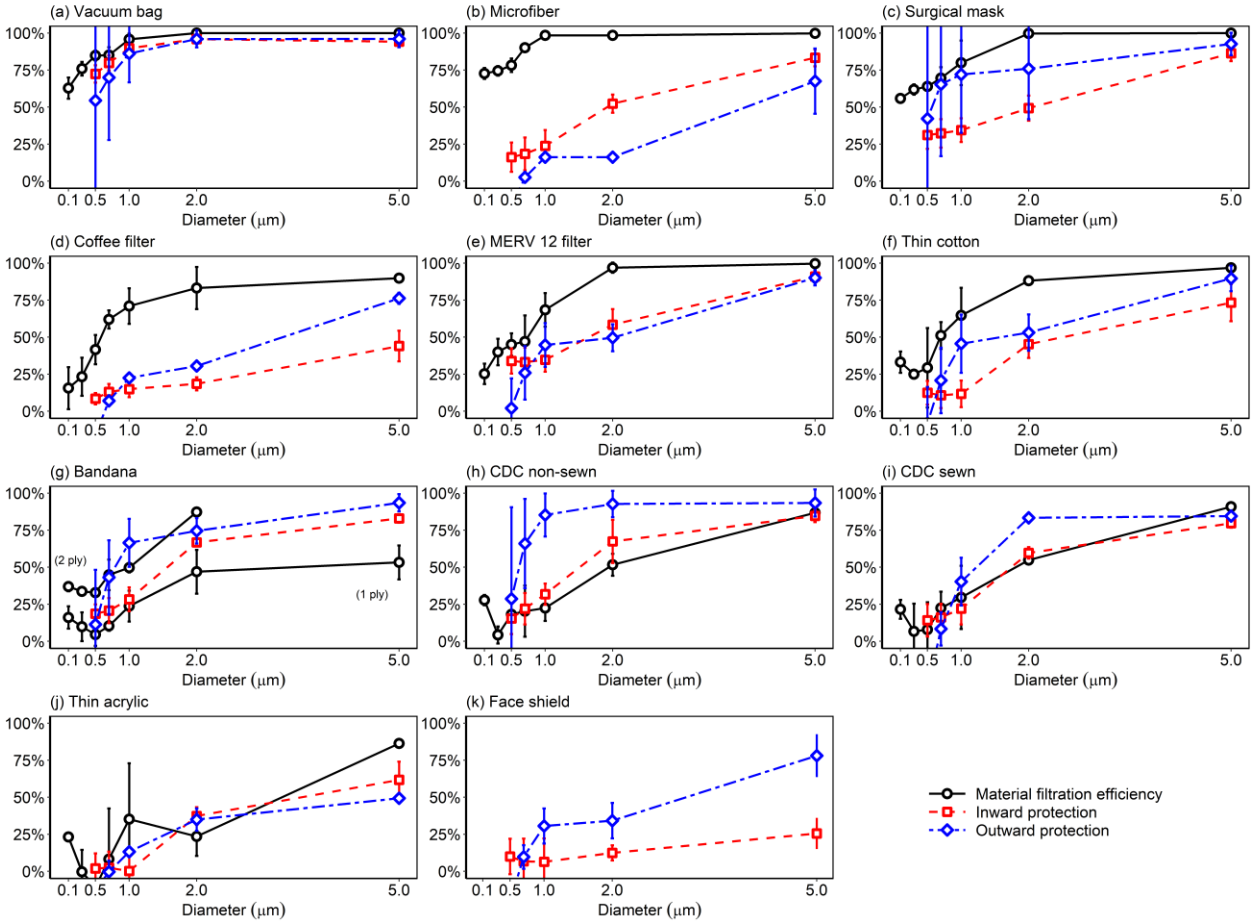

Figure 3-5. Inward and outward protection efficiency of 10 masks and a face shield. These efficiencies are defined for close-range, face-to-face interactions. The face shield was not tested for material filtration efficiency because it did not allow air flow through the material. Error bars represent the standard deviations of triplicates.

Most of the materials exhibited a much better material filtration efficiency for particles >1 μm than for smaller ones, as shown by the black solid line in Figure 3-5. The vacuum bag, microfiber, surgical mask, and MERV 12 filter achieved 90% or higher efficiency at 2 μm, and thin cotton and coffee filter were around 80% efficient at this size. The 2-ply bandana performed much better than the 1-ply bandana, with efficiencies of ~75% and <40% at 2 μm, respectively. The CDC non-sewn and CDC sewn mask materials had efficiencies of ~50% at 2 μm, and their efficiencies increased with particle size to up to 75% at 5 μm. The thin acrylic still ranked at the bottom. Its efficiency was <30% at 2 μm but reached 75% at 5 μm.

Figure 3-6 shows the pressure drop across all materials, measured at a flow rate of 3.0 L/min

through a sample 25 mm in diameter. Microfiber had the highest pressure drop, nearly 1000 Pa, followed by the coffee filter and thin cotton at ~380 Pa. The pressure drop through the other materials was <150 Pa, among which the thin acrylic and MERV 12 filter had the lowest values, ~70 Pa. We further related the pressure drop to the material filtration efficiency using a filter quality factor (Q), as defined by equation (3-4),[35,37] where $FE(D_P)$ is the material filtration efficiency at a particle size of D_P, and ΔP is the pressure drop:

$$Q(D_P) = -\frac{ln(1 - FE(D_P))}{\Delta P} \tag{3-4}$$

We chose 0.3 μm as the representative particle size for the calculation of Q for ease of comparison with other studies (Figure 3-6b). Since pressure drop is directly correlated with the breathability of the material, a high Q means a high filtration efficiency can be achieved with a low pressure drop, indicating that the material is efficient and easy to breathe through. The vacuum bag and MERV 12 filter, which are both designed to filter out particles, had the highest Q of all the materials (~10×10^{-3} Pa^{-1}). The surgical mask also performed well, with an average Q of 7.6×10^{-3} Pa^{-1}, not significantly different from Q of the previous two. These results are comparable to those reported in another study conducted under similar conditions [20]. The Q values of the thin cotton, bandana (2 ply), and the other fabrics were <5×10^{-3} Pa^{-1}, similar to previously reported values.[19,20] Notably, an increase in the number of layers of the bandana resulted in an increase in Q.

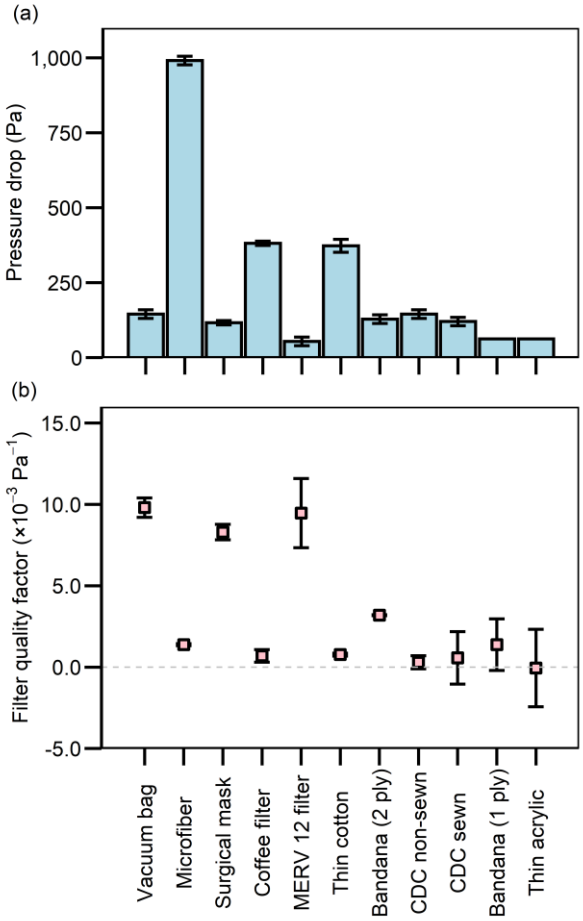

Figure 3-6. Pressure drop and filter quality factor at 0.3 μm of 10 mask materials, sorted on the basis of material filtration efficiency (Figure 3-4). The bandana appears twice because it was tested in both 1-ply and 2-ply configurations. Error bars represent standard deviations of triplicates. In panel (a), there are no error bars for the last two materials as the measurements fell below the detection limit of the pressure gauge.

SEM images of the materials' structure can partly explain the differences in the performance. The vacuum bag, which had the highest material filtration efficiency, had the smallest-diameter fibers and such a compact structure that the pores or intervals between fibers were the least perceptible among all the materials (Figure 3-1a). The fibers of the microfiber cloth were also more tightly woven than those of other materials (Figure 3-1b), resulting in good filtration efficiency. The materials with low efficiency were generally loosely woven, such as the bandana (1 ply), 200-thread-count pillow case used for the CDC non-sewn mask, cotton t-shirt used for the CDC sewn mask, and thin acrylic (Figure 3-1g-j). However, the tightness of the weave was not the only factor

influencing the filtration efficiency. For example, the fiber intervals were large for the surgical mask, yet it was composed of multiple layers of different materials,[19] which made it unique from other materials. That fabric structure alone does not explain filtration efficiency also applies to the filter quality factors. For instance, the vacuum bag had a compact texture yet a low pressure drop, resulting in a high *Q* value. Likewise, the surgical mask was not tightly woven, but it was more efficient and thus had a higher *Q* than many other materials. The number of layers,[17] the properties of the fibers including diameter and electrostatic charges,[20,37-39] and the material composition[19,20] all contribute to differences in filter quality factors.

3.4.3. Inward and outward protection efficiency

In this study, the inward protection efficiency (*IPE*) quantifies the capability of a mask, as worn on a manikin, to protect the wearer by filtering out particles moving in the inward direction through the mask, from the surrounding air to the wearer's respiratory tract. The outward protection efficiency (*OPE*) quantifies the capability of a mask for source control, to filter out particles moving in the outward direction through the mask, from the wearer to the surrounding air. After being made into a mask, the vacuum bag still ranked first for protection efficiency in both directions, with its *IPE* and *OPE* curves close to the material filtration efficiency curve (Figure 3-5a), especially for particles larger than 1 μm. Both *IPE* and *OPE* were >50% at 0.5 μm and >90% for particles larger than 2 μm. However, there were large variations in *OPE* for particles smaller than 0.7 μm. The *IPE* and *OPE* were also similar to the respective material filtration efficiency for the CDC-sewn and thin acrylic masks (Figure 3-5i, j), though their performance was much worse than that of the vacuum bag. The *OPEs* of the CDC sewn mask and thin acrylic mask were ~75% and ~50%, respectively, for particles larger than 2 μm, and both masks were not effective at blocking particles smaller than 0.7 μm. Notably, the *OPE* of the CDC sewn mask was slightly higher than its *IPE* at 2.0 μm, whereas no significant differences (p>0.05) between *OPE* and *IPE* were observed across all sizes for the thin acrylic mask.

In contrast, the microfiber and coffee filter masks had a much worse *IPE* and *OPE* than their material filtration efficiency (Figure 3-5b, d), indicating leakage and a poor fit. The *OPE* for the

microfiber mask was <25% for particles smaller than 2 μm, a difference of >50 percentage points compared to its material filtration efficiency. Its *IPE* was slightly better but still 20–50 percentage points lower than its material filtration efficiency for particles smaller than 2 μm. Similar trends were also observed for the coffee filter, except that its *OPE* was slightly higher than its *IPE* at particle sizes larger than 2 μm.

For the surgical mask, thin cotton, and MERV 12 filter, the differences between *OPE* or *IPE* and material filtration efficiency were moderate, usually within 25 percentage points (Figure 3-5c, e, f). The *OPEs* of the surgical mask and thin cotton mask were higher than their *IPEs* but not significantly; and these efficiencies were lower than the corresponding material filtration efficiency. In particular, the average *OPE* of the surgical mask was substantially better than its *IPE* at particle sizes ranging from 0.7 to 2 μm, but given the large variability in *OPE*, such differences were not statistically significant ($p>0.05$). There were no significant differences ($p>0.05$) between *IPE* and *OPE* for the MERV 12 filter across all sizes.

The bandana, CDC non-sewn mask, and the face shield had unique forms. The bandana was folded in half in a triangle to mimic how people would normally wear it; its *IPE* and *OPE* fell in between the single-layered and double-layered material filtration efficiency (Figure 3-5g), with the *OPE* higher than *IPE* at a particle size of 1 μm ($p<0.05$). The CDC non-sewn mask, whose fit can be adjusted by tightening or loosening the straps, had an *OPE* that was significantly ($p<0.05$) higher than the material filtration efficiency at sizes ranging from 1 to 2 μm. It is likely that stretching or loosening the fabric altered its filtration efficiency. Its average *OPE* was also higher than the *IPE*, whereas no significant difference was found between its *IPE* and material filtration efficiency. The face shield did not block almost any aerosols smaller than 0.7 μm, as expected, for it did not fit closely to the manikin and thus allowed aerosols to travel freely around the shield. However, it exhibited a decent *OPE* for particles at 5 μm (~75%) and an *IPE* of ~25% for such particles.

Figure 3-7 compares the *IPE* and *OPE* across all masks. The vacuum bag mask had the best performance in both directions, while the coffee filter mask, thin acrylic mask, and face shield

ranked at the bottom. The CDC non-sewn mask and surgical mask followed the vacuum bag closely for *OPE* but not *IPE*. Interestingly, the *OPE* values for masks tested spanned a wide range, whereas their *IPE* values were closer, except for the vacuum bag. In addition, direct comparison of the two panels in Figure 3-7 reveals that *OPE* tended to be higher than *IPE*, illustrating that many face coverings work better for source control than protection of the wearer, although the difference was not significant in most cases.

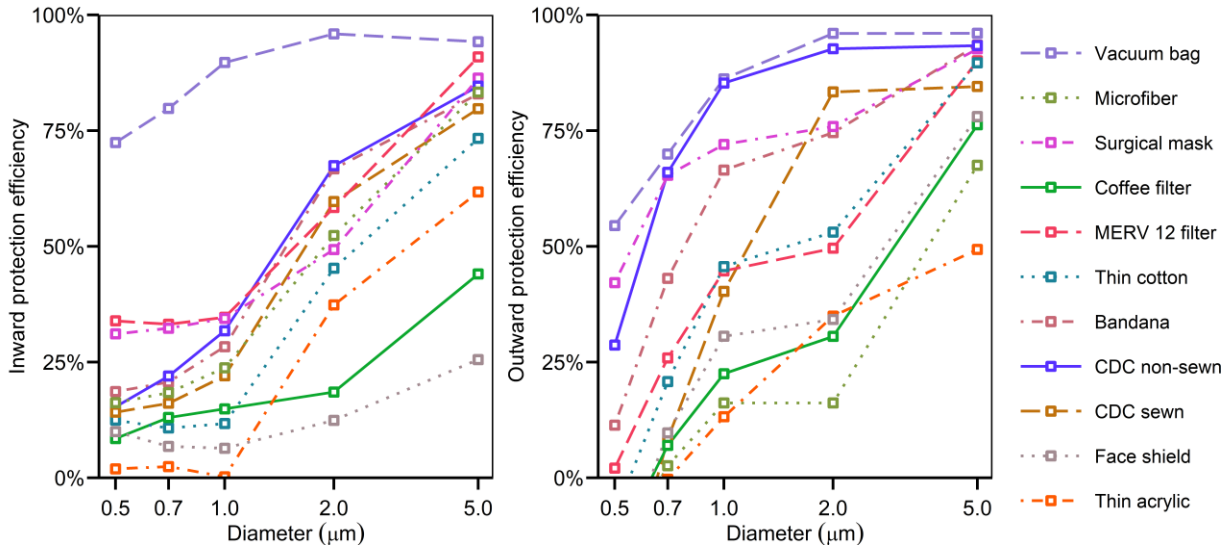

Figure 3-7. Inward and outward protection efficiency for all masks. For improved readability, error bars are not shown here, but they appear in Figure 3-5.

In response to a study that suggested that neck gaiters offer very little protection,[40] we measured the *OPE* of two neck gaiters, one made of thin 100% polyester and another made of a double layer of microfiber fabric that was 87% polyester and 13% elastane. Their average *OPEs* were at least 50% at 1 μm and >90% at 5 μm (Figure S5, S7), similar to the results for the CDC non-sewn mask. When doubled over, the thin polyester neck gaiter achieved an *OPE* of >90% over the size range of 0.5–5 μm (Figure S6). Due to the late addition of these face coverings and expectation of the donors that they be returned in usable condition, we were not able to measure their material filtration efficiency or *IPE*.

Droplet deposition analysis found no stains in the slides for all face coverings, indicating that

all of them were able to prevent droplets larger than 20 μm from spreading 33 cm away. This result indicated that these large droplets either fell to the ground before reaching the inhaling manikin or were absorbed by the mask fabric, as proven by the red stains on the mask after the DDA measurements. We can attribute both mechanisms to the *OPE* of masks according to its definition.

3.5. Discussion

For most of the face coverings tested, those with a high material filtration efficiency also had a better *OPE* and *IPE*. One example is the vacuum bag, which achieved outstanding performance compared to other materials with regards to material filtration efficiency, *IPE*, and *OPE*. It was able to filter out at least 60% of particles when tested on the filter holder (i.e., without leakage) and had an *OPE* and *IPE* of at least 50% and 75%, respectively, for particles 0.5 μm and larger. The MERV 12 filter, surgical mask, thin cotton, and CDC sewn mask also had decent material filtration efficiencies, *OPEs*, and *IPEs*, whereas the thin acrylic mask performed worst or near-worst on all three metrics. However, there were some exceptions, such as the microfiber cloth and coffee filter. The material filtration efficiencies of these two masks were much higher than their *OPEs* and *IPEs* (Figure 3-5b, d). The coffee filter and microfiber were thick and stiff, resulting in a poor fit with larger gaps between the manikin and the mask, through which particles could short circuit the mask. In contrast, the vacuum bag was thin and soft, which allowed it to conform to the face easily and achieve a high *IPE* and *OPE*. Hence, we propose that the stiffness of the material impacts the fit of the mask and can be responsible for large discrepancies between the material filtration efficiency and *OPE* and *IPE*. Additionally, differences in mask use among individuals will lead to variability in fit and thus effectiveness.

The CDC non-sewn mask was another exception. Generally, the *IPE* or *OPE* should be lower than the material filtration efficiency because the latter was tested in a filter holder with no opportunity for leaks. Nonetheless, the CDC non-sewn mask had a higher *OPE* than its material filtration efficiency. This unexpected result may be due to its unique form, resulting in a different way of it being stretched. Its two straps can be adjusted to fit it more tightly to the manikin face, especially to the mouth opening. Hence, the increased pressure caused by the expiratory flow was

not able to push the CDC non-sewn mask outwards to create gaps between masks and the manikin like other conventional masks do,[41-43] minimizing air leakage and bypass through the gaps. The stretching of the fabric may have caused a change in pore size and woven structure, which further impacted the filtration efficiency. In addition, the masks themselves also reduced the expired air velocity, which caused the particles to deposit before they could reach the sampling device, as shown in other studies.[43-45] The combined effects of reduced gaps and reduced air velocity resulted in a uniquely high *OPE* for the CDC non-sewn mask. For other masks with a conventional shape, however, these two effects seemed compensatory during evaluation of *OPE*. While the masks caused a decrease in the expiratory air velocity, they were also pushed outwards by the outgoing flow, creating larger gaps between the masks and manikin. The contradiction in part explained why the differences between *OPE* and *IPE* were not as large as expected for the masks with conventional shapes, and why the bandana achieved an *OPE* better than expected, because it created a larger plenum between itself and the manikin that provided additional containment of the flow to lower the pressure drop and slow the flow jets through the gaps.

During the testing of *IPE*, we noticed that the vacuum through the inhaling manikin can suck the mask tightly against inlet opening, thus reducing the size of any gaps. This can explain the small differences between the material filtration efficiency and *IPE,* except for the coffee filter and microfiber as they were stiff and hard to move. However, this phenomenon also illustrates the tradeoff between breathability and filtration efficiency. Therefore, it is important to select fabrics that can achieve both high filtration efficiency and low pressure drop for making masks.

We also observed variable hydrophobicity of the mask material during the testing of *IPE* and *OPE*. The fabrics (e.g., thin cotton and thin acrylic) and coffee filter were wetted easily by droplets, whereas the filter materials, including the vacuum bag and the MERV 12 filter, were hydrophobic and kept the droplets on the surface of the material. El-Atab et al. developed a reusable hydrophobic mask and proposed that the hydrophobicity of the mask material might contribute to repelling the droplets.[46] However, the role of hydrophobicity in filtration efficiency, *IPE*, and *OPE* remains unclear. We recommend future investigations into the influence of wettability or

hydrophobicity of the face coverings on their performance.

Whether particles actually deposit along the respiratory tract, potentially delivering an inhaled pathogen to a receptor, depends on two factors: (1) their ability to be inhaled into the respiratory tract and (2) their likelihood of depositing. The first can be reduced by a mask, and the second can be predicted as a function of particle size. Accounting for these two factors, we calculated the masked deposition rate (*MD*) by combining the inward protection effectiveness (*IPE*) and the International Commission and Radiological Protection (ICRP) model for the total deposition fraction,[35] as shown in equation (3-5):

$$MD(D_P) = (1 - IPE(D_P))\left(1 - 0.5 \times \frac{1}{1 + 0.00076{D_P}^{2.8}}\right)\left(0.0587 + \frac{0.911}{1 + e^{4.77+1.485ln(D_P)}} + \frac{0.943}{1 + e^{0.508-2.58ln(D_P)}}\right) \quad (3\text{-}5)$$

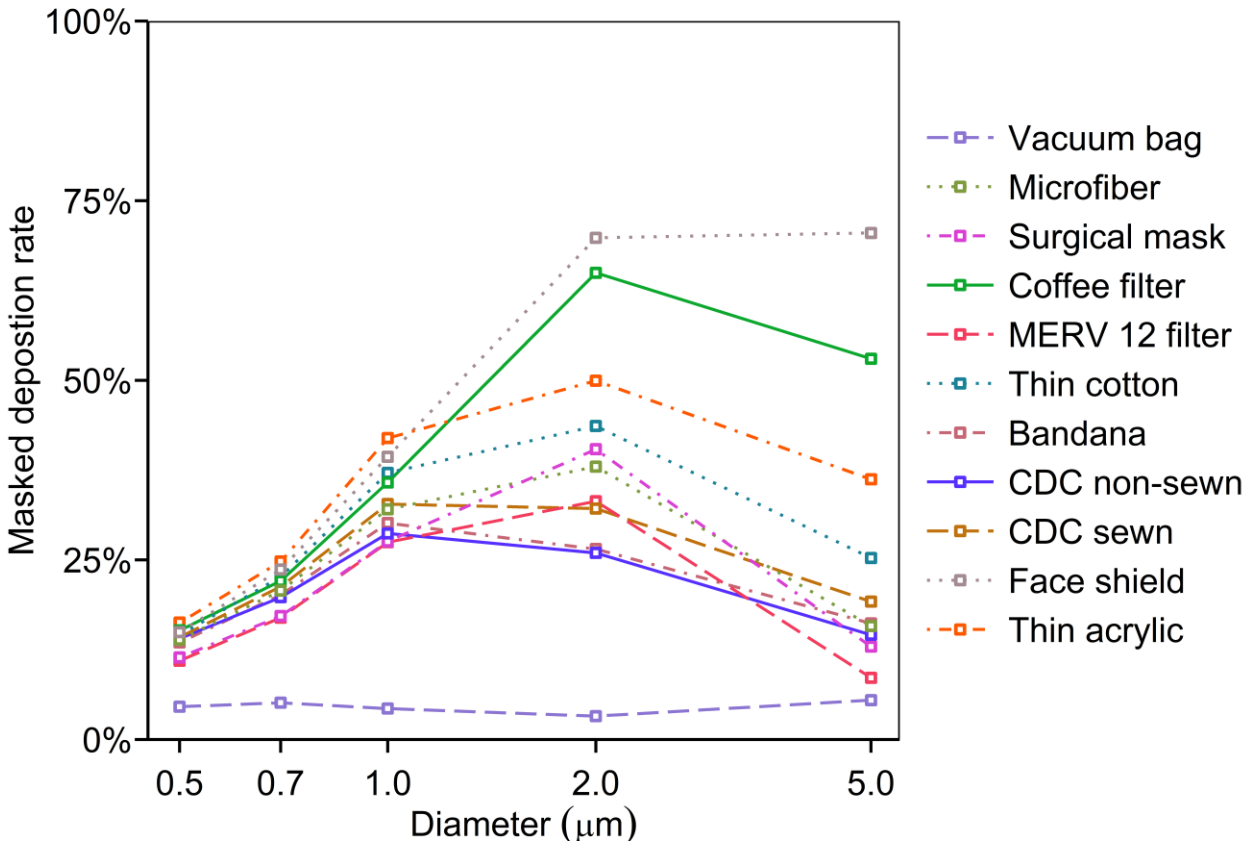

Figure 3-8. Masked deposition rate of 10 masks and a face shield as a function of the aerodynamic diameter.

Figure 3-8 shows the masked deposition rate as a function of particle size. Here, lower values are better. The vacuum bag performed best, with a deposition rate of <10% across all sizes. The thin acrylic mask, the coffee filter mask, and the face shield were the worst, with a 50% or higher deposition rate at a particle size of 2 μm. Although there is considerable concern about exposure to virus in the smaller particles, the particles with the highest deposition rate were those around 2 μm. For example, SARS-CoV-2 RNA has been detected in particles in the size range of 1–4 μm.[12] The smallest particle size considered in this analysis was 0.5 μm, but the deposition efficiency of 0.3 μm particles in the respiratory tract is even lower, so it is possible that concerns about mask efficiency at this size are overstated.

This study was designed to test masks under tightly controlled conditions, which necessitate the use of mechanical particle generation and manikins instead of humans. However, this approach presents several limitations. The manikins are much more rigid than human skin, so masks may not fit as tightly. A study involving a head form with pliable, elastomeric skin found that fit factors of respirators were comparable to those measured on humans,[47] whereas in prior studies with head forms made of more rigid material, the fit factors were not as good.[48] In addition, our manikins did not perfectly mimic human respiratory activities because the aerosol flow traveled in only one direction in the inhaling manikin and the exhaling manikin. As discussed above, inhalation and exhalation will alter the plenum between the mask and the manikin, thus resulting in changes of the pressure drop and expiratory jets. We investigated only one flow rate out of the possible spectrum from gentle breathing to vigorous sneezing.

The experimental setup was designed to measure *OPE* in a close-conversation scenario. With a face covering on the exhaling manikin, the aerosol flow could be diverted downwards or sideways, leading to a longer path length to the inhaling manikin and allowing for more time for particles to be removed by settling. Thus, the *OPE* values reported here are not generalizable to all source control scenarios. In reality, people standing to the side of the emitter may be exposed to more aerosols than indicated by our measurements. This possibility merits further investigation in a follow-up experiment with measurements in multiple locations. Moreover, the chamber may

restrict the aerosol flow from fully and freely developing as in the real world, although this impact is expected to be small based on the radius of the jet and dimensions of the chamber[49] On the other hand, the chamber isolated sampling activities from the internal flow field. As in all experiments, there are tradeoffs among simulating a real-world situation, controlling variables, and managing the limitations of equipment. Because an aerosol generator that produces a uniform distribution of particles spanning a wide range of sizes does not exist, compromises are required in the experimental design. For example, large particles were formed by coagulation of small particles, and thus an excessive number of small particles was present, causing some detection issues. Development of methods to produce large concentrations of supermicron particles would be very useful for future studies.

After multiple measurements of the same masks, the fabrics may be overloaded with particles and then release them back to the flow, resulting in resuspension of the particles (Figure S8, S9). Additionally, masks fit differently on different head shapes. Therefore, the performance of the masks on a human face under real-world conditions will certainly vary from the experimental results in this study. However, there are still some advantages of manikin heads over human faces, as the particle emissions from human clothes and other activities may interfere with the measurements. Particularly, the friction between human faces, jaws, and mask fabrics can release small fabric pieces into the flow stream, complicating the measurement.[50] We did not test multiple layers of fabric, as prior work has shown that the material filtration efficiency is readily predicted by combining individual layers in series.[17] An exception is that the *OPE* of the doubled-over neck gaiter was much greater than expected from combining a single layer in series. When folded over, the neck gaiter was much more difficult to stretch over the manikin. It fit more tightly, so the pores between fibers were probably smaller than in the single-layer configuration, and performance was greatly improved.

Based on these results and other studies,[17] we recommend a three-layer mask consisting of two outer layers of a very flexible, tightly woven fabric and an inner layer consisting of a material designed to filter out particles. The inner layer could be a high efficiency particulate air (HEPA)

filter, a MERV 14 or better filter,[51] or a vacuum bag. This approach enables a good fitting mask with high performance in both directions. If the filter material is 60% efficient at the most penetrating particle size and the outer layers are 20% efficient (Figure 1), the mask would have a minimum efficiency of 74%. At a particle size of 1 μm, where filter materials can easily have an efficiency of 75% and common fabrics 40%, the overall efficiency would be greater than 90%.

Acknowledgments

Jin Pan was supported by an Edna B. Sussman Foundation fellowship. Virginia Tech's Fralin Life Sciences Institute and Institute for Critical Technology and Applied Science provided additional support for this work. Elizabeth Cantando acquired SEM images. TSI Inc. generously loaned the Flow Focusing Monodisperse Aerosol Generator 1520 to the Marr lab. This work used shared facilities at the Virginia Tech National Center for Earth and Environmental Nanotechnology Infrastructure (NanoEarth), a member of the National Nanotechnology Coordinated Infrastructure (NNCI), supported by NSF (ECCS 1542100 and ECCS 2025151).

Supporting information

To verify the influence of a neutralizer on the material filtration efficiency, we connected an aerosol neutralizer (soft X-ray type neutralizer XRC-05, HCT CO., Ltd, Republic of Korea) after the Collison nebulizer. We tested an N95 and found no significant difference in efficiency (p > 0.05) whether the neutralizer was on or off, as determined by the Student's t-test (Figure S1). Figure S2 shows the results with microfiber cloth. The filtration efficiency when the neutralizer was off was slightly lower, but there was no significant difference over the whole range whether the neutralizer was on or off (p > 0.05). We also tested the N95 with Kr-85 radioactive neutralizer (3012, TSI Inc., MN, USA) and found no significant difference (p > 0.05) (Figure S3). Error bars represent standard deviations of duplicates.

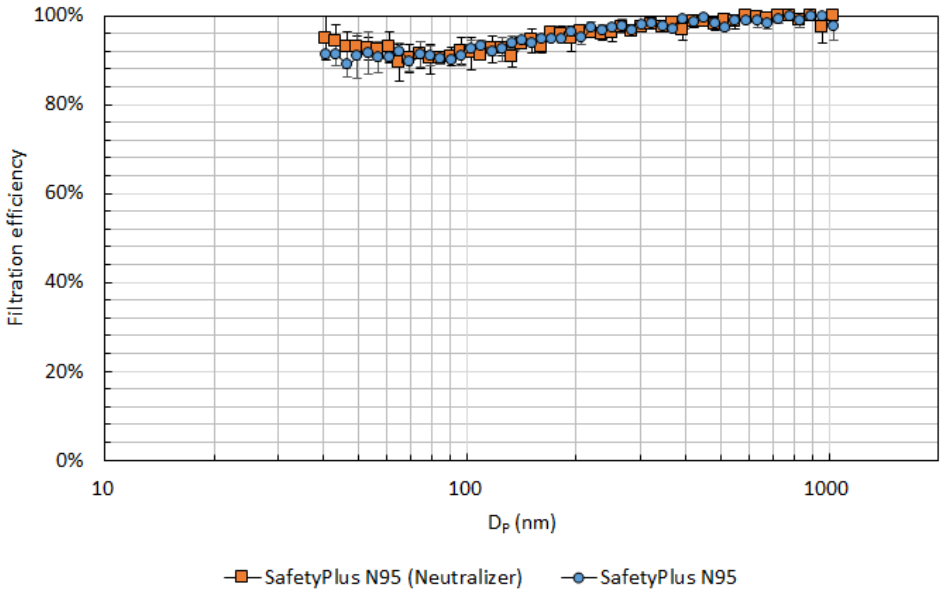

Figure S1. Material filtration efficiency of an N95 with and without a neutralizer (soft X-ray).

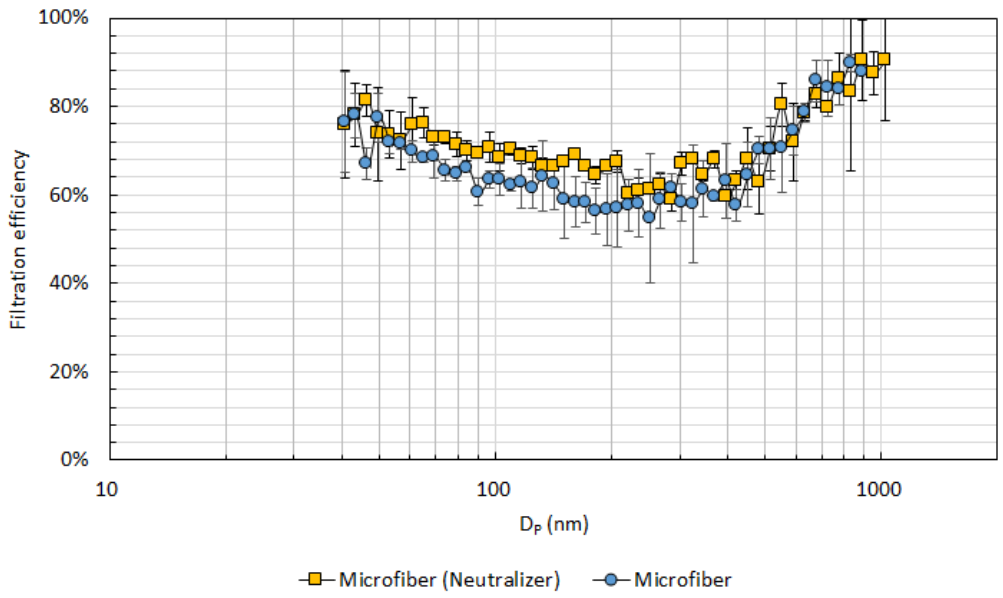

Figure S2. Material filtration efficiency of microfiber cloth with and without a neutralizer (soft X-ray).

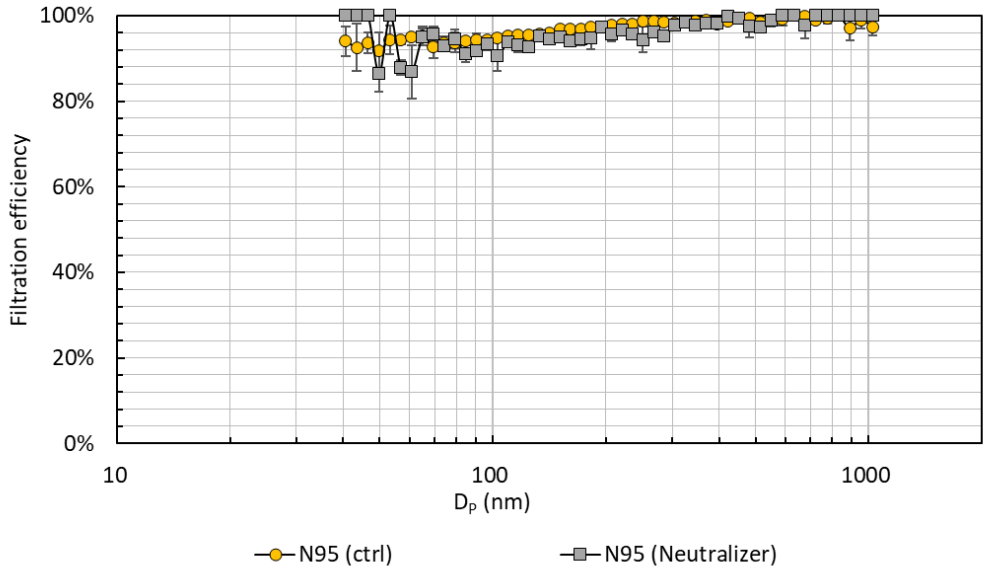

Figure S3. Material filtration efficiency of an N95 with and without a neutralizer (Kr-85).

(a) Vacuum bag mask

(b) Microfiber mask

(c) Surgical mask

(d) Coffee filter mask

(e) MERV 12 filter mask

(f) Thin cotton mask

(g) Bandana

(h) CDC non-sewn

(i) CDC sewn

(j) Thin acrylic mask

(k) Face shield

Figure S4. Masks on the manikin.

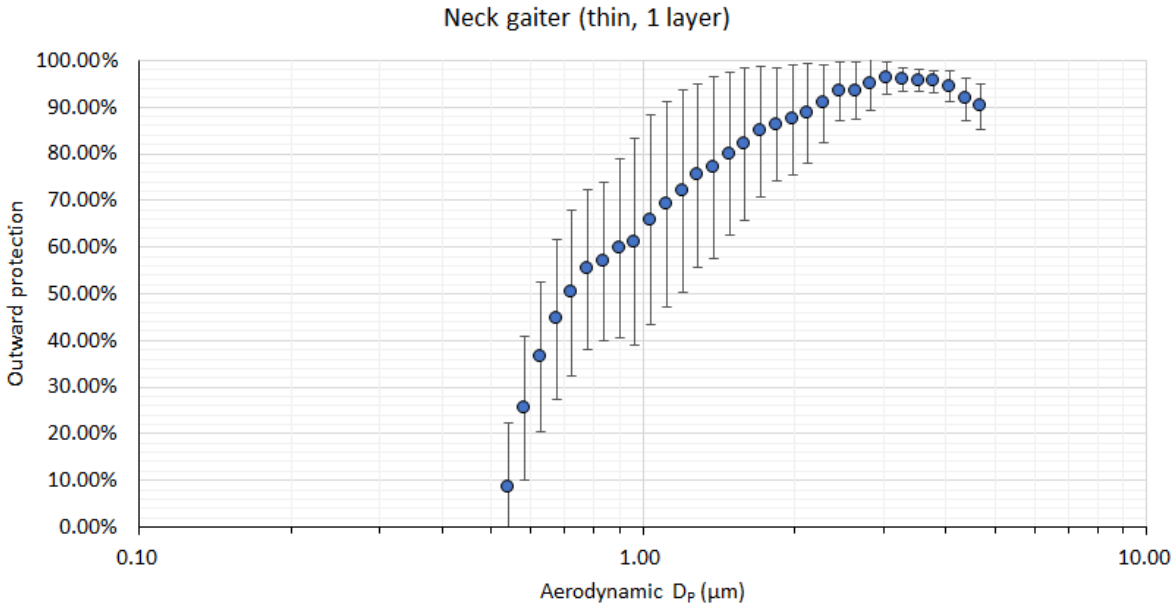

Figure S5. Outward protection efficiency of a thin, polyester neck gaiter (1 ply).

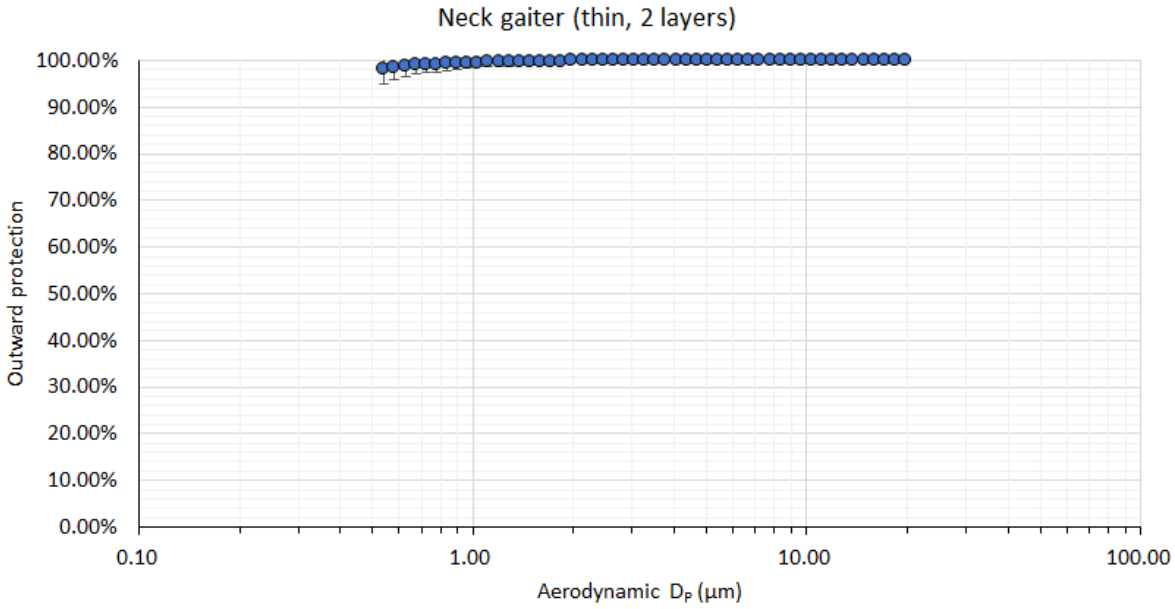

Figure S6. Outward protection efficiency of a thin, polyester neck gaiter (2 ply).

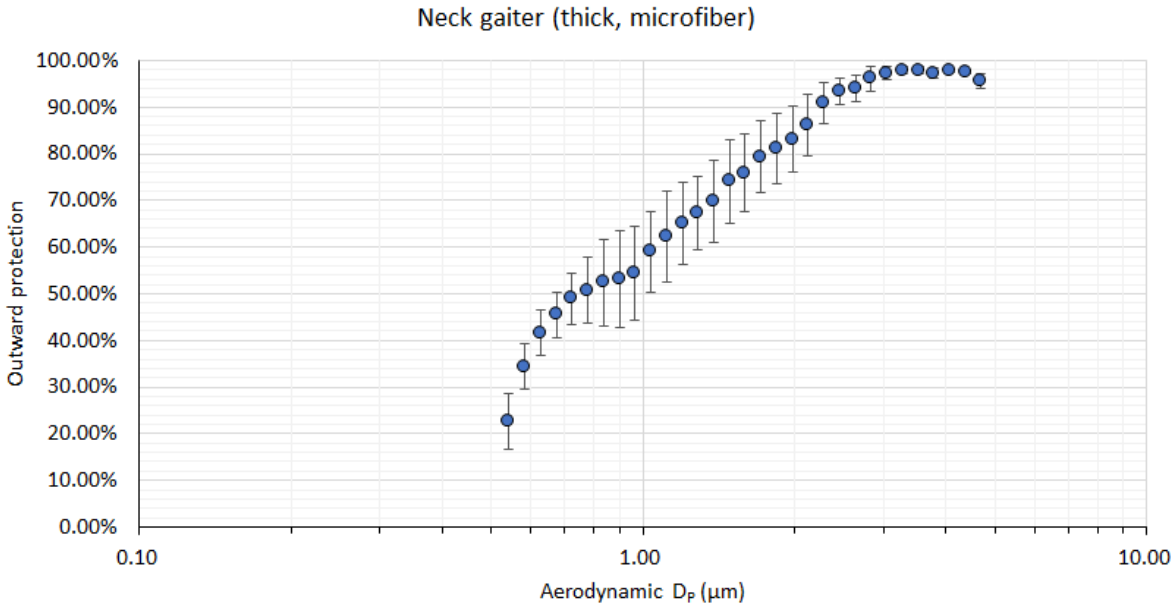

Figure S7. Outward protection efficiency of a double-layer, microfiber, polyester and elastane neck gaiter.

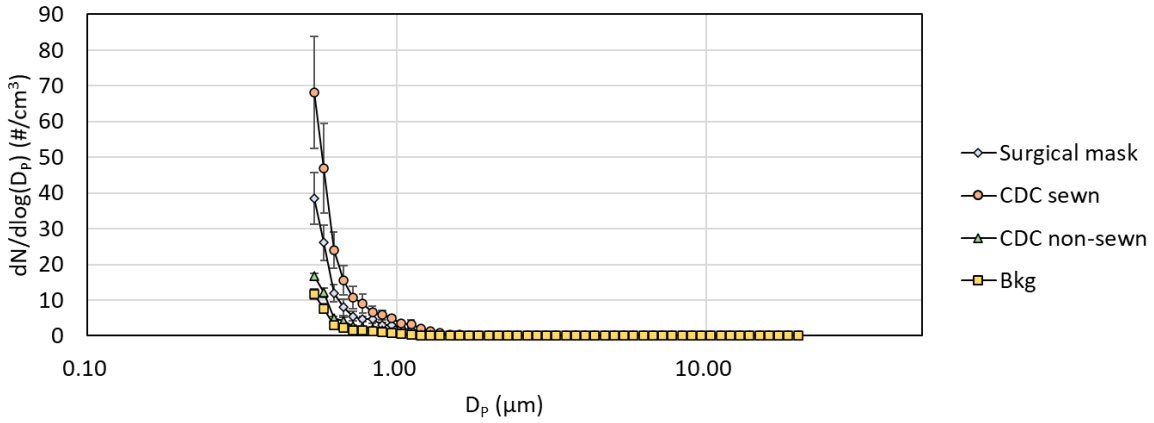

Figure S8. Particle concentration and size distributions when first blowing clean air through these masks after multiple rounds of testing.

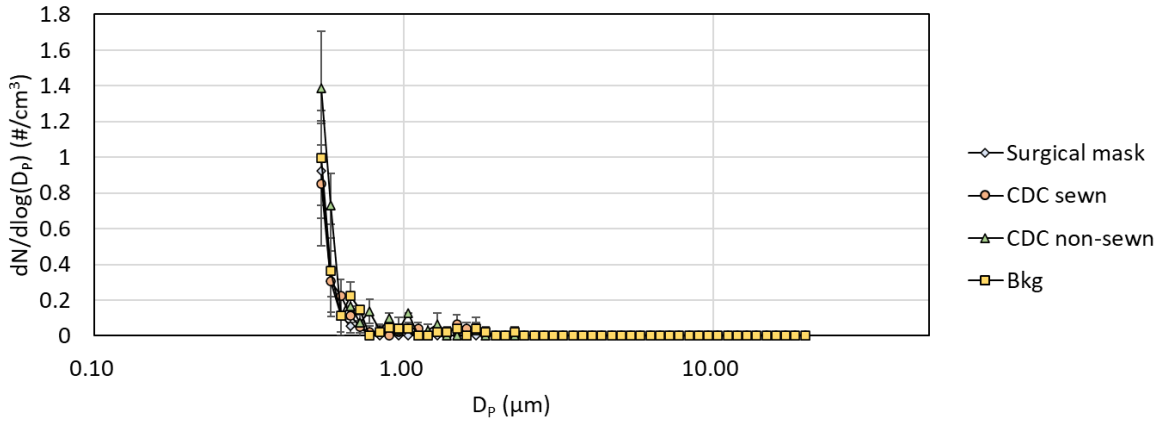

Figure S9. Particle concentration and size distributions after blowing clean air for 15 minutes through the same masks depicted in Figure S8.

References

1. Allen JG, Marr LC. Recognizing and controlling airborne transmission of SARS-CoV-2 in indoor environments. *Indoor Air.* 2020;30(4):557-558.
2. Morawska L, Tang JW, Bahnfleth W, et al. How can airborne transmission of COVID-19 indoors be minimised? *Environment International.* 2020;142:105832.
3. Asadi S, Bouvier N, Wexler AS, Ristenpart WD. The coronavirus pandemic and aerosols: Does COVID-19 transmit via expiratory particles? *Aerosol Science and Technology.* 2020;54(6):635-638.
4. Hadei M, Hopke PK, Jonidi A, Shahsavani A. A Letter about the Airborne Transmission of SARS-CoV-2 Based on the Current Evidence. *Aerosol and Air Quality Research.* 2020;20(5):911-914.
5. Prather KA, Wang CC, Schooley RT. Reducing transmission of SARS-CoV-2. *Science.* 2020;368(6498):1422.
6. Howard J, Huang A, Li Z, et al. An evidence review of face masks against COVID-19. *Proceedings of the National Academy of Sciences.* 2021;118(4):e2014564118.
7. The Economist. Masks probably slow the spread of covid-19. 2020; https://www.economist.com/science-and-technology/2020/05/28/masks-probably-slow-the-spread-of-covid-19. Accessed 10/23, 2020.
8. Wong SH, Teoh JYC, Leung C-H, et al. COVID-19 and Public Interest in Face Mask Use. *American Journal of Respiratory and Critical Care Medicine.* 2020;202(3):453-455.
9. Lyu W, Wehby GL. Community Use Of Face Masks And COVID-19: Evidence From A Natural Experiment Of State Mandates In The US. *Health Affairs.* 2020;39(8):1419-1425.
10. Jefferson T, Foxlee R, Del Mar C, et al. Physical interventions to interrupt or reduce the spread of respiratory viruses: systematic review. *BMJ.* 2008;336(7635):77-80.
11. Xiao J, Shiu EYC, Gao H, et al. Nonpharmaceutical Measures for Pandemic Influenza in Nonhealthcare Settings-Personal Protective and Environmental Measures. *Emerging infectious diseases.* 2020;26(5):967-975.
12. Chia PY, Coleman KK, Tan YK, et al. Detection of air and surface contamination by SARS-CoV-2 in hospital rooms of infected patients. *Nature Communications.* 2020;11(1):2800.
13. Makison Booth C, Clayton M, Crook B, Gawn JM. Effectiveness of surgical masks against influenza bioaerosols. *Journal of Hospital Infection.* 2013;84(1):22-26.
14. Milton DK, Fabian MP, Cowling BJ, Grantham ML, McDevitt JJ. Influenza Virus Aerosols in Human Exhaled Breath: Particle Size, Culturability, and Effect of Surgical Masks. *PLOS Pathogens.* 2013;9(3):e1003205.
15. Leung NHL, Chu DKW, Shiu EYC, et al. Respiratory virus shedding in exhaled breath and efficacy of face masks. *Nature Medicine.* 2020;26(5):676-680.
16. van der Sande M, Teunis P, Sabel R. Professional and Home-Made Face Masks Reduce Exposure to Respiratory Infections among the General Population. *PLOS ONE.* 2008;3(7):e2618.
17. Drewnick F, Pikmann J, Fachinger F, Moormann L, Sprang F, Borrmann S. Aerosol

filtration efficiency of household materials for homemade face masks: Influence of material properties, particle size, particle electrical charge, face velocity, and leaks. *Aerosol Science and Technology.* 2020:1-17.
18. Rengasamy S, Eimer B, Shaffer RE. Simple Respiratory Protection—Evaluation of the Filtration Performance of Cloth Masks and Common Fabric Materials Against 20–1000 nm Size Particles. *The Annals of Occupational Hygiene.* 2010;54(7):789-798.
19. Zhao M, Liao L, Xiao W, et al. Household Materials Selection for Homemade Cloth Face Coverings and Their Filtration Efficiency Enhancement with Triboelectric Charging. *Nano Letters.* 2020;20(7):5544-5552.
20. Zangmeister CD, Radney JG, Vicenzi EP, Weaver JL. Filtration Efficiencies of Nanoscale Aerosol by Cloth Mask Materials Used to Slow the Spread of SARS-CoV-2. *ACS Nano.* 2020;14(7):9188-9200.
21. Konda A, Prakash A, Moss GA, Schmoldt M, Grant GD, Guha S. Response to Letters to the Editor on Aerosol Filtration Efficiency of Common Fabrics Used in Respiratory Cloth Masks: Revised and Expanded Results. *ACS Nano.* 2020;14(9):10764-10770.
22. Mueller W, Horwell CJ, Apsley A, et al. The effectiveness of respiratory protection worn by communities to protect from volcanic ash inhalation. Part I: Filtration efficiency tests. *International Journal of Hygiene and Environmental Health.* 2018;221(6):967-976.
23. La Scola B, Le Bideau M, Andreani J, et al. Viral RNA load as determined by cell culture as a management tool for discharge of SARS-CoV-2 patients from infectious disease wards. *Eur J Clin Microbiol Infect Dis.* 2020;39(6):1059-1061.
24. Lindsley WG, Blachere FM, Law BF, Beezhold DH, Noti JD. Efficacy of face masks, neck gaiters and face shields for reducing the expulsion of simulated cough-generated aerosols. *Aerosol Science and Technology.* 2020:1-9.
25. Yang W, Elankumaran S, Marr LC. Concentrations and size distributions of airborne influenza A viruses measured indoors at a health centre, a day-care centre and on aeroplanes. *Journal of the Royal Society, Interface.* 2011;8(61):1176-1184.
26. Hu J, Lei C, Chen Z, et al. Distribution of airborne SARS-CoV-2 and possible aerosol transmission in Wuhan hospitals, China. *National Science Review.* 2020;7(12):1865-1867.
27. Yan J, Grantham M, Pantelic J, et al. Infectious virus in exhaled breath of symptomatic seasonal influenza cases from a college community. *Proceedings of the National Academy of Sciences.* 2018;115(5):1081.
28. Marr LC, Tang JW, Van Mullekom J, Lakdawala SS. Mechanistic insights into the effect of humidity on airborne influenza virus survival, transmission and incidence. *Journal of the Royal Society Interface.* 2019;16(150):20180298-20180298.
29. Johnson GR, Morawska L, Ristovski ZD, et al. Modality of human expired aerosol size distributions. *Journal of Aerosol Science.* 2011;42(12):839-851.
30. Zhou J, Wei J, Choy K-T, et al. Defining the sizes of airborne particles that mediate influenza transmission in ferrets. *Proceedings of the National Academy of Sciences.* 2018;115(10):E2386.
31. Centers for Disease Control and Prevention. How to Make Masks. 2020;

https://www.cdc.gov/coronavirus/2019-ncov/prevent-getting-sick/how-to-make-cloth-face-covering.html. Accessed 10/23, 2020.
32. Gupta JK, Lin C-H, Chen Q. Characterizing exhaled airflow from breathing and talking. *Indoor Air.* 2010;20(1):31-39.
33. Xie X, Li Y, Sun H, Liu L. Exhaled droplets due to talking and coughing. *Journal of The Royal Society Interface.* 2009;6(suppl_6):S703-S714.
34. Lindsley WG, Reynolds JS, Szalajda JV, Noti JD, Beezhold DH. A Cough Aerosol Simulator for the Study of Disease Transmission by Human Cough-Generated Aerosols. *Aerosol Science and Technology.* 2013;47(8):937-944.
35. Hinds WC. *Aerosol technology: properties, behavior, and measurement of airborne particles.* New York: John Wiley & Sons; 1999.
36. Oberg T, Brosseau LM. Surgical mask filter and fit performance. *American Journal of Infection Control.* 2008;36(4):276-282.
37. Podgórski A, Bałazy A, Gradoń L. Application of nanofibers to improve the filtration efficiency of the most penetrating aerosol particles in fibrous filters. *Chemical Engineering Science.* 2006;61(20):6804-6815.
38. Konda A, Prakash A, Moss GA, Schmoldt M, Grant GD, Guha S. Aerosol Filtration Efficiency of Common Fabrics Used in Respiratory Cloth Masks. *ACS Nano.* 2020;14(5):6339-6347.
39. Ou Q, Pei C, Chan Kim S, Abell E, Pui DYH. Evaluation of decontamination methods for commercial and alternative respirator and mask materials – view from filtration aspect. *Journal of Aerosol Science.* 2020;150:105609.
40. Fischer EP, Fischer MC, Grass D, Henrion I, Warren WS, Westman E. Low-cost measurement of face mask efficacy for filtering expelled droplets during speech. *Science Advances.* 2020;6(36):eabd3083.
41. Liu BYH, Lee J-K, Mullins H, Danisch SG. Respirator Leak Detection by Ultrafine Aerosols: A Predictive Model and Experimental Study. *Aerosol Science and Technology.* 1993;19(1):15-26.
42. Lei Z, Yang J, Zhuang Z, Roberge R. Simulation and Evaluation of Respirator Faceseal Leaks Using Computational Fluid Dynamics and Infrared Imaging. *The Annals of Occupational Hygiene.* 2013;57(4):493-506.
43. Mittal R, Ni R, Seo J-H. The flow physics of COVID-19. *Journal of Fluid Mechanics.* 2020;894:F2.
44. Hsiao T-C, Chuang H-C, Griffith SM, Chen S-J, Young L-H. COVID-19: An Aerosol's Point of View from Expiration to Transmission to Viral-mechanism. *Aerosol and Air Quality Research.* 2020:905-910.
45. Tang JW, Liebner TJ, Craven BA, Settles GS. A schlieren optical study of the human cough with and without wearing masks for aerosol infection control. *Journal of The Royal Society Interface.* 2009;6(suppl_6):S727-S736.
46. El-Atab N, Qaiser N, Badghaish H, Shaikh SF, Hussain MM. Flexible Nanoporous Template for the Design and Development of Reusable Anti-COVID-19 Hydrophobic Face

Masks. *ACS Nano.* 2020;14(6):7659-7665.
47. Bergman MS, He X, Joseph ME, et al. Correlation of Respirator Fit Measured on Human Subjects and a Static Advanced Headform. *Journal of Occupational and Environmental Hygiene.* 2015;12(3):163-171.
48. Bergman MS, Zhuang Z, Hanson D, et al. Development of an advanced respirator fit-test headform. *Journal of occupational and environmental hygiene.* 2014;11(2):117-125.
49. Xu G, Antonia R. Effect of different initial conditions on a turbulent round free jet. *Experiments in Fluids.* 2002;33(5):677-683.
50. Asadi S, Cappa CD, Barreda S, Wexler AS, Bouvier NM, Ristenpart WD. Efficacy of masks and face coverings in controlling outward aerosol particle emission from expiratory activities. *Scientific Reports.* 2020;10(1):15665.
51. Azimi P, Zhao D, Stephens B. Estimates of HVAC filtration efficiency for fine and ultrafine particles of outdoor origin. *Atmospheric Environment.* 2014;98:337-346.

4. Survival of aerosolized SARS-CoV-2 on masks

Jin Pan[a], Aaron J. Prussin II[a], Seth A. Hawks[b], Nisha K. Duggal[b], Linsey C. Marr[a*]

[a] Civil and Environmental Engineering, Virginia Tech, Blacksburg, VA 24061, USA

[b] Department of Biomedical Sciences and Pathobiology, Virginia-Maryland College of Veterinary Medicine, Blacksburg, VA 24061, USA

[*] Corresponding author: lmarr@vt.edu (L. Marr).

4.1. Abstract

The potential for masks to act as fomites in the transmission of SARS-CoV-2 in real-world situations is not well understood. In theory, a person could touch a contaminated mask and transfer virus to their mucus membranes, but for infection to occur, the virus must maintain infectivity while on the mask, among other steps in the process. Several studies have evaluated the persistence of SARS-CoV-2 on different types of masks, but the methods relied on inoculating the surface with unrealistically large droplets containing the virus. Under such conditions, survival of SARS-CoV-2 may be prolonged, and hence the potential for fomite transmission may be exaggerated. In this study, we contaminated the masks in a more realistic way: we aerosolized a suspension of SARS-CoV-2 in saliva at a realistic titer and used a vacuum pump to pull the aerosol through six different types of masks. SARS-CoV-2 lost all detectable infectivity within an hour at 28°C, 80% RH on an N95, surgical mask, polyester mask, and two different cotton masks. The virus was still viable on a nylon/spandex mask. SARS-CoV-2 RNA remained stable for an hour on most of the masks. Differences in particle collection efficiency and elution efficiency among the masks influenced the results. The potential for masks contaminated with SARS-CoV-2 aerosols to act as fomites appears to be less than indicated by studies involving inocula with very large droplets.

4.2. Introduction

Although SARS-CoV-2 appears to be transmitted mainly via the airborne route,[1-5] the fomite route may also contribute to transmission. Two critical processes in this route are the ability of the virus to survive on a surface and the efficiency of its transfer from the surface to people's hands. Previous studies have assessed the survival of SARS-CoV-2 in droplets on different surfaces, including plastics, metals, fabrics, and personal protective equipment.[6-13] Despite such efforts, only a few studies focused on survival of SARS-CoV-2 on fabrics, and fewer still on cloth masks. Given that universal masking has been advised by many public agencies as a high-priority precaution, masks could be a potentially important fomite, as they directly collect exhaled aerosols and droplets,[14,15]

In studies of survival of SARS-CoV-2 on textiles, the most commonly tested materials are cotton and meltblown, non-woven polypropylene, which is used in surgical masks and respirators. One study reported that SARS-CoV-2 lost infectivity on cotton t-shirts after 4 hours,[8] whereas two other studies found that SARS-CoV-2 remained infectious for up to 72 hours .[9,11] The maximum reported reduction of SARS-CoV-2 on cotton was 90% after 5.57 days.[10] SARS-CoV-2 in droplets seemed to persist on polyester for only a short duration: 2.5 hours on a t-shirt made of 85% polyester and 15% elastane,[11] and 4 hours on 65% polyester and 35% cotton.[13] SARS-CoV-2 survived on surgical masks for 4-7 days.[6,9,11] Of note, SARS-CoV-2 remained viable on the outer layer of surgical masks for 7 days and on the inner layer for only 4 days.[6] These studies were conducted at temperatures between 20°C and 22°C and at relative humidities (RH) between 35% and 65%, except for one study in which the conditions were not specified. Virus viability varies with temperature and RH. Two studies tested the persistence of SARS-CoV-2 on N95 masks, and the results differed greatly, ranging from 2 days at 25°C and 70% RH[12] to up to 21 days at 20°C and 35-40%.[8] Three studies tested survival of SARS-CoV-2 on Tyvek; they reported that virus was undetectable after 2 days at 25°C and 70% RH[12], 7 days at 22°C and 45% RH,[11] and 21 days at 20°C and 35-40%,[8] respectively. To summarize, SARS-CoV-2 applied to materials in droplets larger than 5 μL can remain viable for the longest period on N95 masks, followed by surgical

masks, cotton, and polyester, and viability is sensitive to temperature and RH.

Though SARS-CoV-2 in large droplets was able to survive for up to multiple days on many different materials, such prolonged survival under lab-controlled conditions deviates from observations in the built environment, where researchers have found viral RNA but no viable virus.[16-23] These discrepancies might result from differences between lab-controlled and real-world environments, and more importantly, the size of the droplets used to inoculate surfaces in laboratory experiments. Objects may become fomites after virus-laden aerosols and droplets exhaled by an infected person deposit on the surface,[24-26] but respiratory droplets are mostly <100 μm in diameter,[27,28] which corresponds to a volume of 5×10^{-4} μL at most, orders of magnitude smaller than the droplets (>5 μL) used to mimic contaminated surfaces in previous studies.[6-13] Size influences the evaporation rate of these droplets, and evaporation rate influences virus survival.[29] Therefore, it is essential to examine droplets of realistic size when exploring the survival of viruses on surfaces.

We quantified the persistence of SARS-CoV-2 on six different types of masks using a more realistic approach to contaminate the masks. First, we aerosolized a suspension of SARS-CoV-2 in saliva at a realistic titer, and then we used a vacuum pump to pull the aerosol through the masks to mimic what happens when a person inhales. We expected that the aerosolized SARS-CoV-2 would lose infectivity on the mask fabric within an hour, more quickly than the hours to days observed in previous studies using very large droplets.

4.3. Methods and materials

4.3.1. Masks

We acquired six popular, commercially available masks for testing. Table 4-1 shows the models and materials of these masks in detail. We tested new masks that had not been washed or otherwise treated. The amount of virus that is captured on a mask depends on its material filtration efficiency, so we measured this property as a function of particle size using the method described in Chapter 3.2.2 with a few modifications. In short, we generated particles from a 2% NaCl solution using a

medical nebulizer (AIRIAL). The particles filled a 280 L polyethylene chamber (Sigma AtmosBag, Sigma–Aldrich, ON, Canada) containing a small fan to promote mixing. We measured particle concentrations and size distributions over the range from 0.04 to 1 μm using a scanning mobility particle sizer (SMPS 3936, TSI Inc., MN, USA) and from 0.5 to 5 μm using an aerodynamic particle sizer (APS 3321, TSI Inc., MN, USA). We mounted circular pieces of each material in a 25 mm stainless steel filter holder (Advantec, Cole Parmer, IL, USA), which was connected to a pump (AirChek XR5000, SKC Ltd., PA, USA) whose flow rate was adjusted to maintain the total flow rate at 2 L/min when combined with the SMPS or APS. We calculated the filtration efficiency of each mask material using equation (3-1). We conducted these experiments in duplicate using two different pieces from each mask.

Table 4-1. Masks tested in this study.

Name	Inner layer	Middle layer	Outer layer
N95 respirator	Polyester	Polypropylene	Polyester
Surgical mask	Melt-blown, non-woven polypropylene		
Polyester	Cotton blend	Cotton blend	100% Polyester
Cotton knit	100% cotton knit		
Cotton poplin	100% cotton poplin		
Nylon/spandex	90% Nylon, 10% Spandex	Polypropylene	90% Nylon, 10% Spandex

4.3.2. Virus preparation

We passaged the SARS-CoV-2 strain USA-WA1/2020 (NR-52281, BEI Resources, Manassas, VA) in Vero E6 cells once and subsequently in Vero cells once, as described in Hawks et al.[30] All experiments were conducted in a biosafety level 3 (BSL-3) laboratory. The initial titer of harvested viruses was 7-$\log_{10}$ PFU/mL. The virus stock was further diluted in pooled human saliva (Lot 33265, Innovative Research, MI, USA) to 5-$\log_{10}$ PFU/mL, which was used for subsequent SARS-CoV-2 aerosol generation.

4.3.3. Aerosol generation and mask contamination

We evaluated the stability of SARS-CoV-2 aerosols on the masks in an induction chamber with

a sliding top (Stoelting Company, IL, USA) with dimensions of 23 cm (L) × 12.7 cm (W) × 12.7 cm (H) (Figure 4-1). A medical nebulizer (AIRIAL) with a flow rate of 5 L/min was connected to the side of the chamber through a port. We filled the nebulizer's cup with 1 mL of virus suspension in saliva. Three 25 mm stainless steel filter holders (Advantec, Cole Parmer, IL, USA) were positioned inside the chamber, each connected to a high-efficiency particulate air filter capsule (Filter, 3/8" FNPT, 10" long, HEPA Grade, TSI Inc., MN, USA) and a pump (AirChek XR5000, SKC Ltd., PA, USA) located outside the chamber (Figure 4-1). Each pump ran at a flow rate of 2 L/min, resulting in a total flow rate of 6 L/min removed from the chamber. Make-up air entered the chamber through a slit on the top, through the partially open lid, as shown in Figure 4-1. A sensor (HOBO UX100-011, Onset Corporation; Bourne, MA) inside the chamber monitored temperature and RH. A small fan was installed in front of the aerosol inlet to mix the air inside the chamber. The entire experiment was contained in a biosafety cabinet in a BSL-3 laboratory.

We ran an experiment to verify that the three filter holders experienced similar concentrations of particles. Using an optical particle counter (AeroTrak 9306, TSI Inc., MN, USA), we measured the particle concentration and size distribution through each filter holder. For biosafety reasons, we nebulized saliva alone, without virus, for this experiment (Figure S1). There were no significant differences among the three filter holders in terms of the number of particles and size distribution. These values remained stable for the first two minutes of nebulization (Figure S1).

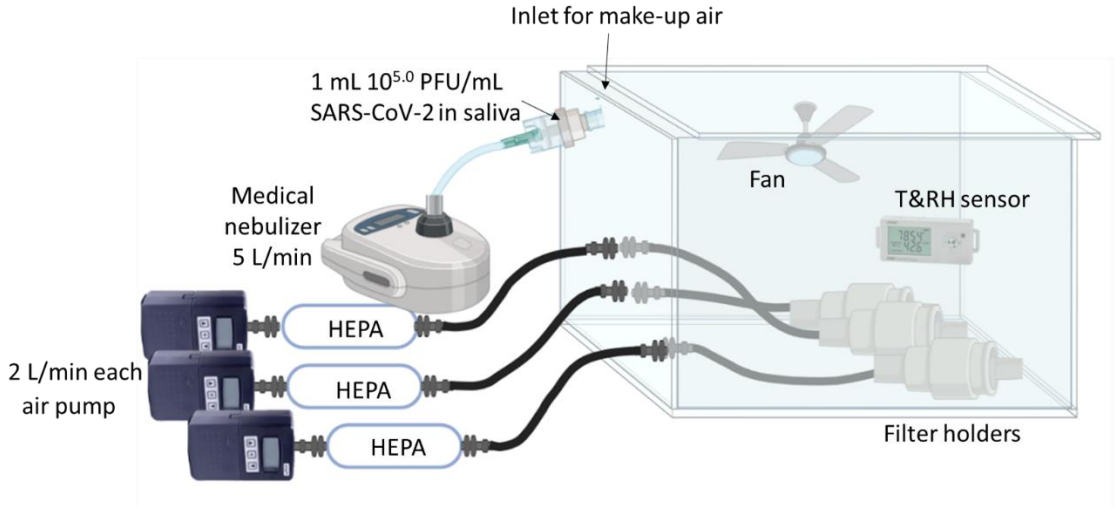

Figure 4-1. Schematic of the setup for aerosol generation and mask contamination.

To test each mask in triplicate, we cut three circular pieces, 25 mm in diameter, from the mask and placed them in the filter holders. For each experiment, we first turned on the three pumps and then the nebulizer. Sample collection proceeded for 3 min, after which only the nebulizer was turned off. We allowed the pumps to run for another minute to remove most of the remaining aerosols from the chamber. We then opened the chamber and immediately transferred the mask pieces into sterile Petri dishes. We incubated the mask pieces at 28°C and 80% RH, similar conditions that a mask worn by humans would experience, for 1 hr. For comparison, we also prepared samples at time zero following the same contamination protocol, with no incubation. We prepared and incubated the 1-hr samples first, followed by the time zero samples, and eluted them together. We cleaned and refilled the nebulizer with 1 mL SARS-CoV-2 solution after each aerosolization. To minimize cross-contamination, we wiped the chamber and filter holders with 70% ethanol between each experiment.

4.3.4. Mask fabric elution, plaque assay, and RT-qPCR.

We subjected each mask piece to bead beating (Qiagen tissuelyser II, Hilden, Germany) in a 2-mL microcentrifuge tube filled with 1 mL of BA-1 buffer[31] and two 2.8-mm stainless steel beads (Benchmark Scientific, NJ, USA), oscillating for 1 min at 25 Hz. To estimate elution efficiency, we also eluted mask pieces onto which we had pipetted ten 1 µL SARS-CoV-2 droplets; additional

details can be found in the Supporting Information. Once the materials were eluted, we immediately transferred the eluates into a -80°C freezer to preserve the virus for both plaque assay and RNA extraction. We determined the amount of viable virus recovered from each piece by plaque assay, as described in Chapter 2.3.3, except that we only did one instead of six 10-fold dilutions. The limit of detection (LOD) of the assay was 5 plaque forming units (PFU) per piece, and we assigned this value to the results that were below the LOD when calculating statistics. To extract and quantify RNA gene copies (gc) in the eluates, we followed the method described in Chapter 2.3.3. The LOD was 17 gc/piece based on the gene copy number at 40 cycles.

4.4. Results and discussion

4.4.1. Material filtration efficiency

We determined the material filtration efficiency of the masks listed in Table 4-1 as a function of aerodynamic diameter to evaluate their ability to collect SARS-CoV-2-laden aerosols (Figure 4-2). Particle concentrations in the size range of 0.1 to 1 μm were measured by SMPS while those in the range of 2 to 4 μm were measured by APS. The efficiencies shown are not continuous due to the differences in detection methods between SMPS and APS.

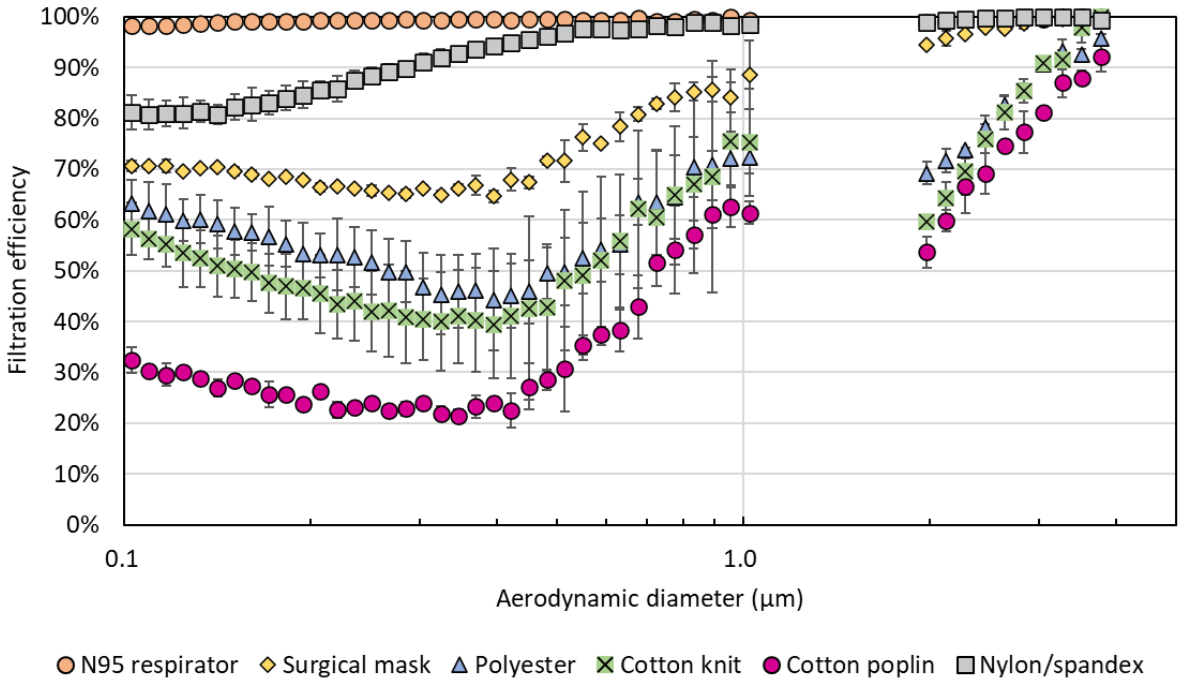

Figure 4-2. Material filtration efficiency of masks. Error bars represent standard deviation of duplicates.

The N95 respirator had the highest filtration efficiency: >95% across all particle sizes, as expected. The nylon/spandex mask performed second best, with a minimum filtration efficiency of ~80%. The surgical mask maintained a filtration efficiency above 60%. The other cloth masks had much lower filtration efficiencies; their minima were below 50%. All the masks showed a higher filtration efficiency at 2-4 µm. In this size range, the N95 respirator and nylon mask had filtration efficiencies of nearly 100%, while the cotton poplin mask performed worst (filtration efficiency >50%).

4.4.2. Stability of SARS-CoV-2 in aerosols on mask fabrics

Figure 4-3 shows the number of infectious SARS-CoV-2 virions in terms of plaque forming units (PFU) detected on mask pieces at 0 hr and 1 hr. Due to varying particle collection efficiency of the different masks, each collected different amounts of virus. In addition, the elution efficiency may vary across masks. These two factors combined result in different starting titers across masks at time zero.

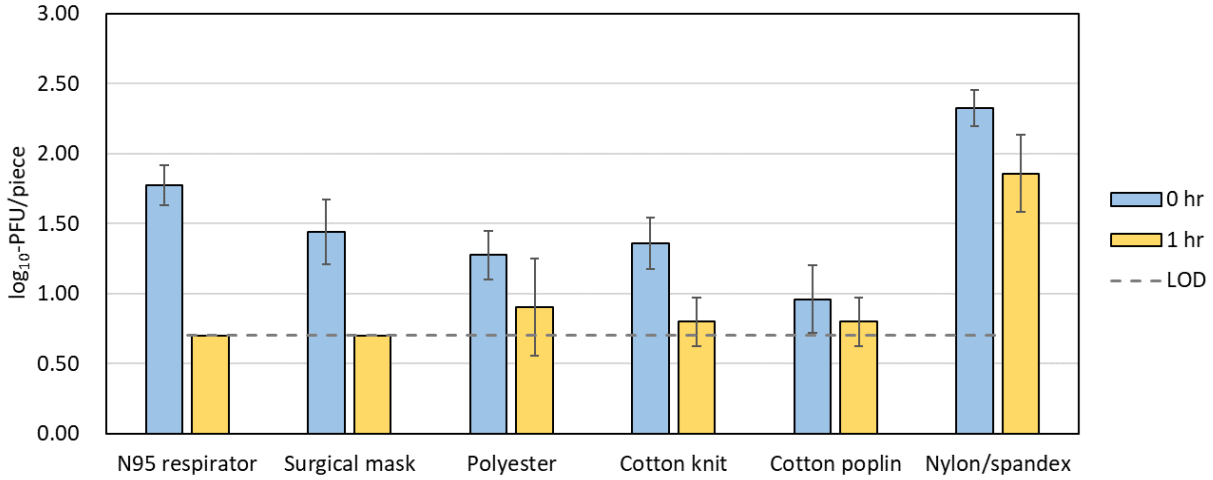

Figure 4-3. Stability of SARS-CoV-2 aerosols on masks. Error bars indicate the standard deviation of triplicates.

There was no detectable infectious virus on the N95 respirator and the surgical mask after 1 hr. The decay rate was at least 1.1-$\log_{10}$ PFU/hr for the N95 respirator and 0.7-$\log_{10}$ PFU/hr for the surgical mask. There was very little detectable infectious virus on the two cotton masks. The decay rates were 0.16- and 0.56-$\log_{10}$ PFU/hr on the poplin and knit cotton, respectively. Likewise, the amount of infectious virus on the polyester mask was close to the limit of detection after 1 hr. An exception was the nylon/spandex mask. The decay rate was <0.5-$\log_{10}$ PFU/hr, and considering its high starting titer, there was still around 1.9-$\log_{10}$ on the mask piece after 1 hr of incubation.

If most virus on masks is deposited in aerosol form, it is likely that it will lose infectivity within an hour as opposed to much longer durations of several hours to days suggested in previous studies that applied inocula in unrealistically large droplets.[6-10,12,13,32]Among those studies, the lowest titer applied was 5×10^4 $TCID_{50}$ per piece.[12] Here, we applied a comparable amount of virus in aerosols to each mask piece, based on the amount of virus aerosolized (1 mL of suspension containing 10^5 PFU/mL), the amount pulled through each piece (1/3 each), and the material filtration efficiency (20-100%). SARS-CoV-2 concentrations on the order of 1-10 $TCID_{50}$ or gc per liter of air have been detected in patient rooms in hospitals,[33,34] so it would take ~100-1000 minutes to load a high-quality mask with the amount of virus used in this study if we assume an inhalation rate of 10 L/min, and this load would be distributed over a larger area of the mask than

the 25 mm circular pieces used here. We expect members of the general public to encounter less virus in the air typically, so their masks would be less contaminated than in our experiments, and virus would decay at a rate faster than it accumulates on the mask. It is still possible that transient exposure to a high concentration of aerosolized virus followed by touching of the mask within minutes could lead to the transfer of infectious virus to fingers or another surface.

There are several reasons for differences between our findings and those of other studies. Aerosolized virus is pulled through a mask, and individual particles will be captured on fibers at various depths through the material. In contrast, virus that is pipetted onto a mask in large droplets may remain on the surface of the mask, where it is easier to remove and may be more prone to aggregation, which protects viruses from decay.[35] Factors that affect the survival of SARS-CoV-2, such as the equilibration time,[36] solute concentration (e.g. salts and proteins),[29,36,37] solute distribution,[38] and pH distribution,[39] are all impacted by the size of aerosols or droplets. Therefore, SARS-CoV-2 in small aerosols (<5 μm in diameter) tends to decay much faster than in large droplets (50 μL).[7]. These results also suggest that risk of fomite transmission via masks might be exaggerated in past findings due to the use of unrealistic inocula, although most these studies are limited by the use of culture media rather than actual respiratory fluid, except one study that used mucin, bovine serum albumin, and tryptone to mimic typical virus-containing fluids.[8]

4.4.3. Persistence of SARS-CoV-2 RNA

Figure 4-4 shows that the amount of SARS-CoV-2 RNA on most masks did not change over 1 hr, consistent with previous findings.[8,32] No significant differences (p>0.05, Student's t-test) were observed between 0 hr and 1 hr for the surgical, polyester, cotton poplin, cotton knit, and nylon/spandex masks. Similar to the results for infectious virus, the number of gene copies detected also depended on the collection and elution efficiency, and thus differed among masks. The nylon/spandex mask had the highest number of gene copies, for its filtration efficiency was above 90%, while the cotton poplin mask had the lowest number in part because of its low filtration efficiency. Moreover, the N95, which should have presented the highest number of gene copies due to its excellent filtration efficiency, showed fewer gene copies than did the nylon/spandex

mask at both 0 hr and 1 hr. This may be due to a lower elution efficiency from its comparatively thicker and stiffer material; bead beating may have been less effective on it compared to more flexible materials. In addition, hydrophobicity and other related physical properties might impact the elution efficiency.

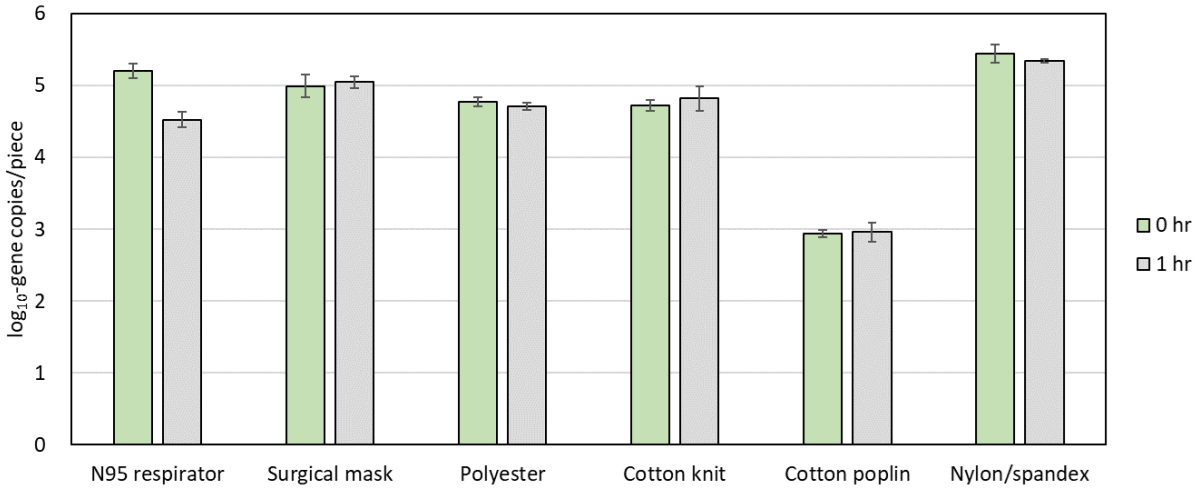

Figure 4-4. Number of gene copies recovered from masks. Error bars indicate the standard deviation of triplicates.

In addition, the N95 respirator exhibited a significantly lower number of gene copies after 1 hr compared to 0 hr (p<0.05, Student's t-test). The difference may have been due to inconsistency in aerosol production by the nebulizer with this mask. Developing a more consistent method to generate aerosols will be crucial to reduce the uncertainties in the aerosolization process and beneficial to future studies of this kind.

Acknowledgements

Virginia Tech's Center for Emerging, Zoonotic, and Arthropod-borne Pathogens, Fralin Life Sciences Institute, and Institute for Critical Technology and Applied Science provided support for this work. The authors thank Dr. Peter Vikesland and Dr. David Schmale at Virginia Tech for helpful discussions.

Supporting information

Methods and materials

Aerosol generation and mask contamination

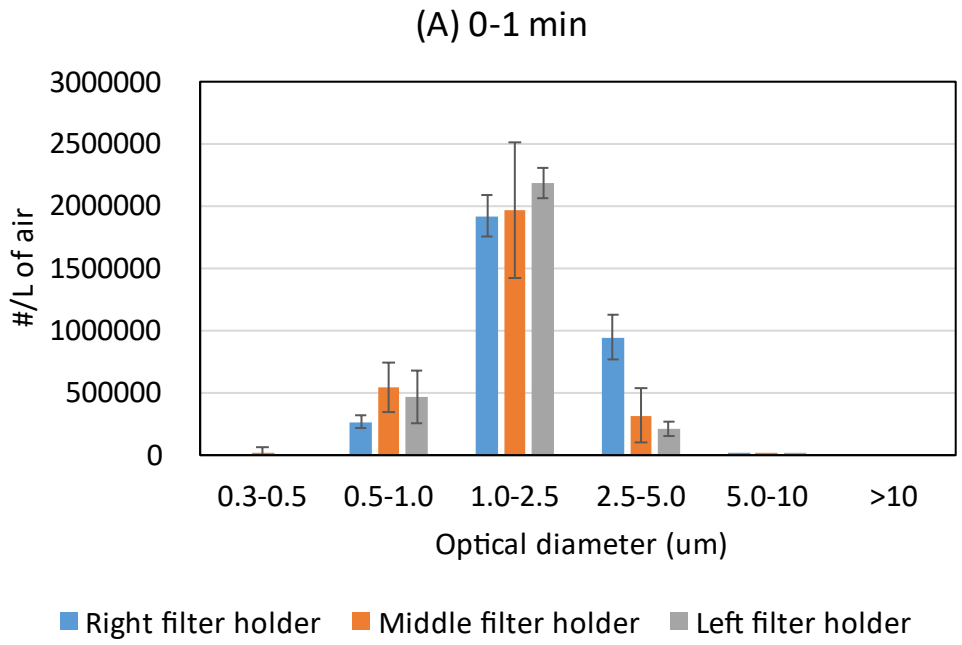

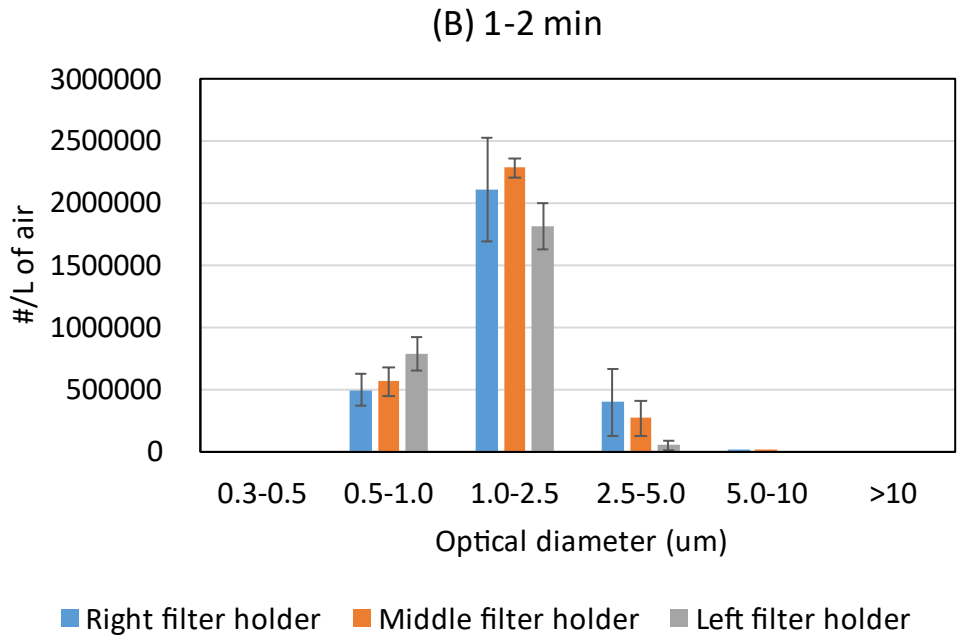

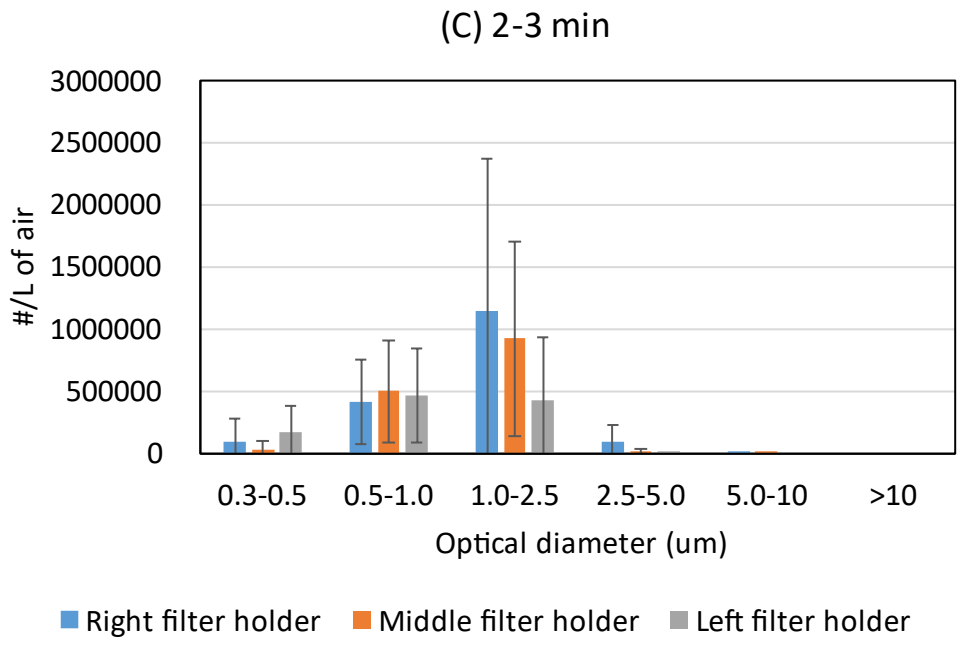

Figure S1. Size distribution and concentration of aerosols generated by the medical nebulizer with saliva from (a) 0 to 1 min, (b) 1 to 2 min, and (c) 2 to 3 min. The detection was conducted from three blank filter holders independently.

Elution efficiency

We estimated the elution efficiency by pipetting ten 1-μL SARS-CoV-2 droplets ($10^{5.0}$ PFU/mL in saliva) directly on the surface of the mask materials, which were later subjected to 5 min of air drying in the hood. The drying time of 5 min is designed to match the treatment of the masks in experiments with aerosols, during which they experienced 4 min of aerosolization plus 1 min of removal and transfer. We eluted these samples and conducted plaque assay following the methods described in the main text, and we compared the results to titer of the virus stock to calculate the elution efficiency (Figure S2). Of note, results based on large droplets cannot be truly representative of the elution efficiency based on aerosols, so these data merely served as a qualitative benchmark.

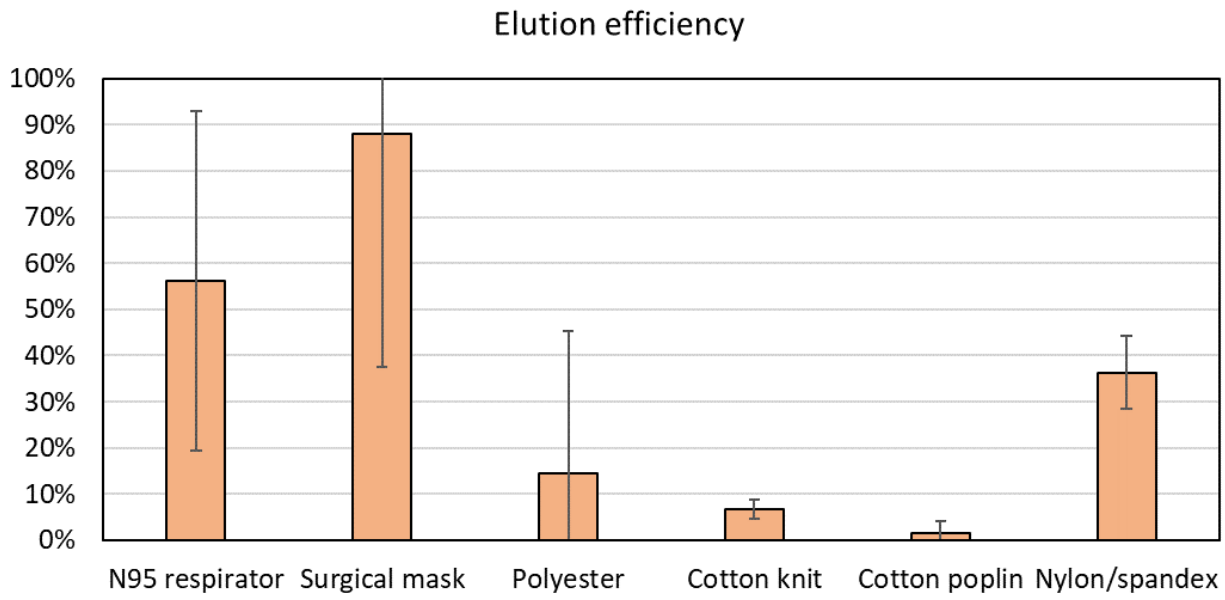

Figure S2. Elution efficiency of mask fabrics loaded with ten 1-μL SARS-CoV-2 droplets ($10^{5.0}$ PFU/mL in saliva)

Reference

1. Allen JG, Marr LC. Recognizing and controlling airborne transmission of SARS-CoV-2 in indoor environments. *Indoor Air.* 2020;30(4):557-558.
2. Morawska L, Tang JW, Bahnfleth W, et al. How can airborne transmission of COVID-19 indoors be minimised? *Environment International.* 2020;142:105832.
3. Asadi S, Bouvier N, Wexler AS, Ristenpart WD. The coronavirus pandemic and aerosols: Does COVID-19 transmit via expiratory particles? *Aerosol Science and Technology.* 2020;54(6):635-638.
4. Hadei M, Hopke PK, Jonidi A, Shahsavani A. A Letter about the Airborne Transmission of SARS-CoV-2 Based on the Current Evidence. *Aerosol and Air Quality Research.* 2020;20(5):911-914.
5. Prather KA, Wang CC, Schooley RT. Reducing transmission of SARS-CoV-2. *Science.* 2020;368(6498):1422.
6. Chin AWH, Chu JTS, Perera MRA, et al. Stability of SARS-CoV-2 in different environmental conditions. *The Lancet Microbe.* 2020;1(1):e10.
7. van Doremalen N, Bushmaker T, Morris DH, et al. Aerosol and Surface Stability of SARS-CoV-2 as Compared with SARS-CoV-1. *New England Journal of Medicine.* 2020;382(16):1564-1567.
8. Kasloff SB, Leung A, Strong JE, Funk D, Cutts T. Stability of SARS-CoV-2 on critical personal protective equipment. *Scientific Reports.* 2021;11(1):984.
9. Liu Y, Li T, Deng Y, et al. Stability of SARS-CoV-2 on environmental surfaces and in human excreta. *Journal of Hospital Infection.* 2021;107:105-107.
10. Riddell S, Goldie S, Hill A, Eagles D, Drew TW. The effect of temperature on persistence of SARS-CoV-2 on common surfaces. *Virology Journal.* 2020;17(1):145.
11. Paton S, Spencer A, Garratt I, et al. Persistence of Severe Acute Respiratory Syndrome Coronavirus 2 (SARS-CoV-2) Virus and Viral RNA in Relation to Surface Type and Contamination Concentration. *Applied and Environmental Microbiology.*87(14):e00526-00521.
12. Kwon T, Gaudreault NN, Richt JA. Environmental Stability of SARS-CoV-2 on Different Types of Surfaces under Indoor and Seasonal Climate Conditions. *Pathogens.* 2021;10(2).
13. Harbourt DE, Haddow AD, Piper AE, et al. Modeling the stability of severe acute respiratory syndrome coronavirus 2 (SARS-CoV-2) on skin, currency, and clothing. *PLOS Neglected Tropical Diseases.* 2020;14(11):e0008831.
14. Ruiz-Bastián M, Rodríguez-Tejedor M, Rivera-Núñez MA, Group SA-C-W. Detection of SARS-CoV-2 genomic RNA on surgical masks worn by patients: Proof of concept. *Enferm Infecc Microbiol Clin (Engl Ed).* 2021:S0213-0005X(0221)00006-00009.
15. Dargahi A, Jeddi F, Ghobadi H, et al. Evaluation of masks' internal and external surfaces used by health care workers and patients in coronavirus-2 (SARS-CoV-2) wards. *Environmental Research.* 2021;196:110948.
16. Yamagishi T, Ohnishi M, Matsunaga N, et al. Environmental Sampling for Severe Acute

Respiratory Syndrome Coronavirus 2 During a COVID-19 Outbreak on the Diamond Princess Cruise Ship. *J Infect Dis.* 2020;222(7):1098-1102.
17. Wang J, Feng H, Zhang S, et al. SARS-CoV-2 RNA detection of hospital isolation wards hygiene monitoring during the Coronavirus Disease 2019 outbreak in a Chinese hospital. *Int J Infect Dis.* 2020;94:103-106.
18. Zhou J, Otter JA, Price JR, et al. Investigating SARS-CoV-2 surface and air contamination in an acute healthcare setting during the peak of the COVID-19 pandemic in London. *Clinical Infectious Diseases.* 2020.
19. Ong SWX, Tan YK, Chia PY, et al. Air, Surface Environmental, and Personal Protective Equipment Contamination by Severe Acute Respiratory Syndrome Coronavirus 2 (SARS-CoV-2) From a Symptomatic Patient. *JAMA.* 2020;323(16):1610-1612.
20. Moore G, Rickard H, Stevenson D, et al. Detection of SARS-CoV-2 within the healthcare environment: a multi-centre study conducted during the first wave of the COVID-19 outbreak in England. *Journal of Hospital Infection.* 2021;108:189-196.
21. Döhla M, Wilbring G, Schulte B, et al. SARS-CoV-2 in environmental samples of quarantined households. *medRxiv.* 2020:2020.2005.2028.20114041.
22. Ben-Shmuel A, Brosh-Nissimov T, Glinert I, et al. Detection and infectivity potential of severe acute respiratory syndrome coronavirus 2 (SARS-CoV-2) environmental contamination in isolation units and quarantine facilities. *Clinical Microbiology and Infection.* 2020;26(12):1658-1662.
23. Colaneri M, Seminari E, Novati S, et al. Severe acute respiratory syndrome coronavirus 2 RNA contamination of inanimate surfaces and virus viability in a health care emergency unit. *Clin Microbiol Infect.* 2020;26(8):1094.e1091-1094.e1095.
24. Dumont-Leblond N, Veillette M, Bhérer L, et al. Positive no-touch surfaces and undetectable SARS-CoV-2 aerosols in long-term care facilities: An attempt to understand the contributing factors and the importance of timing in air sampling campaigns. *American Journal of Infection Control.* 2021;49(6):701-706.
25. Zhang R, Li Y, Zhang AL, Wang Y, Molina MJ. Identifying airborne transmission as the dominant route for the spread of COVID-19. *Proceedings of the National Academy of Sciences.* 2020;117(26):14857.
26. Sun J, Tang X, Bai R, et al. The kinetics of viral load and antibodies to SARS-CoV-2. *Clinical Microbiology and Infection.* 2020;26(12):1690.e1691-1690.e1694.
27. Johnson GR, Morawska L, Ristovski ZD, et al. Modality of human expired aerosol size distributions. *Journal of Aerosol Science.* 2011;42(12):839-851.
28. Morawska L, Johnson GR, Ristovski ZD, et al. Size distribution and sites of origin of droplets expelled from the human respiratory tract during expiratory activities. *Journal of Aerosol Science.* 2009;40(3):256-269.
29. Lin K, Marr LC. Humidity-Dependent Decay of Viruses, but Not Bacteria, in Aerosols and Droplets Follows Disinfection Kinetics. *Environmental Science & Technology.* 2020;54(2):1024-1032.
30. Hawks Seth A, Prussin Aaron J, Kuchinsky Sarah C, et al. Infectious SARS-CoV-2 Is

Emitted in Aerosol Particles. *mBio.* 2021;12(5):e02527-02521.
31. Bunning ML, Bowen RA, Cropp CB, et al. Experimental infection of horses with West Nile virus. *Emerging infectious diseases.* 2002;8(4):380-386.
32. Paton S, Spencer A, Garratt I, et al. Persistence of Severe Acute Respiratory Syndrome Coronavirus 2 (SARS-CoV-2) Virus and Viral RNA in Relation to Surface Type and Contamination Concentration. *Applied and Environmental Microbiology.* 2021;87(14):e00526-00521.
33. Lednicky JA, Lauzardo M, Fan ZH, et al. Viable SARS-CoV-2 in the air of a hospital room with COVID-19 patients. *International Journal of Infectious Diseases.* 2020;100:476-482.
34. Chia PY, Coleman KK, Tan YK, et al. Detection of air and surface contamination by SARS-CoV-2 in hospital rooms of infected patients. *Nature Communications.* 2020;11(1):2800.
35. Gerba CP, Betancourt WQ. Viral Aggregation: Impact on Virus Behavior in the Environment. *Environmental Science & Technology.* 2017;51(13):7318-7325.
36. Oswin HP, Haddrell AE, Otero-Fernandez M, et al. The Dynamics of SARS-CoV-2 Infectivity with Changes in Aerosol Microenvironment. *medRxiv.* 2022:2022.2001.2008.22268944.
37. Lin K, Schulte CR, Marr LC. Survival of MS2 and Φ6 viruses in droplets as a function of relative humidity, pH, and salt, protein, and surfactant concentrations. *PLOS ONE.* 2020;15(12):e0243505.
38. Huynh E, Olinger A, Woolley D, et al. Evidence for a semisolid phase state of aerosols and droplets relevant to the airborne and surface survival of pathogens. *Proceedings of the National Academy of Sciences.* 2022;119(4):e2109750119.
39. Wei H, Vejerano Eric P, Leng W, et al. Aerosol microdroplets exhibit a stable pH gradient. *Proceedings of the National Academy of Sciences.* 2018;115(28):7272-7277.

5. Conclusions

5.1. Outcomes of research objective 1

Quantify SARS-CoV-2 RNA concentration and evaluate virus viability in surface swab samples and on HVAC filters collected from university dormitory rooms housing students who tested positive for COVID-19.

We found high prevalence and concentrations of SARS-CoV-2 RNA on commonly touched surfaces (71/125, 56.8%), HVAC filters (15/21, 71.4%), and exhaust grilles (4/6, 66.7%) in dormitory rooms housing infected individuals. Viral RNA concentrations ranged from 10 to $>10^4$ gene copies per swabbed area. Despite the high level of SARS-CoV-2 RNA, we detected no culturable virus on any surface. High concentrations of SARS-CoV-2 RNA on HVAC filters and exhaust grilles indicated that the virus was present in the air and could be re-distributed via the HVAC systems.

5.2. Outcomes of research objective 2

Evaluate the efficiency of cloth masks compared to a surgical mask and a face shield at blocking aerosols and droplets over a wide range of sizes.

We evaluated the material filtration efficiency, inward protection efficiency, and outward protection efficiency of 10 masks and a face shield on a manikin, using NaCl aerosols over the size range of 0.04 μm to >100 μm. The vacuum bag performed best on all three metrics; it was capable of filtering out 60–96% of particles and achieved an outward protection efficiency of 50%–95% and an inward protection efficiency of 75%–96% for particles of aerodynamic diameter 0.5 μm and greater. The thin acrylic performed worst, with a material filtration efficiency of <25% for particles at 0.1 μm and larger, and inward and outward protection efficiencies of <50%. The material filtration efficiency was generally positively correlated with either inward or outward protection effectiveness, but stiffer materials were an exception to this relationship as they did not fit as closely to the manikin. Factors including stiffness of the material, the way of wearing the mask (e.g., earloops vs. tied around the head), and material hydrophobicity affected the fit of the

mask and thus its performance. Future studies may focus on the influence of material properties on the fit of the mask, and how the transmission of real viruses, including SARS-CoV-2, is altered by wearing the masks.

5.3. Outcomes of research objective 3

Evaluate the persistence of aerosolized SARS-CoV-2 on different types of masks.

We developed a method to contaminate masks with aerosolized SARS-CoV-2 in a realistic manner. On most of the masks tested, including an N95, surgical mask, polyester mask, cotton knit mask, and cotton poplin mask, the virus lost infectivity within one hour. The exception was a nylon/spandex mask. SARS-CoV-2 RNA remained stable on the masks for at least 1 hr. These results suggest that the potential for masks to act as fomites is low. This study also highlighted the importance of applying aerosols of realistic sizes during the contamination process to assess the risk of fomite transmission.

APPENDIX A: Correlating indoor and outdoor temperature and humidity in a sample of buildings in tropical climates

Jin Pan[a], Julian Tang[b], Miguela Caniza[c], Jean-Michel Heraud[d], Evelyn Koay[e], Hong Kai Lee[f], Chun Kiat Lee[g], Yuguo Li[h], Alejandra Nava Ruiz[i], Carlos Francisco Santillan-Salas[j], Linsey C. Marr[a*]

a Civil and Environmental Engineering, Virginia Tech, Blacksburg, VA 24061, USA

b Infection, Immunity and Inflammation, University of Leicester, Leicester, UK

c Global Infectious Diseases Program, Department of Infectious Diseases, St. Jude Children's Research Hospital, Memphis, TN 38105, USA

d Virology Unit, Institut Pasteur de Madagascar, Antananarivo 101, Madagascar

e Department of Pathology, Yong Loo Lin School of Medicine, National University of Singapore

f Singapore Immunology Network (SIgN), Agency for Science, Technology and Research (A*STAR), Singapore 138648

g Department of Laboratory Medicine, National University Health System, 119074, Singapore

h Department of Mechanical Engineering, The University of Hong Kong, Pokfulam Road, Hong Kong, China

i Pediatra Infectólogo, Epidemiólogo, Hospital de Especialidades Pediátricas, Tuxtla Gutiérrez Chiapas, México

j Instituto Nacional de Salud del Niño San Borja, Lima, Peru

* Corresponding author. E-mail address: lmarr@vt.edu (L. Marr).

Reprinted with permission from Pan, J., Tang, J., Caniza, M., Heraud, J. M., Koay, E., Lee, H. K., ... & Marr, L. C. (2021). Correlating indoor and outdoor temperature and humidity in a sample of buildings in tropical climates. *Indoor Air*, 31(6), 2281-2295.

A.1. Abstract

The incidence of several respiratory viral infections has been shown to be related to climate. Because humans spend most of their time indoors, measures of indoor climate, rather than outdoor climate, may be better predictors of disease incidence and transmission. Therefore, understanding the relationship between indoor and outdoor climate will help illuminate their influence on the seasonality of diseases caused by respiratory viruses. Indoor-outdoor relationships between temperature and humidity have been documented in temperate regions, but little information is available for tropical regions, where seasonal patterns of respiratory viral diseases differ. We have examined indoor-outdoor correlations of temperature, relative humidity (*RH*), and absolute humidity (*AH*) over a 1-year period in each of seven tropical cities. Across all cities, the average monthly indoor temperature was 25±3°C (mean ± standard deviation) with a range of 20–30°C. The average monthly indoor *RH* was 66±9% with a range of 50–78%, and the average monthly indoor *AH* was 15±3 g/m^3 with a range of 10–23 g/m^3. Indoor *AH* and *RH* were linearly correlated with outdoor *AH* when the air-conditioning (AC) was off, suggesting that outdoor *AH* may be a good proxy of indoor humidity in the absence of AC. All indoor measurements were more strongly correlated with outdoor measurements as distance from the equator increased. Such correlations were weaker during the wet season, especially when AC was in operation. These correlations will provide insight for assessing the seasonality of respiratory viral infections using outdoor climate data, which is more widely available than indoor data, even though transmission of these diseases mainly occurs indoors.

Key words: temperature, humidity, indoor, respiratory virus, climate, outdoor

A.2. Introduction

Temperature and humidity are associated with a variety of human health maladies. Both factors have been found to contribute to cardiovascular disease;[1-5] and humidity, which affects heat stress and hydration rate, has also been linked to heat-related deaths and all-cause mortality.[6-8] These factors are also associated with the incidence of certain respiratory infections caused by viruses such as SARS-CoV-2,[9,10] influenza virus,[11,12] and respiratory syncytial virus (RSV).[13,14] The seasonality of some respiratory viral infections has been attributed to the effect of temperature and humidity on virus stability and transmissibility and also on immune responses.[15]

Although numerous studies have suggested that there is an association between meteorological conditions, various health conditions, and respiratory viral disease seasonality,[15] nearly all such studies are based on data from outdoor weather stations or output from meteorological models. Given the scarcity of indoor temperature and humidity data, using outdoor measurements has been common practice in the study of climate and health. However, as humans spend most of their time indoors, especially in more developed countries,[16] the indoor climate, rather than the outdoor climate, is likely to be a better indicator of health.[17,18] Most respiratory virus transmission likely occurs indoors.[14,19] Of course, indoor temperature and humidity are influenced by outdoor conditions, but indoor conditions may also be controlled by heating, ventilation, and air conditioning (HVAC) or other regulatory systems[20] and are affected by human activities, resulting in discrepancies between indoor and outdoor measurements. Therefore, whether indoor conditions can be represented by outdoor measurements remains questionable.

There have been several recent studies on indoor-outdoor climate correlations. Two of them based their analyses on data from the northeastern US and drew similar conclusions: indoor temperature is better correlated with outdoor temperature during warm seasons than cool seasons, and outdoor absolute humidity (*AH*) is a good indicator of indoor *AH* across all seasons.[17,21] They also concluded that outdoor relative humidity (*RH*) is not a strong predictor of indoor *RH* year-round. Another study examined the indoor-outdoor correlation in several locations across a range of latitudes, with a focus on temperate regions.[18] The study suggested that actual moisture content

(e.g., *AH*) outdoors was a better proxy for indoor exposure than was *RH*, regardless of season. Two other studies developed models to predict indoor temperature based on outdoor temperature.[22,23] Both studies found a positive correlation between indoor and outdoor temperature, but outdoor temperature alone was not able to fully explain the variability of indoor temperature, even when augmented with solar radiation and dewpoint temperature. Nonetheless, there is little information about indoor-outdoor correlations of temperature and humidity in tropical regions.

Tropical cities have very different meteorological patterns from those in temperate regions. Thus, climate-health seasonality in tropical regions, including that involving respiratory viruses, has been found to differ substantially from that in temperate regions.[24-26] For example, tropical influenza seasonality is not as strong as in temperate regions.[27-29] The seasonal peaks of influenza incidence that are commonly observed in temperate regions are smaller and less distinctive in tropical regions.[19,30] Additionally, the peak timing of both influenza and RSV is more diverse in tropical regions than in temperate regions.[31]

Given the stark differences in climate between tropical and temperate regions, it is crucial to study indoor-outdoor relationships more carefully in order to achieve a global understanding of climate impacts on health. To investigate the relationship between indoor and outdoor temperature and humidity in tropical regions, we collated indoor and outdoor climate data from seven tropical cities, plus one temperate location for reference, and conducted correlation analyses between indoor and outdoor measures. We also explored the seasonal and latitudinal variation of such correlations with the influence of air conditioning (AC) use. The results reveal how well the indoor climate can be represented by outdoor measurements, enabling further advances in the study of climate-health relationships.

A.3. Materials and methods

A.3.1. Indoor measurements

Through personal contacts and St. Jude Children's Research Hospital's PRINCIPAL network, we selected seven study locations in the tropics (latitude -23.5° to 23.5°). Additionally, Blacksburg, Virginia, USA (latitude 37.23°N) served as a temperate reference location. At each location, we

installed three to five temperature and humidity data loggers (HOBO UX100-011A, Onset Corporation; Bourne, MA, USA) in office/academic buildings, hospitals, or residences for at least 12 months. We instructed our collaborators to place the loggers away from vents and out of direct sunlight in a room that is frequently occupied on most days of the week. Loggers were typically located on a shelf or mounted on a wall at a height of 1–2.5 m above the floor. We recorded whether there was an HVAC system in the sampled buildings. In the tropical cities, the buildings sampled had either AC only without heating or lacked indoor climate control. None of the buildings had humidifiers or dehumidifiers. Figure A-1 shows a detailed map of the sampling locations, indicating the number of loggers placed in each type of setting and the presence or absence of an HVAC system. Three of the loggers were placed in different rooms of the same hospital in Tuxtla Gutierrez, so measurements from these are not independent of one another. We do not expect the co-location of the sensors in one city to affect the overall trends.

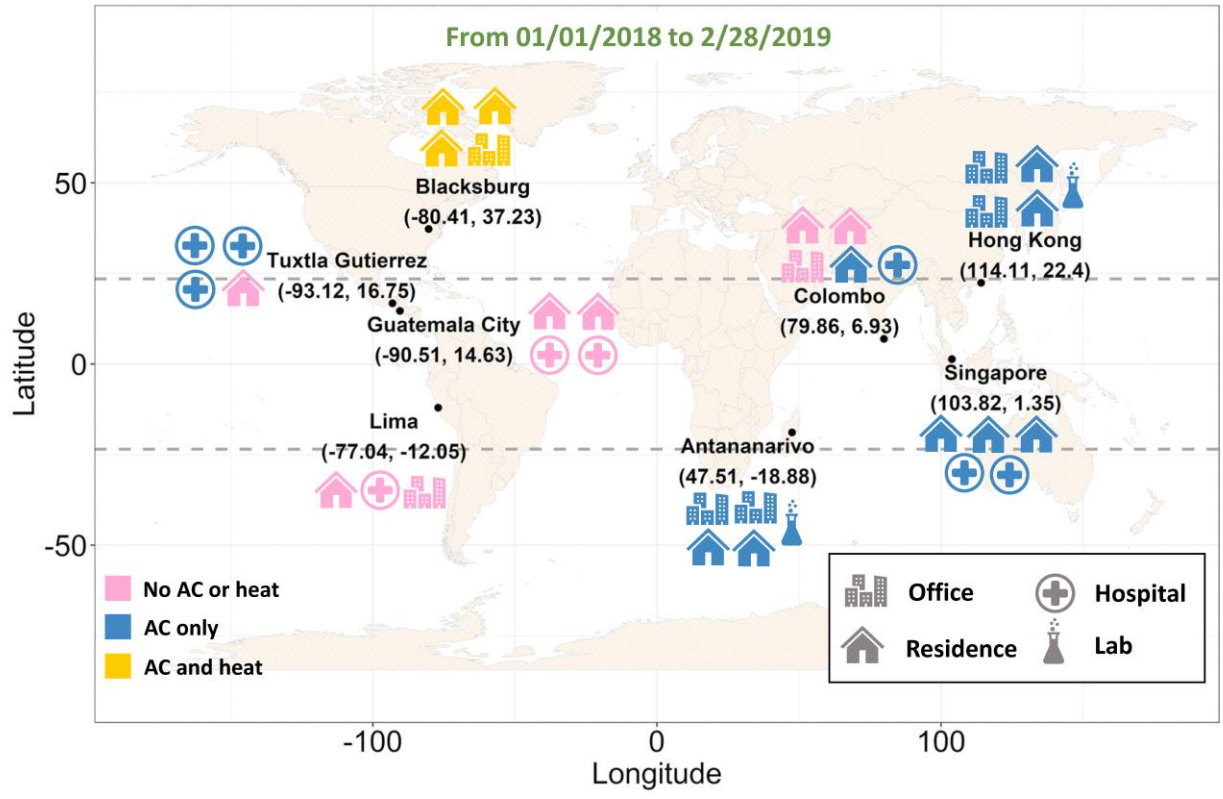

Figure A-1. Locations of 35 temperature and humidity loggers distributed across eight cities (seven tropical and one temperate). The room/building type is indicated by an icon (office, hospital, residence, and lab), and the presence of

air conditioning (AC) and/or heating systems is indicated by the color of the icon. Three of the loggers were placed in different rooms of the same hospital in Tuxtla Gutierrez. The two dashed lines bound the tropical region.

The HOBO data loggers recorded temperature (T, °C) and relative humidity (RH, %) hourly between 1 January 2018 and 28 February 2019 except in Colombo, where the batteries of the loggers died earlier than expected. Prior to distributing them, we confirmed that the sensors' measurements agreed within the manufacturer's specifications by placing them in a constant temperature room, synchronized them, and installed fresh batteries. According to the manufacturer, the sensor measures T with an accuracy of ±0.21°C from 0°C to 50°C, and RH with an accuracy of ±2.5% over the range of 10% to 90% and an accuracy of ±5% at RH below 10% or above 90%. For each hourly measurement, we calculated absolute humidity (AH, g/m^3) based on T (°C) and RH (%) according to Equation (A-1):[32]

$$AH = \frac{1322.7 \times exp\left(\frac{17.625 \times T}{T + 243.04}\right) \times \left(\frac{RH}{100}\right)}{T + 273.15} \quad \text{(A-1)}$$

For additional analyses, we calculated daily averages from the hourly measurements (T, RH, and AH).

A.3.2. Outdoor measurements

We obtained outdoor measurements of temperature and humidity from the closest airport weather station to each city (Table S1). Using code written in Python 3.7, we scraped outdoor data from Weather Underground. The raw data for each city included T, RH, and dew point temperature (T_d), except for Tuxtla Gutierrez, where only T and T_d were recorded. For Tuxtla Gutierrez, we calculated RH (%) from T (°C) and T_d (°C) according to Equation (A-2):[32]

$$RH = 100 \times \frac{exp\left(\frac{17.625 \times T_d}{243.04 + T_d}\right)}{exp\left(\frac{17.625 \times T}{243.04 + T}\right)} \quad \text{(A-2)}$$

Then, we calculated AH (g/m^3) for all cities using Equation (A-1). The temporal resolution of

outdoor measurements varied by city, from 15 minutes to 24 hours. Therefore, we calculated the daily average of outdoor measurements for consistency across cities.

A.3.3. Statistical analyses

The indoor data spanned from 1 January 2018 to 28 February 2019 except those from Colombo, which lacked indoor data after 1 December 2018, and Lima, which lacked data in February 2019. We scraped outdoor data matching the timeframe of all available indoor data, resulting in 424 observations (Colombo has 334 observations). We compared indoor and outdoor conditions using a t-test with a significance level of 0.05. To address our research objectives, we separated the data by season or the operating status of HVAC systems. For season-specific analyses, we divided the data into two seasons: wet season (May to October) and dry season (November to April) in the Northern Hemisphere, and vice versa in the Southern Hemisphere.[33,34] Singapore does not have distinct wet or dry seasons.

For HVAC-specific analyses, we defined three system statuses: "AC on," "AC off," and "heat on." We were not able to record directly the on/off times of HVAC systems in this study, so we assigned a status based on humidity observations. Because AC systems remove water vapor from outdoor air that enters the indoor environment, we established a criterion to differentiate "AC on" and "AC off" conditions. When indoor *AH* minus outdoor *AH* was less than or equal to -5 g/m^3, we assigned the status "AC on," and vice versa. The "heat on" status only occurred in Blacksburg, the reference location, as none of the buildings in tropical cities had a heating system. When indoor *T* minus outdoor *T* was greater than or equal to 15°C, we assigned the "heat on" status. We verified that the assignments matched expectations for the hour of day and time of year in each location by trying several different cutoff values and selecting the ones that generated the most sensible results (e.g., in residences, AC was on during the summer in the evenings on weekdays, when people were expected to be at home).

We tested indoor-outdoor differences using both a Student's t-test, which assumes that the underlying data are normally distributed, and a Wilcoxon test, a nonparametric test that does not require a normal distribution, using a significance level of 0.05 (Table S4). The two tests produced

similar results in terms of identifying differences. To evaluate the relationship between indoor and outdoor measurements, we used an ordinary least squares regression (OLS) model. We also computed the Pearson correlation coefficient (r) to evaluate the strength of the linear correlation by season and by HVAC status. Additionally, we constructed a multivariate OLS model to analyze the collective influence of multiple variables, including building type, season, and AC status, on the respective indoor measurements. We adopted Spearman's correlation (ρ), a nonparametric test assessing monotonic relationship regardless of linearity, to assess the monotonicity between indoor and outdoor variables while AC was on. We conducted all statistical analyses in Python 3.7 and generated all figures using Python 3.7 and R 3.6.1.

A.4. Results

We recorded indoor temperature and humidity in 35 rooms across seven tropical cities and one temperate location over one year and compiled outdoor temperature and humidity data from weather stations at nearby airports. Monthly averages and standard deviations of both indoor and outdoor *T, RH,* and *AH* for all cities appear on a world map (Figure A-2), and the annual averages are shown in Table A-1.

Table A-1. Yearly means in 2018 (standard deviation) of indoor and outdoor measurements.

City	Indoor			Outdoor		
	T (°C)	RH (%)	AH (g/m^3)	T (°C)	RH (%)	AH (g/m^3)
Blacksburg*	22.3 (2.2)	42.2 (14.7)	8.4 (3.4)	12.3 (10.3)	64.2 (19.9)	8.2 (5.5)
Antananarivo	23.5 (2.5)	57.3 (12.3)	12.0 (2.7)	19.4 (4.7)	74.4 (19.1)	12.1 (2.7)
Colombo	29.4 (1.8)	73.3 (8.4)	21.4 (1.9)	27.7 (2.4)	78.8 (1.1)	20.9 (2.0)
Guatemala	22.8 (1.7)	61.6 (7.3)	12.6 (1.8)	19.3 (3.5)	75.3 (16.3)	12.2 (1.8)
Hong Kong	24.0 (3.0)	63.7 (10.8)	14.1 (4.0)	23.6 (5.7)	69.3 (14.1)	15.4 (5.5)
Lima	23.4 (3.1)	67.6 (8.4)	14.1 (1.3)	26.2 (3.3)	73.4 (13.9)	17.7 (1.2)
Singapore	27.0 (2.3)	67.6 (9.9)	17.6 (4.0)	27.9 (2.1)	81.0 (10.6)	21.6 (1.4)
Tuxtla Gutierrez	22.7 (2.4)	68.8 (7.2)	13.9 (1.5)	25.6 (4.1)	64.2 (8.9)	15.3 (2.6)
All tropical cities	24.7 (2.5)	65.7 (9.4)	15.1 (2.7)	24.2 (3.9)	73.8 (13.2)	16.5 (2.8)

A.4.1. Temperature

For cities closer to the equator, such as Colombo and Singapore, the monthly average outdoor temperature was steadily high throughout the year, ranging from 23°C to 30°C with little seasonality (Figure A-2a). In Guatemala City and Tuxtla Gutierrez, which are in between the Tropic of Cancer and the equator, weak temperature seasonality was apparent, as shown by outdoor temperatures that were 4–7°C higher in the wet season than in the dry season. Although Guatemala City is only ~350 km from Tuxtla Gutierrez, its outdoor temperature was 7–10°C lower than Tuxtla Gutierrez's because of its higher altitude (1500 m vs. 500 m). In tropical cities that are farther from the equator, such as Hong Kong and Antananarivo, the monthly average outdoor temperature ranged from 15°C to 30°C and was 10–15°C higher in the respective hemisphere's summer compared to winter, showing a stronger seasonality than in other tropical cities.

Indoor conditions were more consistent across locations. The monthly average indoor temperature of all tropical cities fell within the range of 20–30°C, averaging 24.7±2.5°C (mean ± standard deviation). In Guatemala City and Antananarivo, the indoor temperatures were 0–5°C higher than outdoors, as opposed to other tropical cities where the difference was smaller.

A.4.2. Humidity

Indoor and outdoor *RH* were highest in Colombo and Singapore, where the monthly averages were above 70%. In both cities, indoor *RH* was slightly lower than outdoor *RH* (Figure A-2b). The outdoor *RH* of Guatemala City, Antananarivo, and Tuxtla Gutierrez was similar; all monthly averages exceeded 62%. However, Guatemala City's and Antananarivo's indoor *RH* was 10–15% lower than its outdoor *RH*, whereas indoor *RH* was higher than outdoor *RH* in Tuxtla Gutierrez. In Hong Kong, outdoor *RH* ranged from 54% to almost 80%, showing a relatively large seasonal difference, but indoor *RH* was still lower than outdoor *RH*.

The average monthly indoor *RH* in tropical cities was 66±9%, considerably higher than in the temperate city, which averaged 42±15%. Over the course of the year, the indoor *RH* of each tropical city followed the same temporal trend as its respective outdoor *RH*. In contrast, indoor *RH* was substantially lower than outdoor *RH* in the temperate location (Blacksburg) during wintertime,

when heating is the norm. Although some tropical cities exhibited seasonality, their seasonal fluctuations in *RH* were much weaker compared to those in Blacksburg.

Outdoor *AH* varied widely among cities. In Singapore and Colombo, outdoor *AH* remained above 18 g/m^3 throughout the year without obvious seasonality. Outdoor *AH* in Guatemala (10–13 g/m^3) and Tuxtla Gutierrez (12–18 g/m^3) was much lower. Outdoor *AH* in Antananarivo and Hong Kong was 14–21 g/m^3 and 8–22 g/m^3, respectively; it exhibited strong seasonality in both cities. There was a large difference in *AH* (up to 13 g/m^3) between the wet and dry seasons in these two cities.

The average monthly indoor *AH* in tropical cities was 15±3 g/m^3 (8±3 g/m^3 in the temperate city). In Guatemala City and Colombo, where there was little AC control (two rooms in Colombo had individual AC units), indoor *AH* followed the trend of outdoor *AH* over the year, with indoor *AH* slightly higher than outdoor *AH*. In Hong Kong, indoor *AH* was generally 5–10 g/m^3 lower than outdoor *AH* during the wet season due to the removal of water vapor by AC systems but was roughly equal to outdoor *AH* during the dry season. In Antananarivo, the difference between indoor and outdoor *AH* was not significant regardless of season, unlike in Tuxtla Gutierrez where indoor *AH* was lower than outdoor *AH* year-round. In Singapore, AC was in use during most of the year, so its indoor *AH* was always lower than outdoor *AH* by 4–5 g/m^3 on average.

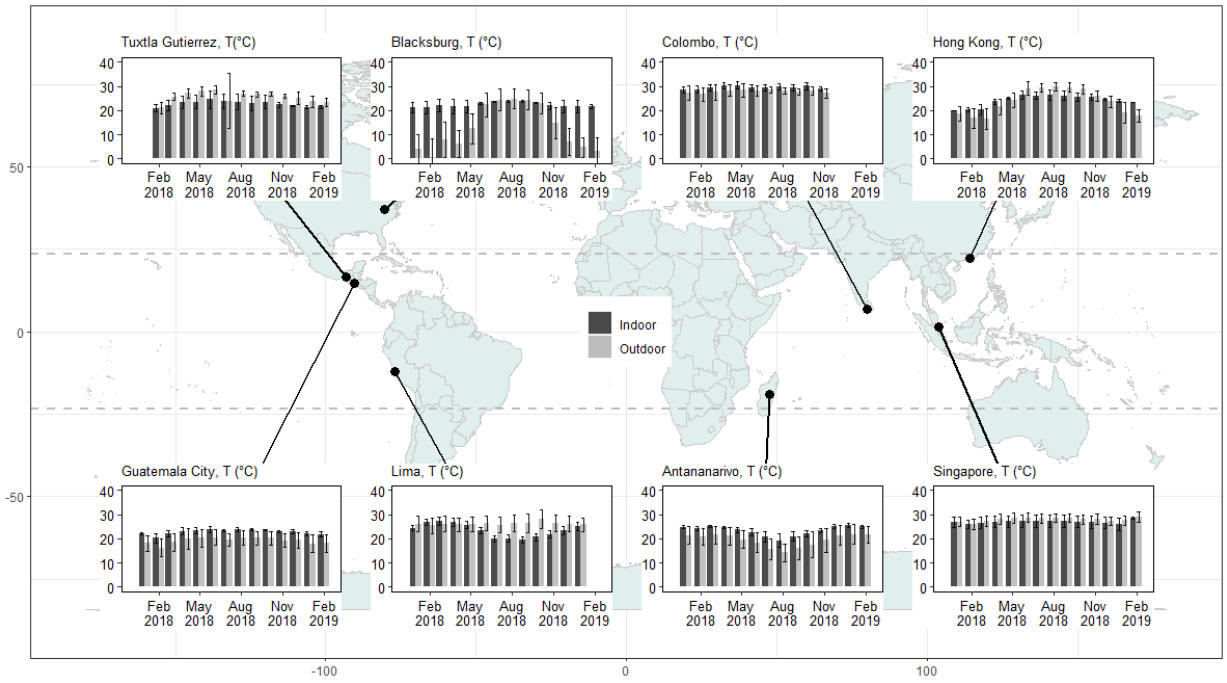

(a) Monthly temperature

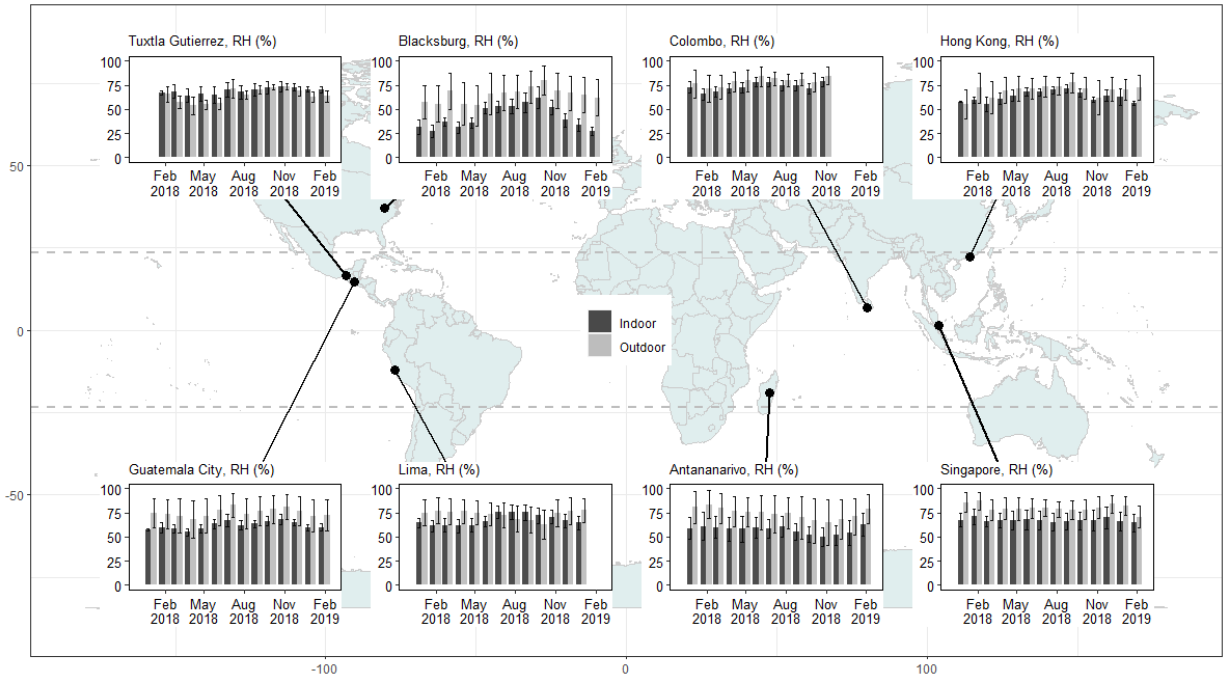

(b) Monthly relative humidity

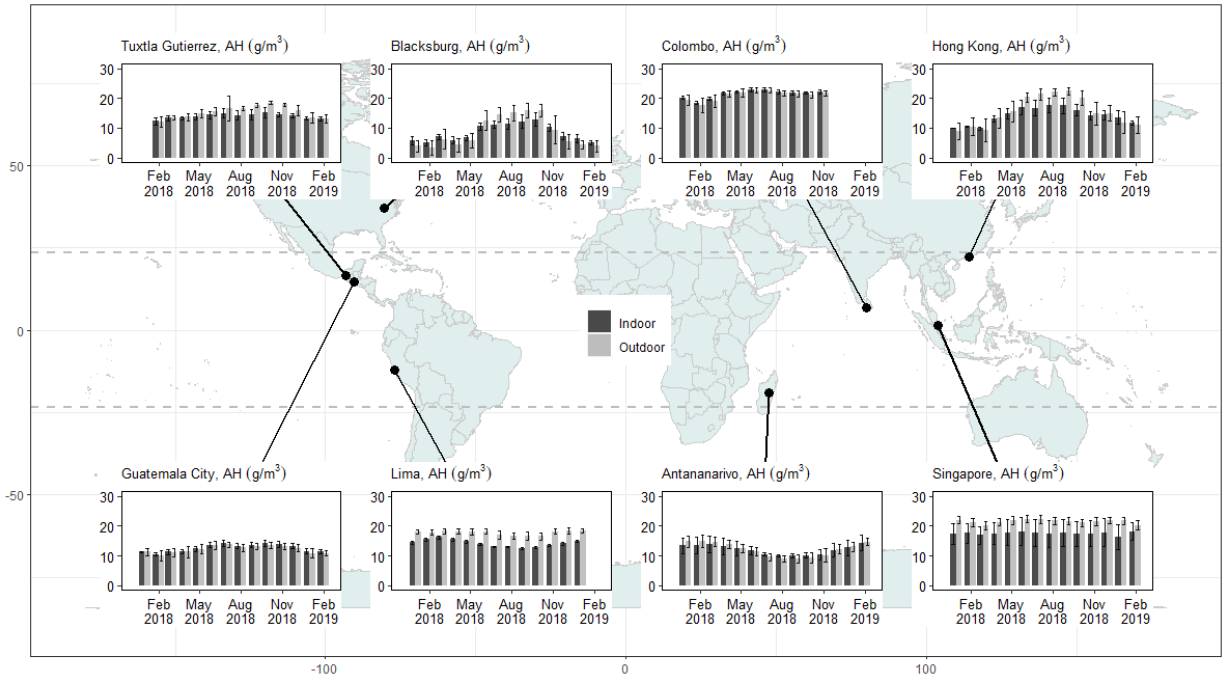

(c) Monthly absolute humidity

Figure A-2. Monthly time series of indoor and outdoor (a) T (°C), (b) RH (%), and (c) AH (g/m^3) for all cities

A.4.3. Correlation between indoor and outdoor temperature and humidity

We analyzed daily (24-hour average) indoor-outdoor correlations between four sets of variables: indoor T vs. outdoor T, indoor RH vs. outdoor RH, indoor AH vs. outdoor AH, and indoor RH vs. outdoor AH. The reason for examining the fourth set is that we expect outdoor water vapor to penetrate indoors, resulting in nearly the same AH indoors and outdoors; and because indoor temperatures fall in a narrow range, indoor RH should be strongly correlated with indoor AH. Thus, we propose that outdoor AH can serve as a proxy for indoor RH.

Figure A-3 shows scatterplots of the indoor-outdoor relationships for three representative cities. Guatemala City represents cities with low penetration of AC systems, such as Colombo in this study. Hong Kong represents cities with greater penetration of AC systems, such as Antananarivo and Tuxtla Gutierrez. Because of its proximity to the equator, Singapore had a slightly different climate pattern compared to other tropical cities in this study. The slope and R^2 for all eight cities are presented in Table S2.

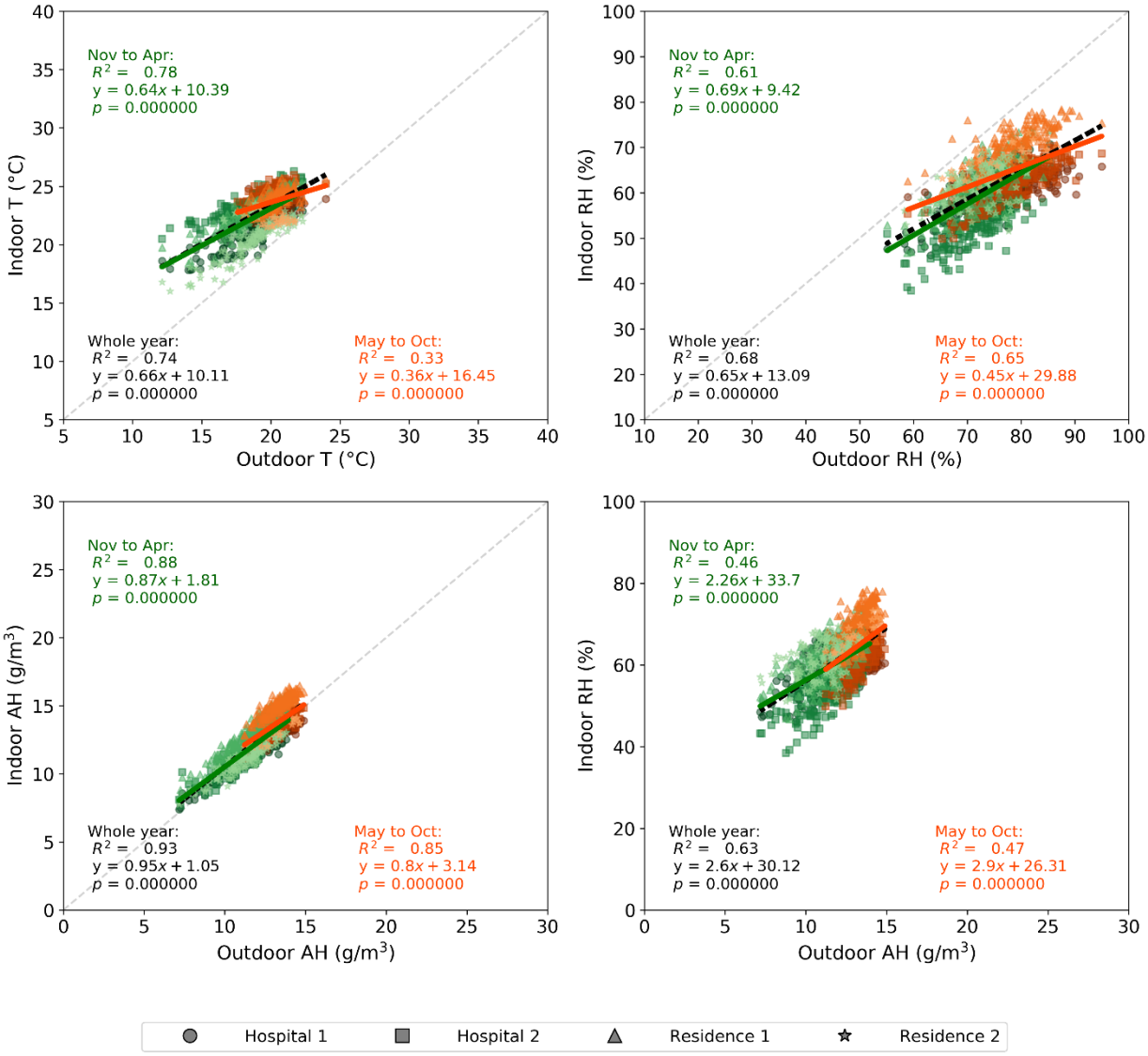

(a) Guatemala City

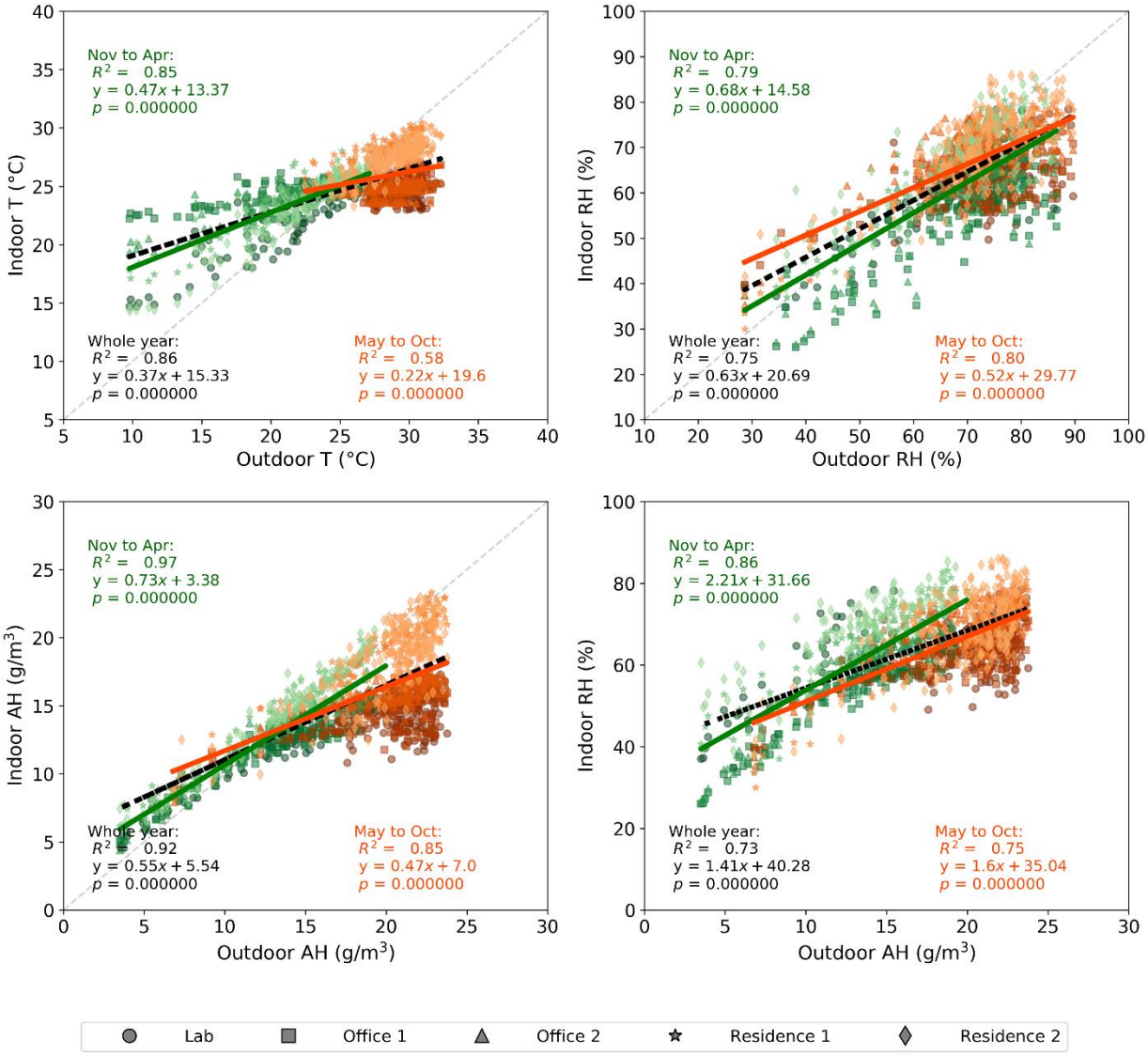
Nov to Apr:
R^2 = 0.85
y = 0.47x + 13.37
p = 0.000000
Whole year:
R^2 = 0.86
y = 0.37x + 15.33
p = 0.000000
May to Oct:
R^2 = 0.58
y = 0.22x + 19.6
p = 0.000000
Indoor T (°C)
Outdoor T (°C)
Nov to Apr:
R^2 = 0.79
y = 0.68x + 14.58
p = 0.000000
Whole year:
R^2 = 0.75
y = 0.63x + 20.69
p = 0.000000
May to Oct:
R^2 = 0.80
y = 0.52x + 29.77
p = 0.000000
Indoor RH (%)
Outdoor RH (%)
Nov to Apr:
R^2 = 0.97
y = 0.73x + 3.38
p = 0.000000
Whole year:
R^2 = 0.92
y = 0.55x + 5.54
p = 0.000000
May to Oct:
R^2 = 0.85
y = 0.47x + 7.0
p = 0.000000
Indoor AH (g/m^3)
Outdoor AH (g/m^3)
Nov to Apr:
R^2 = 0.86
y = 2.21x + 31.66
p = 0.000000
Whole year:
R^2 = 0.73
y = 1.41x + 40.28
p = 0.000000
May to Oct:
R^2 = 0.75
y = 1.6x + 35.04
p = 0.000000
Indoor RH (%)
Outdoor AH (g/m^3)
Lab
Office 1
Office 2
Residence 1
Residence 2

(b) Hong Kong

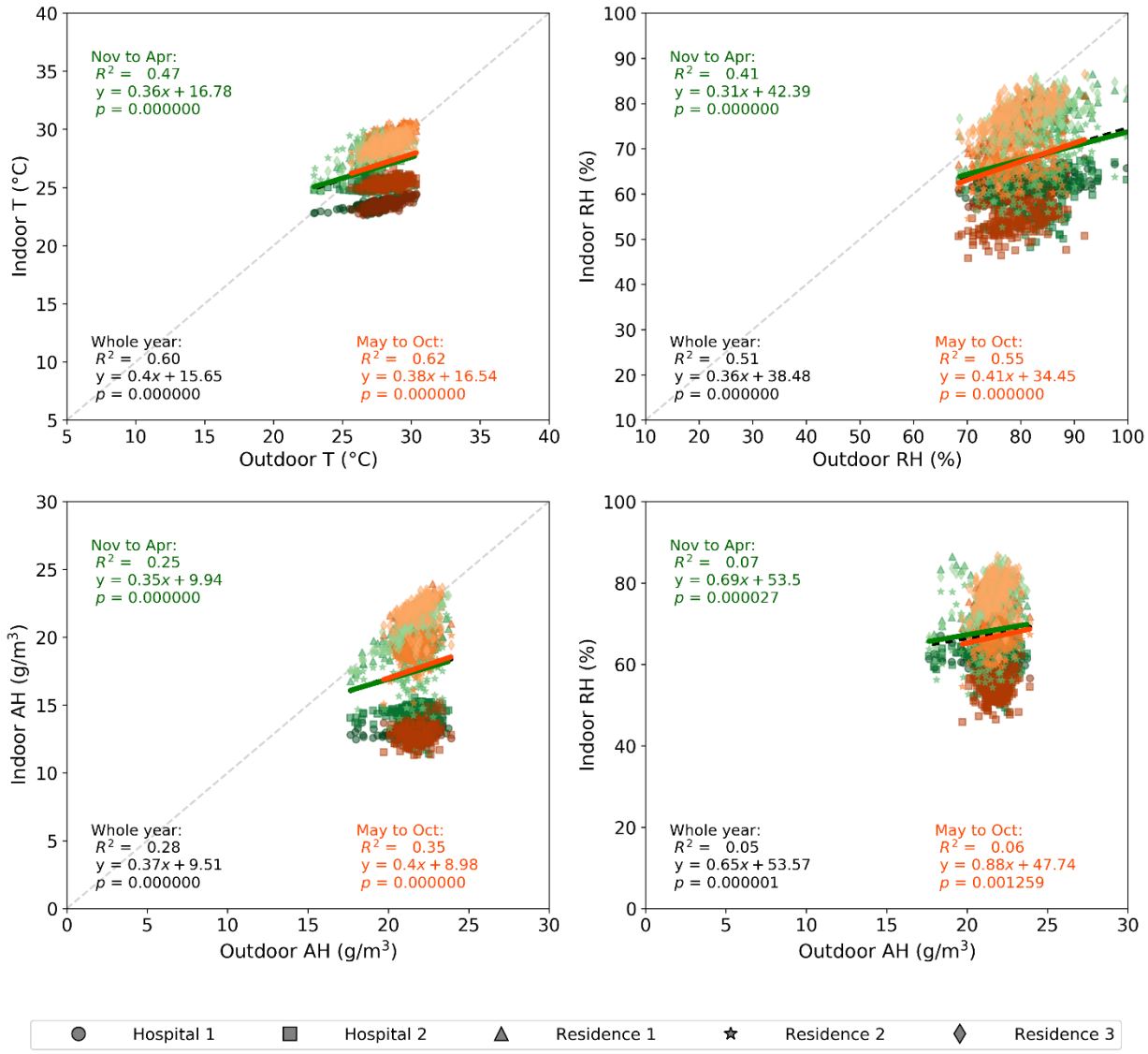

(c) Singapore

Figure A-3. Correlation between daily indoor and outdoor measurements of temperature and humidity in (a) Guatemala City, (b) Hong Kong, and (c) Singapore, separated by season. Green markers represent the dry season (November to April) and orange markers represent the wet season (May to October). Least-squares linear regression lines are shown in their respective colors, and the 1:1 line is shown by a gray dashed line where relevant.

Table A-2. Variation of Pearson's *r* by building type, latitude, and season in cities ordered north to south. Multiple values in a cell indicate that there were multiple sensors in a certain building type. $p < 0.05$ except in Lima.

(a) Wet season.

Latitude	Building type	Correlation			
		Indoor *T* (°C) vs.	Indoor *RH* (%) vs.	Indoor *AH* (g/m³)	Indoor *RH* (%) vs.

		Outdoor T (°C)	Outdoor RH (%)	vs. Outdoor AH (g/m^3)	Outdoor AH (g/m^3)
Blacksburg (37.2 °N)	Residence	0.35, 0.85, 0.75	0.47, 0.37, 0.55	0.65, 0.58, 0.87	0.66, 0.21, 0.69
	Office	0.71	0.56	0.83	0.74
Hong Kong (22.4 °N)	Residence	0.21, 0.53	0.37, 0.24	0.37, 0.16	0.33, 0.18
	Office	-0.02, 0.22	0.22, 0.34	0.13, 0.51	0.13, 0.41
	Lab	0.01	0.41	0.18	0.25
Tuxtla Gutierrez (16.8 °N)	Residence	0.24	0.69	0.52	0.42
	Hospital	0.22, 0.11, -0.01	0.64, 0.38, 0.61	0.02, 0.02, 0.24	0.17, 0.10, 0.29
Guatemala City (14.6 °N)	Residence	-0.11, 0.59	0.46, 0.47	0.63, 0.69	0.58, 0.67
	Hospital	0.06, 0.60	0.38, 0.63	0.69, 0.71	0.50, 0.52
Colombo (6.9 °N)	Residence	0.65, 0.56, 0.27	0.62, 0.50, 0.33	0.62, 0.51, 0.61	0.41, 0.35, 0.47
	Office	0.69	0.58	0.26	0.30
	Hospital	0.05	0.25	0.16	0.21
Singapore (1.4 °N)	Residence	0.51, 0.38, 0.41	0.54, 0.08, 0.33	0.36, 0.15, 0.09	0.30, 0.12, 0.11
	Hospital	0.45, 0.25	0.32, 0.09	0.07, 0.06	0.04, 0.06
Lima (12.0 °S)	Residence	0.15	0.42	-0.15	-0.10
	Office	0.21	0.34	-0.10	0.01
	Hospital	0.01	0.16	-0.12	0.06
Antananarivo (18.9 °S)	Residence	0.49, 0.70	0.37, 0.54	0.52, 0.58	0.41, 0.44
	Office	0.57, 0.59	0.43, 0.45	0.62, 0.62	0.57, 0.50
	Lab	0.18	0.18	0.14	0.16

(b) Dry season.

Latitude	Building type	Correlation			
		Indoor T vs. Outdoor T	Indoor RH vs. Outdoor RH	Indoor AH vs. Outdoor AH	Indoor RH vs. Outdoor AH
Blacksburg (37.2 °N)	Residence	0.18, 0.25, 0.24	0.42, 0.36, 0.35	0.73, 0.65, 0.79	0.75, 0.63, 0.76
	Office	0.52	0.54	0.95	0.94
Hong Kong (22.4 °N)	Residence	0.80, 0.87	0.69, 0.71	0.93, 0.93	0.88. 0.76
	Office	0.57, 0.83	0.72, 0.73	0.88, 0.93	0.87, 0.91
	Lab	0.85	0.69	0.92	0.69
Tuxtla Gutierrez (16.8 °N)	Residence	0.84	0.75	0.93	0.43
	Hospital	0.66, 0.28, 0.47	0.66, 0.40, 0.46	0.72, 0.70, 0.70	0.11, 0.54, 0.54
Guatemala City (14.6 °N)	Residence	0.43, 0.52	0.46, 0.27	0.72, 0.72	0.37, 0.39
	Hospital	0.44, 0.70	0.32, 0.54	0.74, 0.70	0.29, 0.50
Colombo (6.9 °N)	Residence	0.59, 0.40, 0.24	0.55, 0.47, 0.35	0.83, 0.80, 0.84	0.47, 0.54, 0.73
	Office	0.65	0.55	0.72	0.47

	Hospital	0.14	0.35	0.78	0.69
Singapore	Residence	0.49, 0.31, 0.49	0.54, 0.06, 0.41	0.40, 0.11, 0.54	0.30, 0.06, 0.35
(1.4 °N)	Hospital	0.46, 0.27	0.31, 0.15	0.14, 0.01	0.11, -0.02
Lima	Residence	0.25	0.24	0.39	-0.12
(12.0 °S)	Office	0.15	-0.02	0.30	-0.37
	Hospital	-0.01	-0.11	0.40	-0.46
Antananarivo	Residence	0.56, 0.75	0.38, 0.54	0.60, 0.66	0.31, 0.40
(18.9 °S)	Office	0.58, 0.59	0.35, 0.44	0.63, 0.63	0.45, 0.33
	Lab	0.22	0.32	0.14	0.07

In Guatemala City, both indoor and outdoor temperature fell within a relatively small range of 12°C to 27°C (Figure A-3a). An increase of 1°C in outdoor temperature was associated with an average increase of ~0.7°C in indoor temperature (slope: 0.66, R^2 = 0.74). The goodness of fit between indoor and outdoor temperature was better during the dry season than the wet season (R^2 of 0.78 vs. 0.33), probably due to the much narrower range of values observed during the wet season. Its indoor *AH* was nearly the same as outdoor *AH* and an increase of 1 g/m^3 outdoors was related to an increase of 0.95 g/m^3 indoors (slope: 0.95, R^2 = 0.93), suggesting that the majority of the indoor water vapor came from outdoors in Guatemala City. Unlike its temperature profile, there was no significant difference of goodness of fit between wet and dry season regarding indoor-outdoor *AH* correlation. Guatemala City's outdoor and indoor *RH* spanned similar ranges: 50–90% outdoors and 40–80% indoors. However, the indoor-outdoor correlation of *RH* was weaker than indoor *T* vs. outdoor *T* and indoor *AH* vs. outdoor *AH*, and there was no apparent seasonal difference. Among the four sets of comparisons, indoor *AH* vs. outdoor *AH* displayed the best goodness of fit (R^2 = 0.88 in the dry season and 0.85 in the wet season). Indoor and outdoor *RH* were less strongly correlated, and indoor *RH* was only weakly correlated with outdoor *AH*.

In Hong Kong, *T*, *RH*, and *AH* spanned a much wider range than in Guatemala City, and differences between the dry season and wet season were more evident (Figure A-3b). The indoor temperature changed by only 0.37 °C for every 1 °C change in outdoor temperature (slope = 0.37, R^2 = 0.86), implying a weaker influence of outdoor temperature on indoor temperature. The correlation between indoor and outdoor temperature was stronger in the dry season (R^2 = 0.85 vs.

R^2 = 0.58), again probably attributable to the much narrower range of temperatures in the wet season. The slope of the indoor-outdoor *AH* correlation was only 0.55, much less than in Guatemala City. Therefore, we speculate that some dehumidification processes were taking place, such that there was a smaller change in indoor *AH* given a 1 g/m^3 change in outdoor *AH*. Such dehumidification effects were stronger in the wet season than the dry season (slope = 0.47 vs. slope = 0.73), as AC systems were more widespread and more commonly used in Hong Kong during the wet season. These effects may also contribute to a weaker indoor-outdoor *AH* correlation in the wet season than in the dry season (R^2 = 0.85 vs. R^2 = 0.97). The indoor *RH* vs. outdoor *AH* correlation was also strong in Hong Kong, especially during the dry season (R^2 = 0.86). In general, the linear correlations of all combinations were much stronger in Hong Kong compared to Guatemala City, except indoor *AH* vs. outdoor *AH*, which was roughly equal in both cities.

In Singapore, the range of each of *T*, *RH*, and *AH* was narrow because its climate does not vary much over the year. Therefore, the indoor-outdoor correlations in Singapore (Figure A-3c) exhibited substantial differences from those in Guatemala City and Hong Kong. The linear correlation was weak for indoor-outdoor combinations regardless of the season due to the clustering of the values in a narrow range (R^2 < 0.6). Interestingly, some indoor measurements, especially *T* and *AH*, in residential buildings were clearly higher than those in hospital buildings, which implied some potential influence on indoor-outdoor correlations from building type. We surmise that the difference is due to heavier use of AC in hospital buildings compared to residential buildings.

The strength of correlations between indoor and outdoor conditions varied by building type, by latitude, and by season (Table A-2, Figure S1). The indoor-outdoor correlation was in general stronger in the dry season than in the wet season, especially for the relationship between indoor *AH* and outdoor *AH* in many locations ($r \geq 0.7$ for most data points in the wet season) (Table A-2, Figure S1). The strength of the indoor-outdoor correlation increased with latitude in the dry season, more so for indoor *RH* vs. outdoor *RH* than for indoor *RH* vs. outdoor *AH*. However, there was no significant trend in the wet season, in part because the use of AC systems in some cities regulated

the indoor environment. The strength of indoor-outdoor correlations in residential buildings was similar to that in the office buildings. However, due to our limited sample size, we do not know if this observation applies more broadly.

A.4.4. Influence of AC systems on the correlation

To investigate the influence of AC systems, we further stratified the data depending on whether the AC system was turned on and then analyzed the same correlations described in the previous section (Figure A-4, Table S3, and Table A-3).

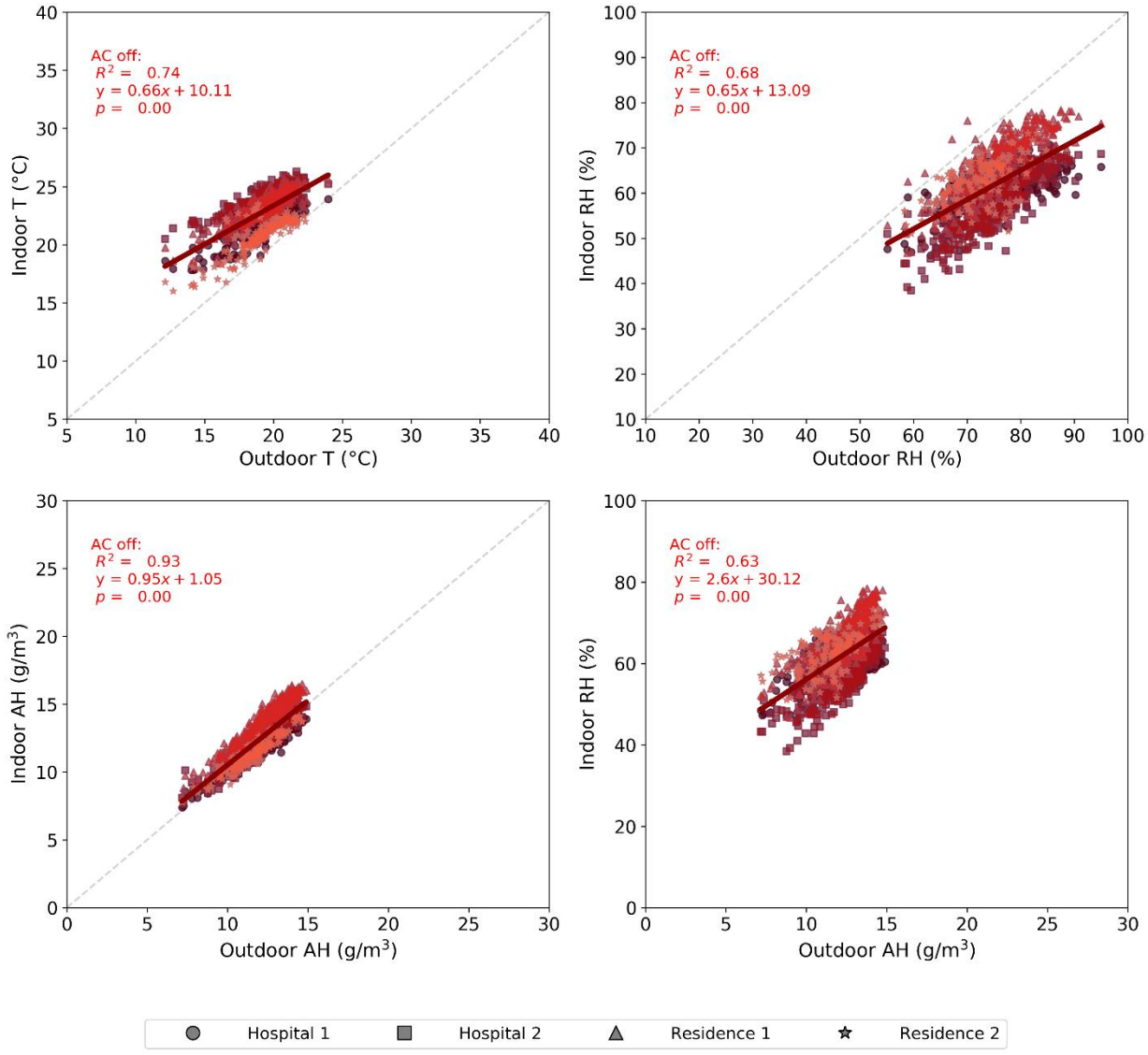

(a) Guatemala City

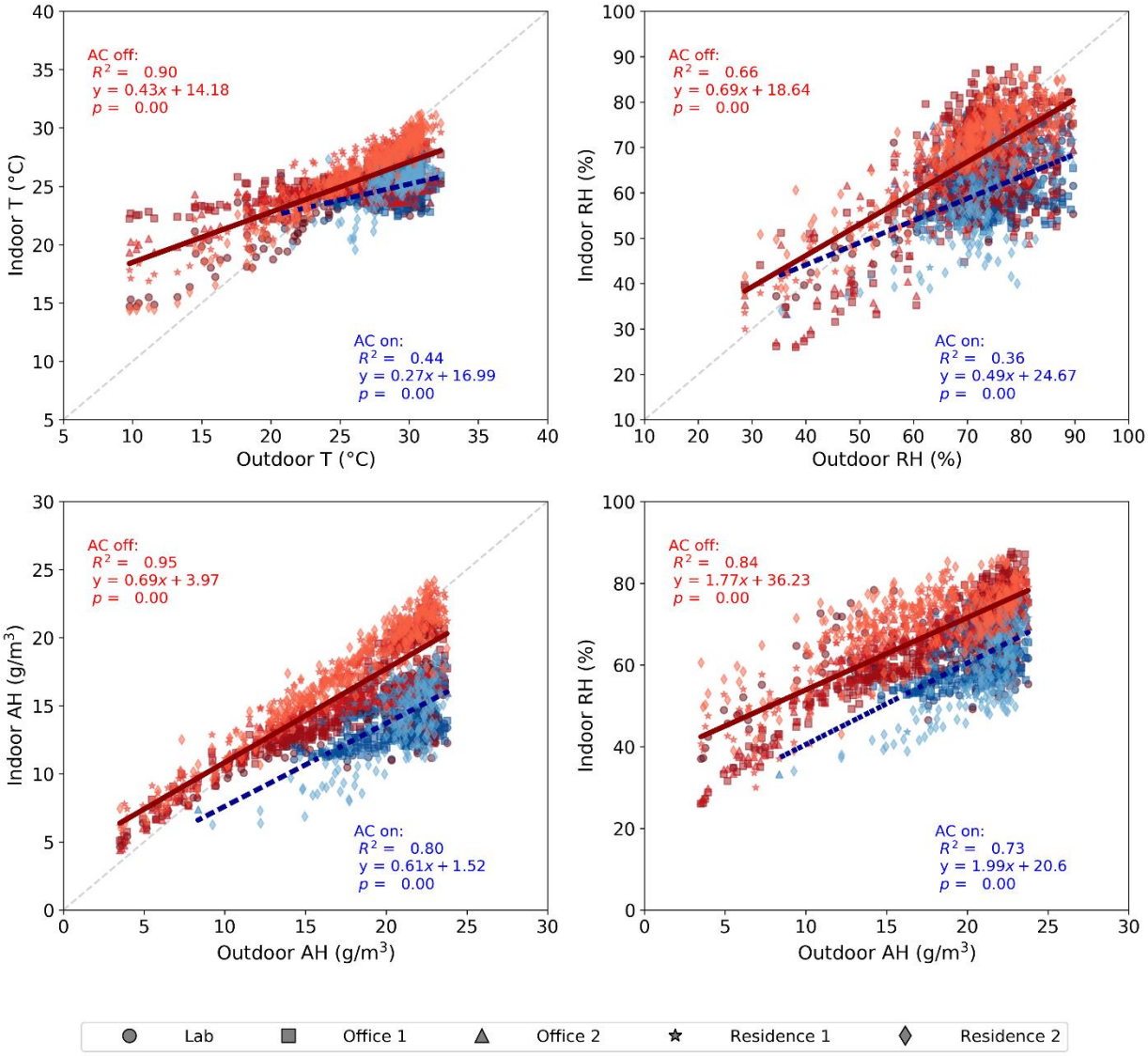
AC off:
R^2 = 0.90
y = 0.43x + 14.18
p = 0.00
AC on:
R^2 = 0.44
y = 0.27x + 16.99
p = 0.00
Indoor T (°C)
Outdoor T (°C)
AC off:
R^2 = 0.66
y = 0.69x + 18.64
p = 0.00
AC on:
R^2 = 0.36
y = 0.49x + 24.67
p = 0.00
Indoor RH (%)
Outdoor RH (%)
AC off:
R^2 = 0.95
y = 0.69x + 3.97
p = 0.00
AC on:
R^2 = 0.80
y = 0.61x + 1.52
p = 0.00
Indoor AH (g/m^3)
Outdoor AH (g/m^3)
AC off:
R^2 = 0.84
y = 1.77x + 36.23
p = 0.00
AC on:
R^2 = 0.73
y = 1.99x + 20.6
p = 0.00
Indoor RH (%)
Outdoor AH (g/m^3)
Lab
Office 1
Office 2
Residence 1
Residence 2

(b) Hong Kong

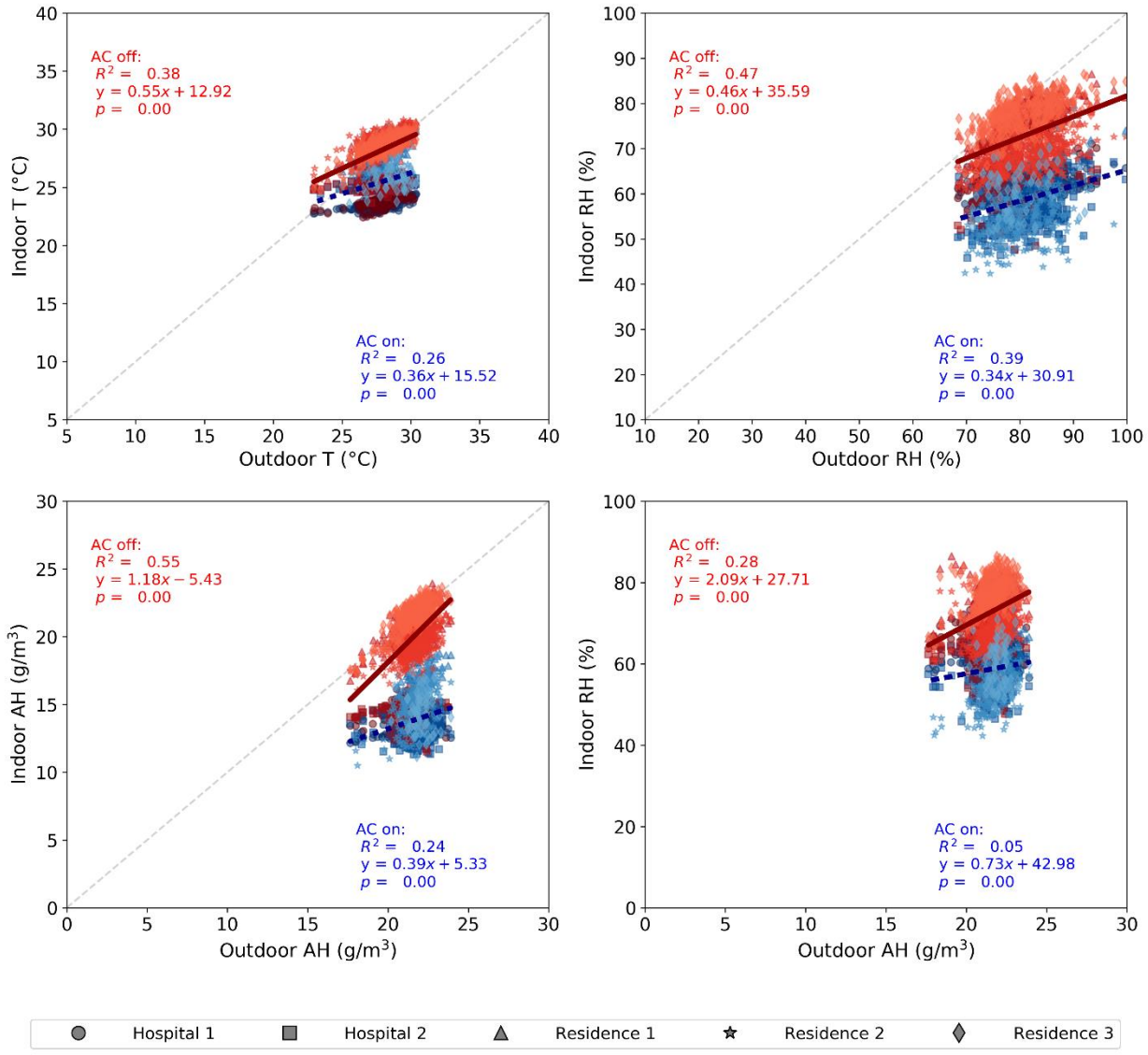

(c) Singapore

Figure A-4. Correlation between daily indoor and outdoor measurements of temperature and humidity in (a) Guatemala City, (b) Hong Kong, and (c) Singapore, separated by AC use. Blue markers represent "AC on" status and red markers represent "AC off" status. Least-squares linear regression lines are shown in their respective colors, and the 1:1 line is shown by a gray dashed line where relevant.

Table A-3 Variation of Pearson's r by building type, by latitude, and by AC status. Multiple values in a cell indicate that there were multiple sensors in a certain building type. Buildings that lacked AC are indicated by "NA". They are included to facilitate direct comparison with Table 2. $p < 0.05$ for all data points except those representing Lima.

(a) AC on

Latitude	Building type	Correlation			
		Indoor *T* vs.	Indoor *RH* vs.	Indoor *AH* vs.	Indoor *RH* vs.

		Outdoor *T*	Outdoor *RH*	Outdoor *AH*	Outdoor *AH*
Blacksburg	Residence	0.61, 0.77, 0.69	0.36, 0.27, -0.05	0.64, 0.29, 0.90	0.33, 0.19, 0.77
(37.2 °N)	Office	0.42	0.45	0.40	0.21
Hong Kong	Residence	-0.01, 0.44	0.36, 0.46	0.61, 0.64	0.51, 0.60
(22.4 °N)	Office	0.23, 0.19	0.20, 0.33	0.50, 0.58	0.45, 0.47
	Lab	0.15	0.47	0.41	0.42
Tuxtla Gutierrez	Residence	NA	NA	NA	NA
(16.8 °N)	Hospital	0.13, 0.11	0.64, 0.50	0.94, 0.65	0.88, 0.60
Guatemala City	Residence	NA	NA	NA	NA
(14.6 °N)	Hospital	NA	NA	NA	NA
Colombo	Residence	0.72	0.21	0.28	0.33
(6.9 °N)	Office	0.49	0.56	0.69	0.28
	Hospital	-0.09	0.26	0.64	0.30
Singapore	Residence	0.34, 0.43, 0.14	0.31, 0.41, 0.30	0.64, 0.54, 0.18	0.49, 0.53, 0.09
(1.4 °N)	Hospital	0.45, 0.26	0.35, 0.20	0.18, 0.05	0.13, 0.06
Lima	Residence	NA	NA	NA	NA
(12.0 °S)	Office	NA	NA	NA	NA
	Hospital	NA	NA	NA	NA
Antananarivo	Residence	0.08, 0.74	0.58, 0.56	0.91, 0.94	0.88, 0.77
(18.9 °S)	Office	0.25, 0.42	0.50, 0.27	0.70, 0.80	0.69, 0.73
	Lab	0.21	0.15	0.49	0.42

(b) AC off

Latitude	Building type	Correlation			
		In *T* vs. Out *T*	In *RH* vs. Out *RH*	In *AH* vs. Out *AH*	In *RH* vs. Out *AH*
Blacksburg	Residence	0.23, 0.76, 0.84	0.59, 0.44, 0.51	0.87, 0.77, 0.95	0.87, 0.64, 0.89
(37.2 °N)	Office	0.84	0.63	0.96	0.93
Hong Kong	Residence	0.83, 0.90	0.68, 0.69	0.92, 0.92	0.76, 0.69
(22.4 °N)	Office	0.62, 0.71	0.60, 0.57	0.92, 0.93	0.92, 0.91
	Lab	0.85	0.64	0.95	0.76
Tuxtla Gutierrez	Residence	0.33	0.75	0.76	0.49
(16.8 °N)	Hospital	0.48, -0.04, 0.33	0.47, 0.37, 0.50	0.69, 0.62, 0.66	-0.01, 0.68, 0.60
Guatemala City	Residence	0.35, 0.53	0.48, 0.30	0.81, 0.76	0.63, 0.50
(14.6 °N)	Hospital	0.37, 0.62	0.35, 0.55	0.83, 0.79	0.49, 0.62
Colombo	Residence	0.61, 0.44, 0.22	0.60, 0.52, 0.42	0.84, 0.83, 0.86	0.51, 0.60, 0.75
(6.9 °N)	Office	0.66	0.58	0.68	0.45
	Hospital	0.16	0.40	0.79	0.71
Singapore	Residence	0.53, 0.41, 0.55	0.58, 0.12, 0.42	0.45, 0.32, 0.50	0.32, 0.20, 0.32
(1.4 °N)	Hospital	0.64, 0.36	0.65, 0.55	0.78, 0.70	0.76, 0.58
Lima	Residence	0.06	0.20	0.34	-0.27

(12.0 °S)	Office	0.02	-0.10	0.32	-0.46
	Hospital	-0.08	-0.19	0.38	-0.48
Antananarivo	Residence	0.64, 0.78	0.38, 0.55	0.79, 0.84	0.28, 0.43
(18.9 °S)	Office	0.64, 0.67	0.41, 0.46	0.85, 0.84	0.57, 0.46
	Lab	0.37	0.40	0.38	0.22

In Guatemala City, none of the buildings in our sample had AC. In this situation, all indoor and outdoor climate metrics were well correlated, especially indoor *AH* and outdoor *AH* (R^2 = 0.93). The correlations were slightly weaker between indoor *RH* and outdoor *RH*/*AH*. As shown by the results for Hong Kong, our criterion for "AC on" highlighted periods when outdoor *T* was greater than 25 °C, but not all such points, as residences were not commonly air conditioned during the workday. Use of AC tended to shift both indoor *RH* and *AH* toward lower values. Compared to "AC on" periods, the indoor-outdoor correlations were stronger when the AC was off. Under these conditions, indoor *AH* was very strongly correlated with outdoor *AH* (R^2 = 0.95), and indoor *RH* was more strongly correlated with outdoor *AH* than with outdoor *RH* (R^2 =0.84 vs. R^2 = 0.66).

In Singapore, no pattern or trend was observed between indoor and outdoor climate; however, the use of AC can explain the clustering of measurements and separation by different building type to some extent. It seemed that these measurements clustered by whether AC systems were in use, and the AC systems tended to run longer in the office buildings as evidenced by a lower average daily indoor temperature and *AH* than in residential buildings. For both Hong Kong and Singapore (indoor *AH* or *T* vs. outdoor *AH* or *T*) when AC was on, the indoor *AH* varied between 13-18 g/m^3, regardless of outdoor *AH*. Indoor temperature hovered around 25^{o}C, regardless of outdoor *T*. This is expected, as AC removes heat and moisture so that the indoor temperature and humidity are maintained at a relatively constant level.

The Pearson's *r* values were modestly higher when AC was off compared to when AC was on across all cities regardless of building type (Table A-3, Figure S2). In particular, the correlation between indoor *AH* and outdoor *AH* in most buildings was quite strong ($r > 0.7$) when AC was off. Similar to season-specific observations, the correlations were stronger at higher latitudes, especially when AC was off.

A.4.5. Multivariate analyses

We also considered the influence of multiple variables on indoor climate using multivariate OLS regression. Table A-4 and Table A-5 present the results of all correlations, including R^2 and coefficients of each independent variable. We used type-II Analysis of Variance (ANOVA) to verify whether the independent variables have significant influence on the respective indoor measurements.

The multivariate OLS model, which utilized outdoor measurements, building type, and season, performed similarly to the single-variable OLS one, which utilized outdoor measurements only and considered data by season, as their R^2 values were close. However, the multivariate OLS analysis generated higher R^2 values than single-variable OLS based on wet season data in most tropical cities. Interestingly, the R^2 of indoor *RH* vs. outdoor *AH* were greatly elevated using the multivariate OLS model in Guatemala City and Antananarivo. We conjecture that the indoor *RH* was more dependent on the characteristics of different building types, including the insulation of building envelopes, the ventilation rate, or even the habits of the residents, in these two cities than in other cities. Moreover, the R^2 of all correlations were much higher in Singapore and Lima with the multivariate OLS than with the single-variable OLS model. These results indicated that all indoor measurements in these two cities were influenced by the building type. In addition, ANOVA results of the multivariate OLS model suggested a non-significant influence of season on indoor *RH* vs. outdoor *RH* and indoor *AH* vs. outdoor *AH* in Singapore. This was expected because Singapore has very little seasonality. As shown in Figure A-3c, there were differences between residential buildings and hospitals. Thus, the addition of building type in the model can better interpret such patterns. Lima exhibited weak indoor-outdoor correlations for all four relationships, in part because the outdoor weather station was far away from the indoor sampling sites; availability of outdoor climate data in Lima was limited. Therefore, including building type, a more relevant variable to the indoor measurements in Lima, can improve the goodness of fit.

We further changed the independent variables in the multivariate OLS model to outdoor measurements, building type, and AC status (instead of season) to investigate the influence of AC

in combination with other variables. The multivariate OLS model performed similarly to the single-variable OLS model with AC off but did much better with AC on. The multivariate OLS model in Singapore, which has no seasonality but high usage of AC, achieved much higher R^2 values than its respective single-variable OLS model when we discarded season and included AC status as an independent variable.

Table A-4. Parameters based on multivariate ordinary least squares regression between indoor measurements, outdoor measurements, building type, and season. Building type (residence, office, hospital, lab) and season (wet, dry), which were categorical variables, were converted to dummy variables in the analysis.

City	Parameters	Correlation			
		Indoor *T* (°C) vs. Outdoor *T* (°C)	Indoor *RH* (%) vs. Outdoor *RH* (%)	Indoor *AH* (g/m^3) vs. Outdoor *AH* (g/m^3)	Indoor *RH* (%) vs. Outdoor *AH* (g/m^3)
Blacksburg (37.2 °N)	R^2	0.21	0.70	0.81	0.74
	Intercept	20.82	9.72	2.95	2.95
	Building type: residence	0.27	8.61	1.73	1.73
	Season: wet	0.36	17.91	0.98	0.98
	Outdoor variable	0.09	0.28	0.44	0.44
Hong Kong (22.4 °N)	R^2	0.68	0.63	0.84	0.65
	Intercept	12.92	17.28	2.66	32.56
	Building type: office	1.20	0.10‡	1.05	0.42‡
	Building type: residence	2.56	6.30	3.90	6.63
	Season: wet	-0.46	4.19	-0.88	-7.16
	Outdoor variable	0.42	0.60	0.62	1.92
Tuxtla Gutierrez (16.8 °N)	R^2	0.61	0.31	0.57	0.28
	Intercept	19.42	51.93	9.03	54.92
	Building type: residence	4.80	-7.76	2.14	-8.51
	Season: wet	0.82	-0.09‡	0.22	-1.31
	Outdoor variable	0.08	0.28	0.29	1.03
Guatemala City (14.6 °N)	R^2	0.52	0.69	0.85	0.62
	Intercept	11.33	14.19	1.40	29.43
	Building type:	-0.43	6.49	1.08	6.41

	residence				
	Season: wet	0.53	3.18	0.56	1.78
	Outdoor variable	0.59	0.58	0.86	2.36
	R^2	0.57	0.57	0.85	0.49
	Intercept	9.62	23.04	3.95	31.95
	Building type:	2.83	-9.07	0.61	-9.07
Colombo	office				
(6.9 °N)	Building type:	2.19	-5.12	1.00	-5.12
	residence				
	Season: wet	-0.09‡	1.86	0.22	0.92
	Outdoor variable	0.65	0.69	0.79	2.18
	R^2	0.87	0.63	0.87	0.59
	Intercept	14.30	30.58	4.83	43.21
Singapore	Building type:	4.12	13.54	7.23	13.53
(1.4 °N)	residence				
	Season: wet	0.20	-0.35‡	0.12‡	-1.80
	Outdoor variable	0.36	0.36	0.39	0.79
	R^2	0.67	0.64	0.57	0.65
	Intercept	20.88	81.03	11.69	100.45
	Building type:	2.20	-10.30	-0.50	-10.30
Lima	office				
(12.0 °S)	Building type:	0.84	-7.00	-0.66	-6.99
	residence				
	Season: wet	4.62	-9.42	1.63	-8.39
	Outdoor variable	-0.04‡	-0.04	0.11	-1.27
	R^2	0.78	0.83	0.81	0.76
	Intercept	12.97	-4.75	1.05	16.94
	Building type:	-2.35	23.71	3.80	23.72
Antananarivo	office				
(18.9 °S)	Building type:	-1.77	24.45	4.35	24.45
	residence				
	Season: wet	0.74	-1.96	0.02‡	-6.84
	Outdoor variable	0.61	0.58	0.63	2.04

Table A-5. Parameters based on multivariate ordinary least squares regression between indoor measurements, outdoor measurements, building type, and AC status. Building type (residence, office, hospital, lab) and AC status (on, off), which were categorical variables, were converted to dummy variables in the analysis. Guatemala and Lima, where we sampled buildings without AC, are not shown here.

City	Parameters	Correlation			
		Indoor *T* (°C)	Indoor *RH* (%)	Indoor *AH*	Indoor *RH* (%)

		vs. Outdoor *T* (°C)	vs. Outdoor *RH* (%)	(g/m^3) vs. Outdoor *AH* (g/m^3)	vs. Outdoor *AH* (g/m^3)
Blacksburg (37.2 °N)	R^2	0.39	0.60	0.88	0.82
	Intercept	18.41	17.29	2.11	18.66
	Building type: residence	0.21	8.79	1.58	7.98
	AC: on	-0.28	-1.68	-3.19	-13.57
	Heat: on	3.08	-16.23	0.28	-3.45
	Outdoor variable	0.22	0.36	0.62	2.33
Hong Kong (22.4 °N)	R^2	0.72	0.60	0.89	0.62
	Intercept	12.93	17.55	2.66	36.28
	Building type: office	0.96	0.28‡	0.64	-0.48‡
	Building type: residence	1.78	7.00	2.57	3.95
	AC: on	-1.50	1.48	-2.63	-5.03
	Outdoor variable	0.44	0.62	0.67	1.63
Tuxtla Gutierrez (16.8 °N)	R^2	0.58	0.32	0.60	0.29
	Intercept	19.35	19.35	8.46	56.14
	Building type: residence	4.84	4.84	2.10	-8.75
	AC: on	-0.76	-0.76	-1.86	-4.72
	Outdoor variable	0.10	0.10	0.33	0.92
Colombo (6.9 °N)	R^2	0.57	0.56	0.85	0.48
	Intercept	20.18	19.67	3.42	29.70
	Building type: office	2.86	-9.07	0.61	-9.07
	Building type: residence	2.26	-5.12	1.00	-5.12
	AC: on	-1.60	-14.70	-6.34	-17.12
	Outdoor variable	0.27	0.74	0.82	2.31
Singapore (1.4 °N)	R^2	0.87	0.67	0.90	0.63
	Intercept	14.10	39.19	5.77	47.75
	Building type: residence	3.25	2.27	3.24	1.95
	AC: on	-0.91	-11.83	-4.19	-12.14
	Outdoor variable	0.40	0.39	0.54	1.10
Antananarivo (18.9 °S)	R^2	0.79	0.85	0.89	0.76
	Intercept	11.36	-3.13	1.04	26.95

Building type: office	-2.92	20.53	2.59	20.64
Building type: residence	-2.34	21.26	3.14	21.36
AC: on	-1.64	-9.11	-3.47	-8.83
Outdoor variable	0.74	0.59	0.73	1.14

‡ $p > 0.05$ tested by type-II ANOVA, indicating this variable did not have significant influence on the respective indoor measurements.

A.5. Discussion

Correlations between indoor and outdoor temperature and humidity in tropical regions are influenced by many parameters including season, AC use, and latitude. In general, latitude is an important factor in the correlations, as the three representative cities – Guatemala City, Hong Kong, and Singapore – exhibited very different patterns. The further the city from the equator, the stronger the linear correlation. This is in part because cities further from the equator experience a stronger seasonality pattern, exhibiting a wider range in their parameter values. Other factors that were not considered in this study, such as human behavior and socioeconomic status, are also likely to influence the pattern.

Seasonal differences have been reported in the temperate regions, where indoor and outdoor temperatures are more strongly correlated during warm seasons than cool seasons,[17,21] as the natural indoor-outdoor temperature differential is smaller during this period. We observed the same pattern in our reference temperate city, Blacksburg. However, this trend did not apply to tropical cities. This is likely due to the use of heating systems in temperate regions (increasing the indoor-outdoor temperature differential), but not tropical cities during cool seasons (dry seasons in tropics).

Indoor *AH* vs. outdoor *AH* had the strongest linear correlation among other indoor-outdoor combinations regardless of building type and latitude, especially during the dry season. This result matches the findings in studies of cities with temperate climates.[17,18] It is partially due to a generally unchanging daily outdoor *AH* and less use of AC systems in the dry season than in the wet season. This result suggests that outdoor *AH* may serve as a good indicator of indoor *AH* for tropical cities except those with widespread use of AC, such as Singapore. Consistent with

previous studies,[17,18] outdoor *RH* was a poor indicator of indoor *RH* because indoor *RH* is determined by both *T* and *AH*, resulting in greater variability. However, outdoor *AH* is a reasonable predictor of indoor *RH* when AC was off and/or during the dry season. Since indoor *RH* and *AH* are associated with many health problems,[6] as well as impacting airborne virus survival,[35,36] it is useful to know that they can be predicted by outdoor parameters.

Season and the use of AC systems influenced the linearity and correlations between indoor and outdoor measurements. Where AC was not in use, such as in Guatemala City, there was very little difference between the dry season and wet season, whereas for cities with greater penetration of AC (such as Hong Kong and Singapore), AC use can better explain the trend and the clustering of measurements than season given generally higher Pearson's *r* when AC was off.

When AC is running, the indoor temperature should be regulated around its set-point, and humidity should also be somewhat controlled, so we first assumed a constant value for AC-controlled indoor conditions. However, a non-zero slope with $p < 0.05$ (Figure A-4) indicates that indoor variables are still correlated with outdoor variables even with the control of AC. We further analyzed the indoor-outdoor correlation using Spearman's ρ without assuming a linear relationship (Table S5). Statistics suggested that indoor and outdoor variables were still correlated ($p < 0.05$) with AC in use except in Colombo and Tuxtla Gutierrez, where the number of days when AC was on is small. These results indicated that the influence of AC on the indoor environment did not totally override the influence of outdoor conditions and other potential parameters. Hence, we applied a multivariate OLS model to achieve a better understanding of the collective influence of these variables on the indoor variables. The multivariate OLS model produced a better goodness of fit than the single-variable OLS model, especially for the cities with heavy AC usage. However, the multivariate model also increases the complexity of data interpretation. For example, the coefficients of the categorical variables (building type, AC status) do not have any physical meaning and are thus less explanatory. Additionally, the multicollinearity among independent variables, such as the correlation between outdoor measurements, AC status, and season, can be a potential issue. Principal component analyses or similar approaches would reduce the

multicollinearity, but these analyses further complicate the interpretation and explanation of variables, especially for a small data set such as that in our study.

While this study presents the most comprehensive set of indoor-outdoor data in tropical regions to date, the limited sample size restricted us from drawing more robust conclusions. For example, we observed that there was no difference of indoor measurements between residential buildings and office buildings in most cities ($p > 0.05$), but we collected measurements from at most three of one type of building in any one city. A larger study might detect differences, although differences in building construction and maintenance practices between cities and within a city might also contribute to a less consistent result in terms of building type.

In addition, we did not include demographic and socio-economic information in the analysis. Notably, the affluence of each city differed, so the penetration rate of AC varied. As we did not track occupancy nor the activities of occupants in each building, we were not able to determine behavioral influences, including actual AC usage, on indoor climate. Humans themselves contribute to indoor heat and water vapor,[37,38] and variation in human behavior may help explain the inconsistency of correlations among different locations even if their outdoor climates were similar (Table S2 and Table S3).

In terms of broader impacts, it is useful to consider these findings in the context of the COVID-19 pandemic. Initial studies have shown that transmission of COVID-19 is related to outdoor temperature and humidity. In general transmission appears to be slower at higher temperature and/or higher humidity,[39-42] consistent with results for influenza and SARS. Several studies have found that COVID-19 spreads faster in locations whose temperature falls in the range of 3-17°C and *AH* lies in the range of 3-9 g/cm^3.[10,43-46] These studies focused on temperate climate zones in the Northern Hemisphere, suggesting that the conditions corresponded to low indoor *RH*. However, these results should be viewed with caution because the datasets were restricted to early-stage outbreaks. It remains to be seen how strongly climate affects COVID-19 incidence and transmission and whether the disease settles into a seasonal pattern.

However, all these studies used outdoor meteorological data in their analyses. Because the

transmission of COVID-19[47] and other respiratory viral diseases occurs mainly indoors, it is critical to consider the indoor environment, either through direct measurements or inferring them using the relationship between outdoor and indoor measurements, such as presented here. Doing so will advance our understanding of the influence of temperature and humidity on the seasonality of certain infectious diseases.

A.6. Conclusion

We have examined indoor-outdoor correlations of temperature, relative humidity (RH), and absolute humidity (AH) over a 1-year period in a sample of buildings in seven tropical cities. Across all cities, the average monthly indoor temperature was 25±3°C (mean ± standard deviation) with a range of 20–30°C. The average monthly indoor RH was 66±9% with a range of 50–78%, and the average monthly indoor AH was 15±3 g/m3 with a range of 10–23 g/m3. The average monthly outdoor temperature, RH, and AH were 24±4°C, 74±13%, 17±3 g/m3, respectively, and the ranges were much larger than seen indoors. The range of outdoor measurements differed greatly among cities. In general, indoor AH and outdoor AH were more strongly correlated than other variables between indoors and outdoors. Indoor AH and RH were linearly correlated with outdoor AH when the air-conditioning (AC) was off, suggesting that outdoor AH may be a good indicator of indoor humidity, both AH and RH, under these conditions. For cities further from the equator, almost all correlations became stronger. Multivariate analyses revealed that building characteristics have a greater influence on indoor climate in some cities and that accounting for AC use improves model prediction. The results of this work can be used to advance our understanding of the relationship between outdoor climate, indoor climate, and health.

Acknowledgments

This research was supported by a grant from the Alfred P. Sloan Foundation as part of its Microbiology of the Built Environment program. The authors thank Kaisen Lin for helpful discussions and Julia Gohlke, Archit Manuja, and AJ Prussin II for handling sensors.

Author contributions

Jin Pan: formal analysis (lead), investigation (lead), methodology (equal), visualization (lead), writing – original draft (lead), writing – reviewing and editing (equal). **Julian Tang:** conceptualization (equal), funding acquisition (equal), project administration (equal), supervision (equal), writing – reviewing and editing (supporting). **Miguela Caniza:** project administration (supporting). **Jean Michel Heraud:** investigation (supporting), writing – reviewing and editing (supporting). **Evelyn Koay:** investigation (supporting), writing – reviewing and editing (supporting). **Hong Kai Lee:** investigation (supporting), writing – reviewing and editing (supporting). **Chun Kiat Lee:** investigation (supporting), writing – reviewing and editing (supporting). **Yuguo Li:** investigation (supporting), writing – reviewing and editing (supporting). **Alejandra Nava Ruiz:** investigation (supporting), writing – reviewing and editing (supporting). **Carlos Francisco Santillan-Salas:** investigation (supporting), writing – reviewing and editing (supporting). **Linsey C. Marr:** conceptualization (equal), funding acquisition (equal), methodology (equal), project administration (equal), supervision (equal), writing – reviewing and editing (equal).

Supporting information

Table S1. Locations of outdoor weather stations

City	Latitude and longitude	Location
Blacksburg[†]	37.3 °N, 79.96 °W	Roanoke Regional Airport Station
Antananarivo	18.91 °S, 47.52 °E	Ivato International Airport Station
Colombo	6.87 °N, 80.02 °E	Ratmalana Airport Station
Guatemala	14.59 °N, 90.53 °W	La Aurora International Airport Station
Hong Kong	22.26 °N, 113.95 °E	Hong Kong International Airport Station
Lima	9.91 °S, 76.28 °W	Alf. Fap David Figueroa Fernandini Airport Station
Singapore	1.36 °N, 103.99 °E	Singapore Changi Airport Station
Tuxtla Gutierrez	16.75 °N, 93.37 °W	Angel Albino Corzo International Airport Station

[†]Blacksburg is a temperate location used for reference.

Table S2. Slope (R^2) of daily indoor-to-outdoor linear regression by season. Indoor data are averaged across all sensors in a city.

(a) Summer/wet season (May to October for Northern Hemisphere and November to April for Southern Hemisphere)

Correlation	Indoor *T* (°C) vs. Outdoor *T* (°C)	Indoor *RH* (%) vs. Outdoor *RH* (%)	Indoor *AH* (g/m^3) vs. Outdoor *AH* (g/m^3)	Indoor *RH* (%) vs. Outdoor *AH* (g/m^3)
Blacksburg	0.19 (0.80)	0.37 (0.59)	0.4 (0.80)	2.49 (0.80)
Antananarivo†	0.58 (0.67)	0.55 (0.74)	0.62 (0.86)	2.38 (0.56)
Colombo	0.51 (0.35)	0.56 (0.45)	0.64 (0.71)	2.63 (0.32)
Guatemala City	0.36 (0.33)	0.45 (0.65)	0.80 (0.85)	2.90 (0.47)
Hong Kong	0.22 (0.58)	0.52 (0.80)	0.47 (0.85)	1.60 (0.75)
Lima†	-0.04 (0.00)	0.02 (0.00)	-0.30 (0.04)	0.49 (0.01)
Singapore	0.38 (0.62)	0.40 (0.55)	0.40 (0.35)	0.88 (0.06)
Tuxtla Gutierrez	0.03 (0.03)	0.35 (0.52)	0.06 (0.05)	0.81 (0.17)

(b) Winter/dry season (November to April for Northern Hemisphere and May to October for Southern Hemisphere)

Correlation	Indoor *T* (°C) vs. Outdoor *T* (°C)	Indoor *RH* (%) vs. Outdoor *RH* (%)	Indoor *AH* (g/m^3) vs. Outdoor *AH* (g/m^3)	Indoor *RH* (%) vs. Outdoor *AH* (g/m^3)
Blacksburg	0.04 (0.21)	0.23 (0.33)	0.51 (0.81)	1.36 (0.55)
Antananarivo†	0.62 (0.79)	0.63 (0.64)	0.64 (0.84)	1.53 (0.14)
Colombo	0.77 (0.71)	0.74 (0.83)	0.82 (0.94)	2.10 (0.58)
Guatemala City	0.64 (0.78)	0.69 (0.61)	0.87 (0.88)	2.26 (0.46)
Hong Kong	0.47 (0.85)	0.68 (0.79)	0.73 (0.97)	2.21 (0.86)
Lima†	-0.03 (0.00)	-0.08 (0.04)	0.26 (0.27)	-1.93 (0.27)
Singapore	0.36 (0.47)	0.31 (0.41)	0.35 (0.25)	0.69 (0.07)
Tuxtla Gutierrez	0.31 (0.67)	0.33 (0.32)	0.53 (0.74)	1.54 (0.37)

†Southern Hemisphere

Table S3. Slope (R^2) of daily indoor-to-outdoor linear regression by air conditioning status. Indoor data are averaged across all sensors in a city.

(a) Air conditioning off

Correlation	Indoor *T* (°C) vs. Outdoor *T* (°C)	Indoor *RH* (%) vs. Outdoor *RH* (%)	Indoor *AH* (g/m^3) vs. Outdoor *AH* (g/m^3)	Indoor *RH* (%) vs. Outdoor *AH* (g/m^3)
Blacksburg	0.12 (0.70)	0.43 (0.33)	0.51 (0.93)	2.04 (0.87)
Antananarivo	0.71 (0.90)	0.54 (0.66)	0.65 (0.94)	0.95 (0.20)
Colombo	0.64 (0.54)	0.74 (0.73)	0.83 (0.94)	2.32 (0.60)
Guatemala City	0.66 (0.74)	0.64 (0.68)	0.94 (0.93)	2.56 (0.63)
Hong Kong	0.43 (0.90)	0.69 (0.66)	0.69 (0.95)	1.77 (0.84)
Lima	-0.27 (0.04)	-0.23 (0.13)	0.55 (0.22)	-3.46 (0.35)
Singapore	0.55 (0.38)	0.46 (0.47)	1.18 (0.55)	2.09 (0.28)
Tuxtla Gutierrez	0.15 (0.23)	0.33 (0.42)	0.36 (0.60)	0.93 (0.27)

(b) Air conditioning on

Correlation	Indoor *T* (°C) vs. Outdoor *T* (°C)	Indoor *RH* (%) vs. Outdoor *RH* (%)	Indoor *AH* (g/m^3) vs. Outdoor *AH* (g/m^3)	Indoor *RH* (%) vs. Outdoor *AH* (g/m^3)
Blacksburg	0.2 (0.60)	0.19 (0.20)	0.46 (0.76)	1.80 (0.62)
Antananarivo	0.46 (0.25)	0.58 (0.26)	0.71 (0.35)	2.68 (0.27)
Colombo	-0.13 (0.00)	0.17 (0.02)	0.98 (0.41)	1.04 (0.03)
Guatemala City[†]	--	--	--	--
Hong Kong	0.27 (0.44)	0.49 (0.36)	0.61 (0.80)	1.99 (0.73)
Lima[†]	--	--	--	--
Singapore	0.36 (0.26)	0.34 (0.39)	0.39 (0.24)	0.73 (0.05)
Tuxtla Gutierrez	-0.18 (0.03)	0.14 (0.02)	0.98 (0.72)	3.00 (0.18)

[†]No AC systems installed.

Table S4. Differences (t statistics & w statistics) between indoor measurements and outdoor measurements. ↑ means indoor measurement is higher than the corresponding outdoor measurements, and ↓ is vice versa; -- means no significant difference. If not indicated in the data, there was no seasonal difference between indoors and outdoors.

Correlation	Indoor *T* (°C) vs. Outdoor *T* (°C)	Indoor *RH* (%) vs. Outdoor *RH* (%)	Indoor *AH* (g/m^3) vs. Outdoor *AH* (g/m^3)
Blacksburg	↑ (19.06* & 40.80*, winter) ↑ (1.47, $p = 0.14$ & 3.66*, summer)	↓ (-19.03* & -24.78*)	-- (1.74, $p = 0.08$ & -1,11, $p = 0.27$)
Antananarivo	↑ (19.52* & 25.09*)	↓ (-23.91* & -39.67*)	-- (-1.43, $p = 0.15$ & -1.15, $p = 0.25$)
Colombo	↑ (17.45* & 21.93*)	↓ (-12.02* & -12.07*)	↑ (3.76* & 3.41*)
Guatemala City†	↑ (22.13* & 34.87*)	↓ (-21.76* & -32.55*)	↑ (3.87* & 3.73*)
Hong Kong	↓ (-5.95* & -3.14*)	↓ (-9.82* & -7.09*)	↓ (-12.68* & -13.96*, wet season) -- (-1.11, $p = 0.27$ & -0.5, $p = 0.6$, dry season)
Lima†	↓ (-13.9* & -17.16**)	↓ (-8.60* & - 9.06*)	↓ (-23.21* & 46.70*)
Singapore	↓ (-13.24* & -14.20*)	↓ (-24.18* & -45.07*)	↓ (-24.37* & -73.70*)
Tuxtla Gutierrez	↓ (-17.32* & -13.81*)	↑ (8.36* & 9.51*)	↓ (-9.87* &-10.62*)

†No AC systems installed.

* $p < 0.05$ if not stated otherwise.

Table S5. Spearman coefficient between indoor measurements and outdoor measurements when AC was on.

Correlation	Indoor T (°C) vs. Outdoor T (°C)	Indoor RH (%) vs. Outdoor RH (%)	Indoor AH (g/m^3) vs. Outdoor AH (g/m^3)	Indoor RH (%) vs. Outdoor AH (g/m^3)
Blacksburg	0.64*	0.59*	0.77*	0.66*
Antananarivo	0.44*	0.62*	0.71*	0.60*
Colombo	0.03, $p = 0.85$	-0.00, $p = 0.99$	0.61*	0.13, $p = 0.34$
Guatemala City†	--	--	--	--
Hong Kong	0.76*	0.47*	0.88*	0.81*
Lima†	--	--	--	--
Singapore	0.52*	0.60*	0.44*	0.19*
Tuxtla Gutierrez	-0.04, $p = 0.84$	0.10, $p = 0.60$	0.84*	0.23, $p = 0.24$

† No AC systems installed.

* $p < 0.05$ if not stated otherwise.

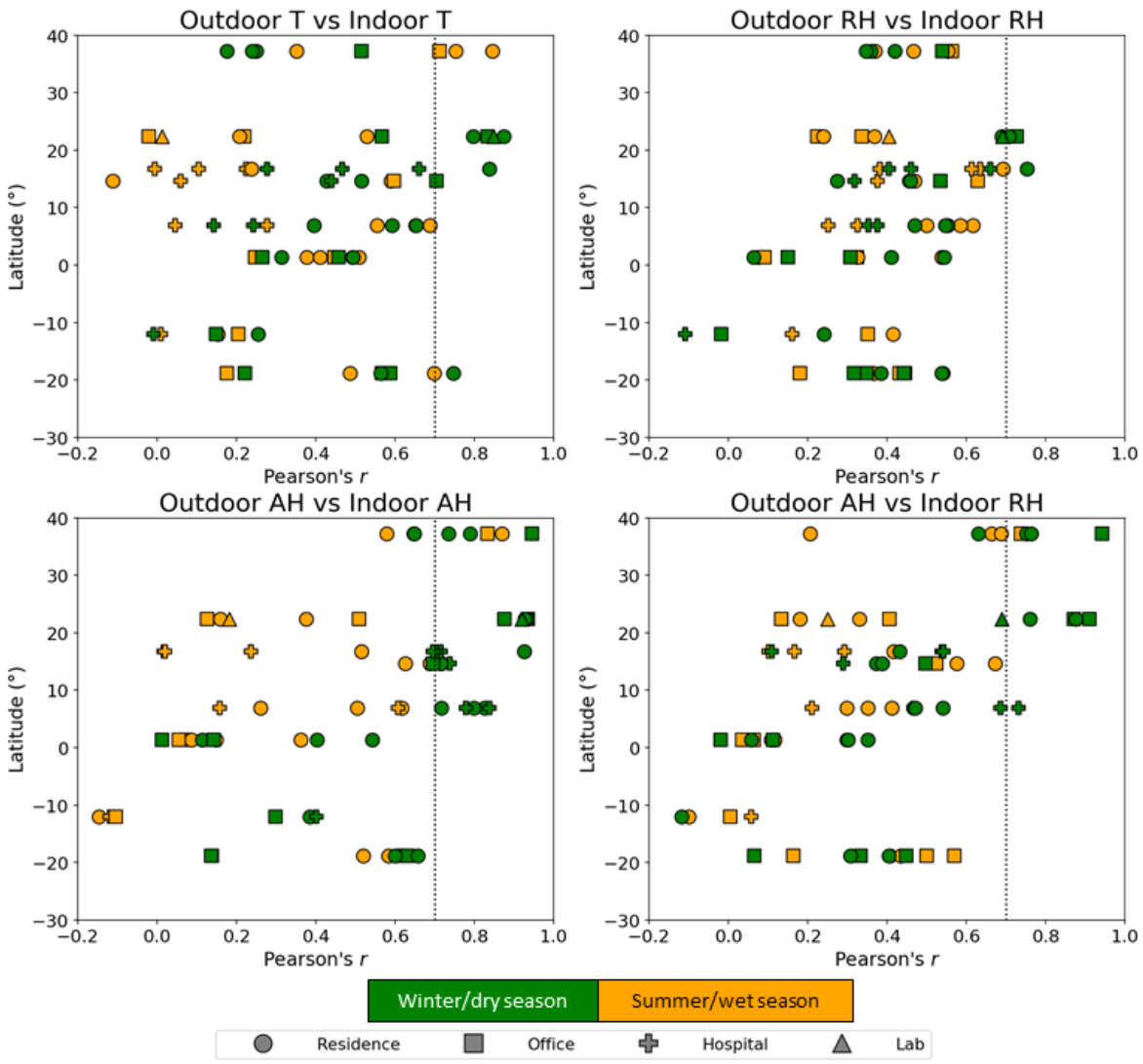

Figure S1. Variation of Pearson's *r* by building type, latitude, and season. Green markers represent winter/dry seasons, and orange markers represent summer/wet seasons. The shape of the markers represents the building type, as indicated in the legend. $p < 0.05$ for all data points except those representing Lima (latitude: 12.05°S).

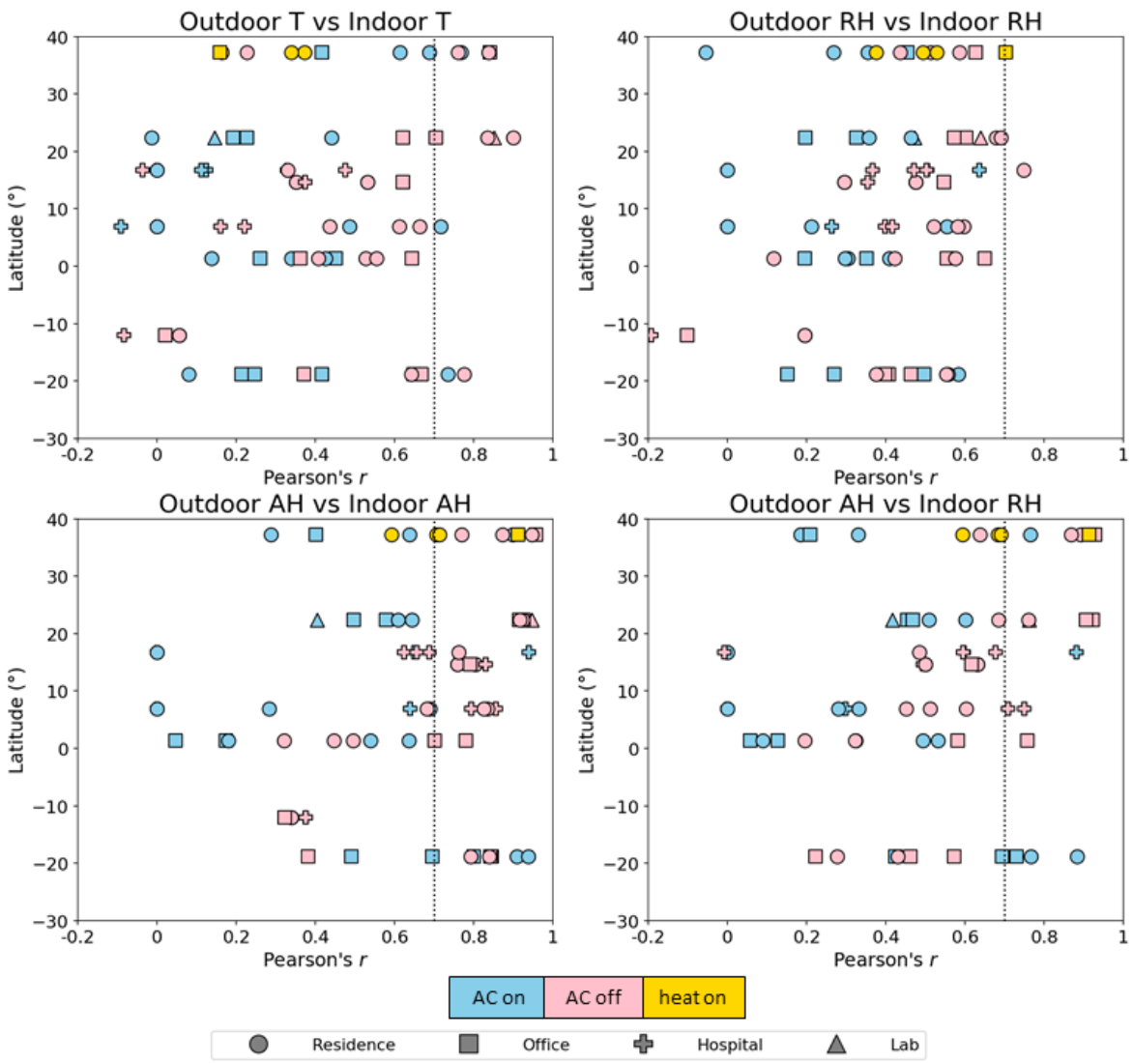

Figure S2. Variation of Pearson's r by building type, latitude, and AC status. Blue markers represent "AC on", pink markers represent "AC off", and yellow markers represent "heat on" (for Blacksburg only). The shape of the markers represents the building type, as indicated in the legend. $p < 0.05$ for all data points except those representing Lima (latitude: 12.05°S).

References

1. Conlon KC, Rajkovich NB, White-Newsome JL, Larsen L, O'Neill MS. Preventing cold-related morbidity and mortality in a changing climate. *Maturitas.* 2011;69(3):197-202.
2. Schwartz J, Samet JM, Patz JA. Hospital admissions for heart disease: The effects of temperature and humidity. *Epidemiology.* 2004;15(6):755-761.
3. Lin S, Luo M, Walker RJ, Liu X, Hwang S-A, Chinery R. Extreme high temperatures and hospital admissions for respiratory and cardiovascular diseases. *Epidemiology.* 2009;20(5):738-746.
4. Turner LR, Barnett AG, Connell D, Tonga S. Ambient temperature and cardiorespiratory morbidity: A systematic review and meta-analysis. *Epidemiology.* 2012;23(4):594-606.
5. The Eurowinter Group. Cold exposure and winter mortality from ischaemic heart disease, cerebrovascular disease, respiratory disease, and all causes in warm and cold regions of Europe. *The Lancet.* 1997;349(9062):1341-1346.
6. Davis RE, McGregor GR, Enfield KB. Humidity: A review and primer on atmospheric moisture and human health. *Environmental Research.* 2016;144:106-116.
7. Anderson BG, Bell ML. Weather-related mortality: How heat, cold, and heat waves affect mortality in the United States. *Epidemiology.* 2009;20(2):205-213.
8. Zhang K, Li Y, Schwartz JD, O'Neill MS. What weather variables are important in predicting heat-related mortality? A new application of statistical learning methods. *Environmental Research.* 2014;132:350-359.
9. Wu Y, Jing W, Liu J, et al. Effects of temperature and humidity on the daily new cases and new deaths of COVID-19 in 166 countries. *Sci Total Environ.* 2020;729:139051-139051.
10. Sajadi MM, Habibzadeh P, Vintzileos A, Shokouhi S, Miralles-Wilhelm F, Amoroso A. Temperature, humidity, and latitude analysis to estimate potential spread and seasonality of coronavirus disease 2019 (COVID-19). *JAMA Network Open.* 2020;3(6):e2011834-e2011834.
11. Davis RE, Rossier CE, Enfield KB. The impact of weather on influenza and pneumonia mortality in New York City, 1975–2002: A retrospective study. *PLOS ONE.* 2012;7(3):e34091.
12. Shaman J, Pitzer VE, Viboud C, Grenfell BT, Lipsitch M. Absolute humidity and the seasonal onset of influenza in the continental United States. *PLOS Biology.* 2010;8(2):e1000316.
13. Tang JW, Lai FYL, Wong F, Hon KLE. Incidence of common respiratory viral infections related to climate factors in hospitalized children in Hong Kong. *Epidemiology and Infection.* 2010;138(2):226-235.
14. Tang JW, Loh TP. Correlations between climate factors and incidence—a contributor to RSV seasonality. *Reviews in Medical Virology.* 2014;24(1):15-34.
15. Moriyama M, Hugentobler WJ, Iwasaki A. Seasonality of respiratory viral infections. *Annual Review of Virology.* 2020;7:1.
16. Klepeis NE, Nelson WC, Ott WR, et al. The National Human Activity Pattern Survey

(NHAPS): a resource for assessing exposure to environmental pollutants. *Journal of Exposure Science & Environmental Epidemiology.* 2001;11(3):231-252.
17. Nguyen JL, Schwartz J, Dockery DW. The relationship between indoor and outdoor temperature, apparent temperature, relative humidity, and absolute humidity. *Indoor Air.* 2014;24(1):103-112.
18. Nguyen JL, Dockery DW. Daily indoor-to-outdoor temperature and humidity relationships: A sample across seasons and diverse climatic regions. *International Journal of Biometeorology.* 2016;60(2):221-229.
19. Tang JW, Loh TP. Influenza seasonality. *Current Treatment Options in Infectious Diseases.* 2016;8(4):343-367.
20. Höppe P, Martinac I. Indoor climate and air quality. *International Journal of Biometeorology.* 1998;42(1):1-7.
21. Tamerius JD, Perzanowski MS, Acosta LM, et al. Socioeconomic and outdoor meteorological determinants of indoor temperature and humidity in New York City dwellings. *Weather, Climate, and Society.* 2013;5(2):168-179.
22. Quinn A, Tamerius JD, Perzanowski M, et al. Predicting indoor heat exposure risk during extreme heat events. *Science of The Total Environment.* 2014;490:686-693.
23. White-Newsome JL, Sánchez BN, Jolliet O, et al. Climate change and health: Indoor heat exposure in vulnerable populations. *Environmental Research.* 2012;112:20-27.
24. Epstein PR. Climate and health. *Science.* 1999;285(5426):347.
25. McMichael AJ, Woodruff RE, Hales S. Climate change and human health: present and future risks. *The Lancet.* 2006;367(9513):859-869.
26. Haines A, Kovats RS, Campbell-Lendrum D, Corvalan C. Climate change and human health: Impacts, vulnerability and public health. *Public Health.* 2006;120(7):585-596.
27. Viboud C, Alonso WJ, Simonsen L. Influenza in tropical regions. *PLOS Medicine.* 2006;3(4):e89.
28. Tamerius JD, Nelson Martha I, Zhou Steven Z, Viboud C, Miller Mark A, Alonso Wladimir J. Global influenza seasonality: Reconciling patterns across temperate and tropical regions. *Environmental Health Perspectives.* 2011;119(4):439-445.
29. Tamerius JD, Shaman J, Alonso WJ, et al. Environmental predictors of seasonal influenza epidemics across temperate and tropical climates. *PLOS Pathogens.* 2013;9(3):e1003194.
30. Dowell SF. Seasonality – still confusing. *Epidemiology and Infection.* 2012;140(1):87-90.
31. Bloom-Feshbach K, Alonso WJ, Charu V, et al. Latitudinal variations in seasonal activity of influenza and respiratory syncytial virus (RSV): a global comparative review. *PloS one.* 2013;8(2):e54445.
32. Alduchov OA, Eskridge RE. Improved magnus form approximation of saturation vapor pressure. *Journal of Applied Meteorology.* 1996;35(4):601-609.
33. Worbes M. Annual growth rings, rainfall-dependent growth and long-term growth patterns of tropical trees from the Caparo Forest Reserve in Venezuela. *Journal of Ecology.* 1999;87(3):391-403.
34. De Silva CS, Rushton KR. Groundwater recharge estimation using improved soil moisture

balance methodology for a tropical climate with distinct dry seasons. *Hydrological Sciences Journal.* 2007;52(5):1051-1067.
35. Tang JW. The effect of environmental parameters on the survival of airborne infectious agents. *J R Soc Interface.* 2009;Suppl 6(Suppl 6):S737-746.
36. Marr LC, Tang JW, Van Mullekom J, Lakdawala SS. Mechanistic insights into the effect of humidity on airborne influenza virus survival, transmission and incidence. *J R Soc Interface.* 2019;16(150):20180298-20180298.
37. Tetelin A, Pouget V, Lachaud J, Pellet C. Dynamic behavior of a chemical sensor for humidity level measurement in human breath. *IEEE Transactions on Instrumentation and Measurement.* 2004;53(4):1262-1267.
38. Buettner K. Diffusion of Water and Water Vapor Through Human Skin. *Journal of Applied Physiology.* 1953;6(4):229-242.
39. Qi H, Xiao S, Shi R, et al. COVID-19 transmission in Mainland China is associated with temperature and humidity: A time-series analysis. *Science of The Total Environment.* 2020;728:138778.
40. Ward MP, Xiao S, Zhang Z. Humidity is a consistent climatic factor contributing to SARS-CoV-2 transmission. *Transboundary and Emerging Diseases.* 2020;00(67):3069-3074.
41. Garnett L, Bello A, Tran KN, et al. Comparison analysis of different swabs and transport mediums suitable for SARS-CoV-2 testing following shortages. *Journal of Virological Methods.* 2020;285:113947.
42. Wang J, Tang K, Feng K, et al. Impact of temperature and relative humidity on the transmission of COVID-19: a modelling study in China and the United States. *BMJ Open.* 2021;11:e043863.
43. Gupta S, Raghuwanshi GS, Chanda A. Effect of weather on COVID-19 spread in the US: A prediction model for India in 2020. *Science of The Total Environment.* 2020;728:138860.
44. Bukhari Q, Jameel Y. Will coronavirus pandemic diminish by summer? *Available at SSRN 3556998.* 2020.
45. Ficetola GF, Rubolini D. Containment measures limit environmental effects on COVID-19 early outbreak dynamics. *Science of The Total Environment.* 2021;761:144432.
46. Poole L. Seasonal influences on the spread of SARS-CoV-2 (COVID-19), causality, and forecastabililty (3-15-2020). *Available at SSRN 3554746.* 2020.
47. Qian H, Miao T, Liu L, Zheng X, Luo D, Li Y. Indoor transmission of SARS-CoV-2. *Indoor Air.* 2020;00:1-7.